ANL/NE-12/4

The SAS4A/SASSYS-1 Safety Analysis Code System

Nuclear Engineering Division

ANL/NE-12/4

The SAS4A/SASSYS-1 Safety Analysis Code System

Chapter 3:
Steady-State and Transient Thermal Hydraulics in Core Assemblies

F. E. Dunn
Nuclear Engineering Division
Argonne National Laboratory

January 31, 2012

TABLE OF CONTENTS

LIST OF FIGURES

LIST OF TABLES

NOMENCLATURE

Subscript	Description
c	Coolant
e	Cladding
f	Fuel
g	Plenum gas
kz	Reflector zone
p	Gas plenum region
si	Structure inner node
so	Structure outer node
1	Beginning of the time step
2	End of the time step

Symbol	Description	Units
A_c	Coolant flow area	m^2
A_{ep}	Cross sectional area of the clad in the gas plenum region	m^2
A_g	Cross sectional area of the plenum gas	m^2
A_{fr}, b_{fr}	Coefficients in the friction factor correlation: $f = A_{fr}(Re)^{b_{fr}}$	--
c	Specific heat	J/kg-K
$\overline{c}_c$	Coolant specific heat	J/kg-K
c_e	Cladding specific heat	J/kg-K
$\overline{c}_f$	Average fuel specific heat, averaged over a time step	J/kg-K
c_m	Modified specific heat in the melting range	J/kg-K
c_{mix}	Coolant specific heat in the mixing zone used for re-entry temperature calculation	J/kg-K
c_1,c_2,c_3	Correlation constants used in coolant heat-transfer coefficients	--
D	Right-hand-side terms in the matrix equations for radial temperature profiles	J/m
D_h	Hydraulic diameter	m
d_{sti}	Structure inner node thickness	m
d_{sto}	Structure outer node thickness	m
E_{ec}	Heat flux from clad to coolant, integrated over a time step	J/m^2
E_{sc}	Heat flux form structure to coolant, integrated over a time	J/m^2

Symbol	Description	Units
	step	
f	Friction factor	--
f_i	Fraction of the structure thickness represented by the inner node	--
f_o	Fraction of the structure thickness represented by the outer node	--
g	Acceleration of gravity	m/s^2
h_b	Bond gap conductance	W/m^2-K
h_c	Coolant-film heat-transfer coefficient	W/m^2-K
h_{cond}	Condensation heat-transfer coefficient for sodium vapor	W/m^2-K
H_{eg}	Heat-transfer coefficient form the gas in the gas plenum to the cladding	W/m^2-K
H_{erc}	Heat-transfer coefficient from the cladding or reflector outer node to the coolant	W/m^2-K
h_r	Equivalent radiation heat-transfer coefficient	W/m^2-K
H_{rio}	Heat-transfer coefficient from the structure inner node to the reflector outer node	W/m^2-K
H_{sic}	Heat-transfer coefficient from the structure inner node to the coolant	W/m^2-K
H_{stio}	Heat-transfer coefficient from the structure inner node to the structure outer node	W/m^2-K
i	Radial node number	--
ic	Core channel number	--
I_1	Inertial integral in the momentum equation	m^{-1}
I_2	Acceleration integral in the momentum equation	m/kg
I_3	Friction integral in the momentum equation	m/kg
I_4	Orifice term in the momentum equation	m/kg
I_5	Density integral in the momentum equation	kg/m^2
j	Fuel axial node number	--
jc	Coolant axial node number	--
JC	Axial node number	--
k	Thermal conductivity	W/m-K
k_{ep}	Cladding thermal conductivity in the gas plenum region	W/m-K
$\bar{k}_{i,j}$	Weighted average thermal conductivity for heat flow from node i to j	W/m-K
K_{or}	Orifice coefficient	--

Symbol	Description	Units
L	1 for subassembly inlet, 2 for outlet	--
MZC	Total number of coolant axial nodes	--
m_e	Cladding mass	kg
m_f	Fuel mass	kg
M_{mix}	Mass of sodium in the mixing volume	kg
NC	Radial node number of the coolant node	--
NE	Radial node number for the cladding mid-point	--
NE′	Radial node number for the cladding outer surface node	--
NE″	Radial node number for the cladding inner surface node	--
NN	NT-1	--
N_{ps}	Number of fuel pins represented by a channel	--
NR	Radial node number for the fuel outer surface radius. (note NR=NE″)	--
NSI	Radial node number for the inner structure node	--
NSO	Radial node number for the outer structure node	--
NT	Radial node number for the fuel outer surface temperature node	--
p	Pressure	Pa
p_b	Pressure at the bottom of the subassembly	Pa
p_{b1},p_{b2}	p_b at beginning and end of a time step	Pa
p_{in}	Pressure in the coolant inlet plenum	Pa
$\overline{P}_j$	Heat production rate in axial node j	W
P_r	Radial power shape, per unit mass	--
p_t	Pressure at the top of the subassembly	Pa
p_{t1},p_{t2}	p_t at the beginning and end of a time step	Pa
p_x	Pressure in the coolant outlet plenum	Pa
$\left(\frac{\partial p}{\partial z}\right)_{fr}$	Friction pressure drop	Pa/m
$\left(\frac{\partial p}{\partial z}\right)_{k}$	Orifice pressure drop	Pa/m
Q_c	Coolant heat source due to direct heating by neutrons and gamma rays	W/m^3
Q_{ct}	Total steady-state heat source per unit of coolant volume	W/m^3
Q_{ec}	Heat flow from clad to coolant	W/m^3
q_{fe}	Fuel-to-cladding heat flux	W/m^2

Symbol	Description	Units
Q_{sc}	Heat flow from structure to coolant	W/m^3
$Q_{sm}(i)$	Sum of the heat sources for all radial nodes inside and including node i	W
Q_{st}	Structure heat source due to direct heating by neutrons and gamma rays	W/m^2
Q_v	Heat source per unit volume	W/m^3
r	Radius	m
r_{brp}	Clad inner radius in the gas plenum region	m
Re	Reynolds number	--
R_{ec}	Thermal resistance between clad and coolant	m^2-K/W
R_{ehf}	Thermal resistance of the outer fourth of the cladding	m^2-K/W
r_{erp}	Cladding outer radius in the gas plenum region	m
R_g	Thermal resistance of the gas in the plenum	m^2-K/W
$r_o(i)$	Steady-state radial mesh	m
S_{er}	Perimeter of the cladding or reflector in contact with the coolant	m
S_{st}	Structure perimeter, heat-transfer area per unit height	m
T	Temperature	K
t	Time	s
T_{cin}	Coolant inlet temperature	K
T_{cout}	Coolant outlet temperature	K
T_{eex}	Extrapolated clad temperature	K
T_{eq}	Equilibrium temperature in the mixing volume	K
$\overline{T}_{exp}$	Temperature of the sodium expelled from the subassembly into a mixing volume, averaged over a time step	K
$\overline{T}_f$	Average fuel temperature at an axial node, mass-weighted average	K
T_g	Plenum gas temperature	K
T_{liq}	Liquidus temperature	K
T_{out}	Bulk temperature in the coolant outlet plenum	K
t_{p1}, t_{p2}	Times at the beginning and end of a PRIMAR time step	s
T_{ri}	Reflector inner node temperature	K
T_{ro}	Reflector outer node temperature	K
T_{sol}	Solidus temperature	K
T_o	Temperature at the beginning of a time step	K

Symbol	Description	Units
T_1	Temperature at the beginning of a time step	K
T'_1	Temperature of the coolant entering an axial node at the end of a time step	K
T_2	Temperature at the end of a time step	K
T'_2	Temperature of the coolant entering an axial node at the end of a time step	K
U_{melt}	Heat of fusion	J/kg
v	Velocity	m/s
w	Coolant mass flow rate	kg/s
w_e	Estimated mass flow rate	kg/s
w_{fe}	Thickness of the liquid-sodium film left on the cladding after voiding occurs	m
w_{fr}	Thickness of the liquid-sodium film left on the reflector after voiding occurs	m
w_{fst}	Thickness of the liquid-sodium film left on the structure after voiding occurs	m
w_1,w_2	w at beginning and end of a time step	kg/s
Δw	Change in w during a time step	kg/s
x	Distance	m
x_{I1}(JC)	Nodal contribution to I_1	m^{-1}
x_{I2}(JC)	Nodal contribution to I_2	m/kg
x_{I3}(JC)	Nodal contribution to I_3	
x_{I5}(JC)	Nodal contribution to I_5	kg/m^2
z	Axial position	m
z	Elevation	m
Δz	Node height	m
z_{pb}	Elevation at the bottom of the gas plenum	m
z_{pt}	Elevation at the top of the gas plenum	m
$z_{p\ell\ell}$	Reference elevation of the coolant inlet plenum	m
$z_{p\ell u}$	Reference elevation of the coolant outlet plenum	m
α	Heat capacity terms in the matrix equations for radial temperature profiles	J/m-K
α_e	Cladding thermal expansion coefficient	K^{-1}
α_f	Fuel thermal expansion coefficient	K^{-1}
β	Thermal conductivity terms in the matrix equations for	J/m-K

Symbol	Description	Units
	radial temperature profiles	
γ_c	Fraction of the total heat production that goes directly into the coolant	--
γ_e	Fraction of the total heat production that goes directly into the cladding	--
γ_s	Fraction of the total heat production that goes directly into the structure	--
γ_2	Ratio of the structure perimeter to the cladding perimeter	--
Δr	Radial node size	m
$\Delta r_{i,j}$	Effective radial distance for heat flow from node I to node j	m
Δt	Time-step size	s
Δz	Axial node height	m
ε	Thermal emissivity	--
θ_1,θ_2	Degree of explicitness or implicitness in the solution	--
ρ	Density	kg/m^3
ρ_c	Coolant density	kg/m^3
ρ_{cin}	Coolant density in the inlet plenum	kg/m^3
ρ_{cout}	Coolant density in the outlet plenum	kg/m^3
$(\rho c)_g$	Density times specific heat of the plenum gas	J/m^3-K
$(\rho c)_r$	Density times specific heat for the reflector	J/m^3-K
ρ_e	Cladding density	kg/m^3
σ	Stefan-Bolzmann constant	W/m^2-K^4
τ	Time constant for flow rate changes	s
τ_c	Condensation heat-transfer time constant	s
τ_{ro}	Time constant for temperature changes in the outer reflector node	s
τ_{sti}	Time constant for temperature changes in the inner structure node	s
μ	Coolant viscosity	Pa-s
$\bar{\mu}(JC)$	Average value of μ for node JC	Pa-s
ψ	Source terms in the matrix equations for radial temperature profiles	--

STEADY-STATE AND TRANSIENT THERMAL HYDRAULICS IN CORE ASSEMBLIES

3.1 Introduction

The core assembly thermal hydraulics treatment in SASSYS-1 and SAS4A includes the calculation of fuel, cladding, coolant, and structure temperatures, as well as coolant flow rates and pressure distributions. This treatment includes melting of the fuel and cladding. Boiling of the coolant is also handled, as described in Chapter 12. The relocation of fuel and cladding after pin disruption is described in Chapters 13, 14, and 16; and relocation of molten fuel before pin disruption is described in Chapter 15.

Until recently, all of the core subassembly models in SAS4A and SASSYS-1 were single pin models: a single fuel pin and its associated coolant were used to represent a subassembly; and pin-to-pin variations within a subassembly were ignored. Recently a multiple pin option has been added to the code. A number of pins and their associated coolant can now be used to represent a subassembly, so variations within a subassembly can be accounted for. Currently the multiple pin option is only available for single-phase thermal hydraulics; it does not handle coolant boiling, in-pin fuel relocation, or pin disruption. Therefore, typical SASSYS-1 cases that do not get into coolant boiling can be handled with the multiple-pin model, but typical SAS4A core disruption cases can only be handled with single pin models.

Although SASSYS-1 and SAS4A are mainly transient codes both steady-state and transient temperatures and coolant pressures are calculated. The steady-state solutions are obtained from the transient equations after dropping all time derivatives. In general, the steady-state solutions in the single pin per subassembly model are not obtained by running a transient calculation at constant power and flow until the results approach a steady-state solution. Instead, the steady-state temperatures are obtained rapidly from a direct solution based on conservation of energy and the use of the same spatial finite differencing as used in the transient. On the other hand, a direct steady-state solution for the multiple pin option would be much more complicated, especially if subassembly-to-subassembly heat transfer is included. Therefore, a null transient with powers and flows held constant is used to obtain steady-state conditions for the multiple pin option.

The thermal hydraulics calculations are carried out in a number of separate modules, and each module is designed for a specific type of calculation. A steady-state thermal hydraulics module provides the initial conditions for the transient. The transient temperatures are calculated in a pre-voiding module (TSHTRN) until the onset of boiling. After the onset of boiling, the fuel-pin temperatures are calculated in a separate module (TSHTRV) that couples with the boiling module.

The core thermal-hydraulic routines interact with a number of other modules, as shown in Fig. 3.1-1. Before the onset of voiding, TSHTRN calculates the coolant temperatures used in the hydraulic calculations, whereas the hydraulics routines calculate the coolant flow rates used in TSHTRN. After the onset of voiding, coolant temperatures are calculated in TSBOIL, and this module supplies the heat flux at the cladding outer surface or the fuel outer surface to TSHTRV. TSBOIL uses the cladding

temperatures from TSHTRV in its coolant temperature calculations. The point kinetics module supplies the power level used in the heat-transfer routines, and the heat-transfer routines supply the Doppler feedback reactivity as well as other temperature-dependent reactivity feedback. TSBOIL supplies the voiding reactivity. The inlet plenum temperature computed by PRIMAR-4 is used in calculating the inlet temperature for TSHTRN or TSBOIL, and TSHTRN or TSBOIL provides the subassembly outlet temperatures used by PRIMAR-4 to compute the outlet plenum temperature. If flow reversal occurs in a subassembly, then the outlet plenum temperature computed by PRIMAR-4 is used in calculating the coolant temperature at the top of the subassembly, and the temperature computed by TSHTRN or TSBOIL for the coolant leaving the bottom of the subassembly is used by PRIMAR-4 to calculate the inlet plenum temperature. PRIMAR-4 supplies the inlet and outlet plenum pressures that drive the coolant hydraulics calculations, and the core channel flows are provided to PRIMAR-4 by TSBOIL and the pre-voiding hydraulics. The initial coolant flow rate and pressure distribution are supplied to TSBOIL by the pre-voiding hydraulics routines.

The transient calculations in the codes used a multi-level time step approach, with separate time steps for each module. For the heat-transfer routines, all temperatures are known at the beginning of a heat-transfer step, and the routines calculate the new temperatures at the end of the step. The heat-transfer time step can be longer than the coolant time step or the PRIMAR time step, but the heat-transfer time step can be no longer than the main time step that is used for reactivity feedback and main printouts.

Figure 3.1-2 shows the flow through the pre-voiding core channel thermal hydraulics driver, TSCL0. This routine is entered once for each channel during each coolant time step. The coolant flow rates are calculated before the heat-transfer module (TSHTRN) is called. TSHTRN is only called if the current coolant time step completes a heat-transfer time step. The voiding model, TSHTRV, is described in Chapter 12.

In this chapter, Section 3.2 describes the mesh structure used for heat-transfer calculations. Then, Section 3.3 describes the pre-boiling transient heat-transfer calculations, followed by the steady-state thermal hydraulics calculations in Section 3.4. The pre-voiding transient heat transfer is discussed before the steady-state thermal hydraulics for two reasons. First, as previously mentioned, the codes are primarily transient codes, so the transient calculations are more important. Second, the finite difference approximations were made with the transient calculations in mind, and the steady-state solution was formulated to be consistent with the approximations used in the transient. Section 3.5 describes TSHTRV, the fuel-pin heat-transfer calculations in the boiling module. Section 3.6 describes the treatment of the bond-gap conductance between the fuel and the cladding. Section 3.7 describes modifications to the fuel pin heat transfer calculations for PLUTO2 and LEVITATE. The heat transfer time step control is described in Section 3.8. Section 3.9 describes steady-state and pre-voiding transient hydraulics. Section 3.10 describes the multiple pin option. Subassembly-to-subassembly heat transfers described in Section 3.11. Section 3.12 describes interaction with other modules. It is followed by sections including subroutine descriptions and flowcharts, thermal properties of fuel and cladding, and a description of the input to, and output from, the thermal hydraulic routines.

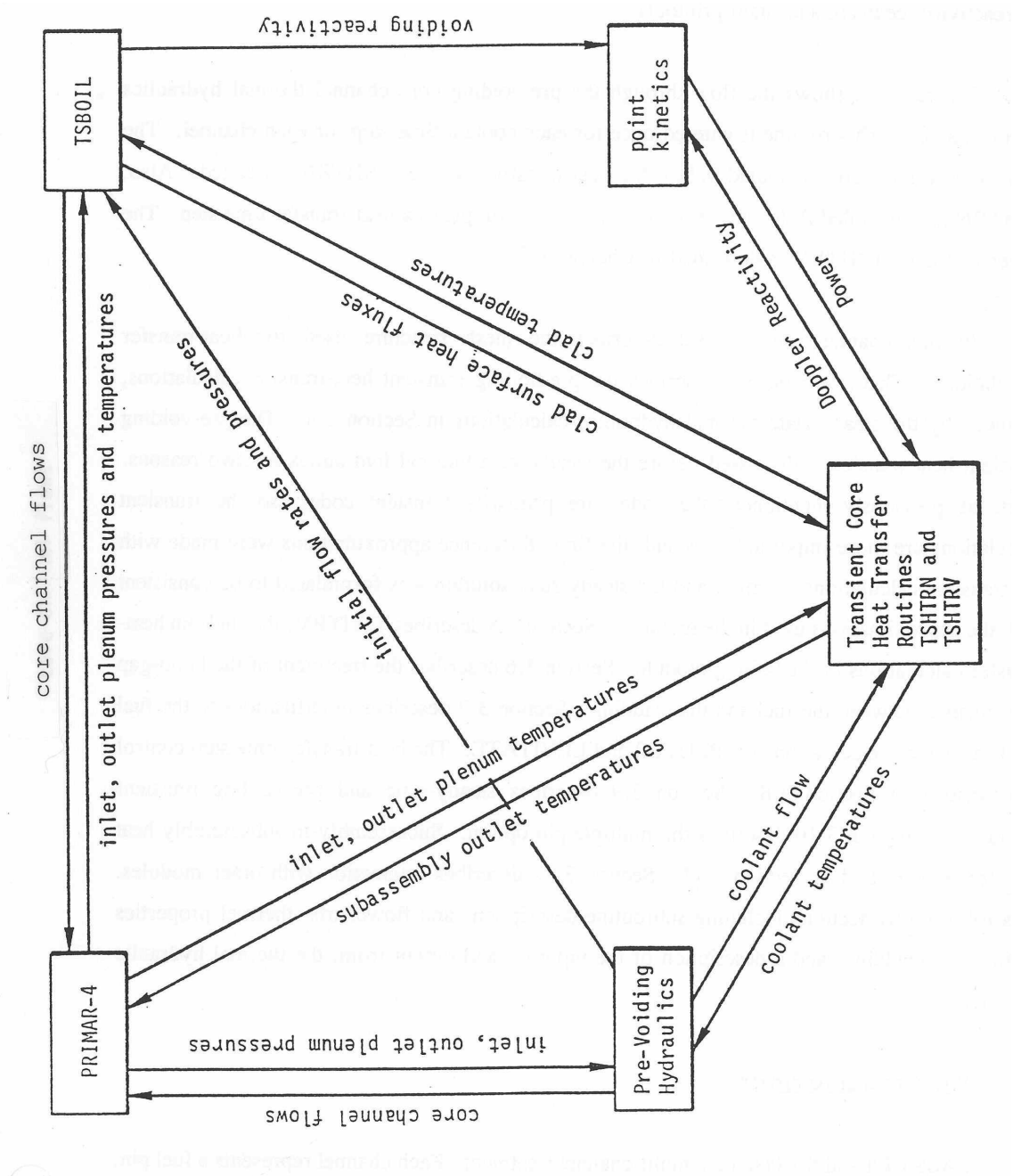

Figure 3.1-1: Interactions of Thermal-Hydraulic Routines with Other Modules

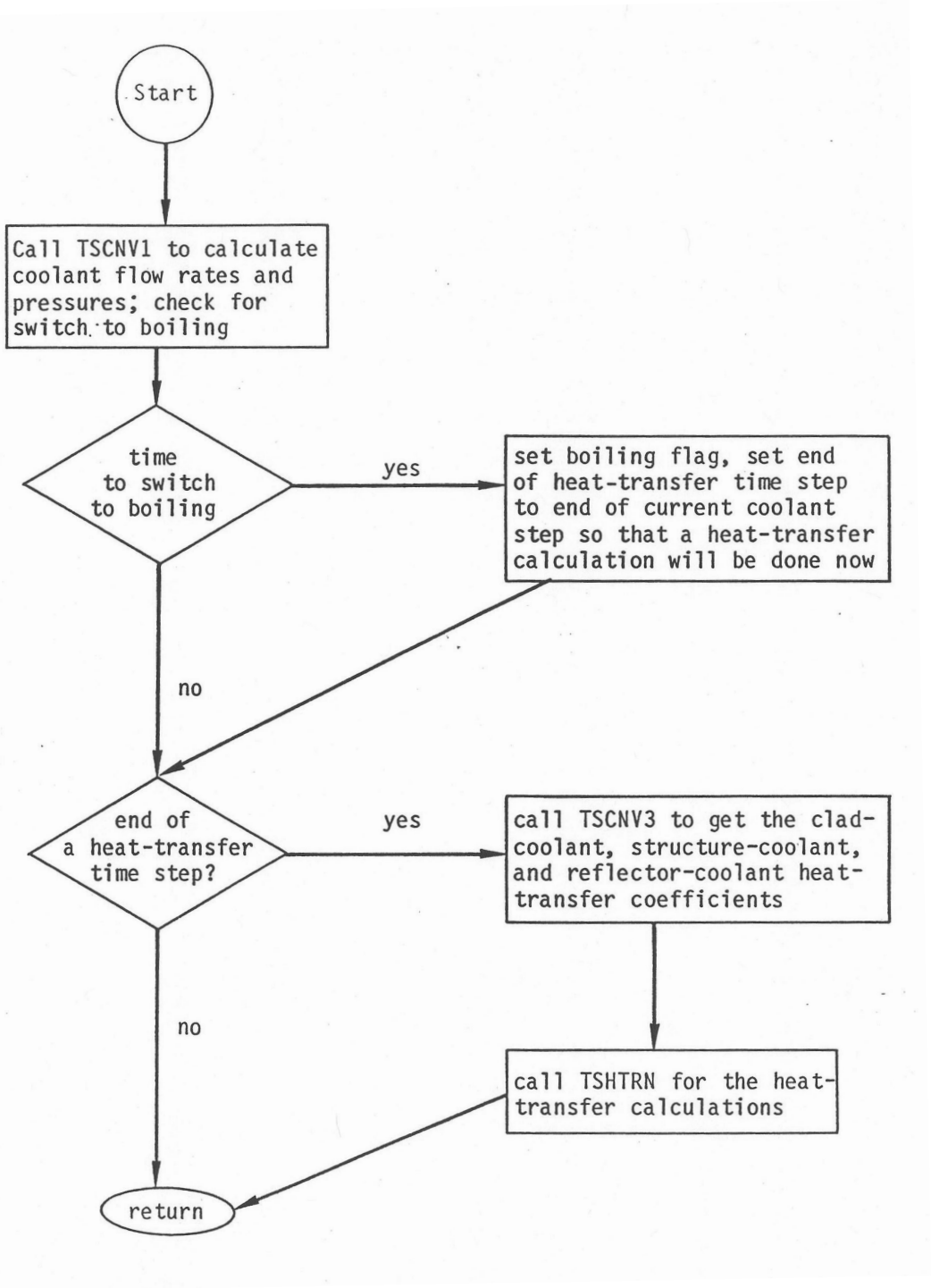

Figure 3.1-2: Flowchart for the Pre-Voiding Core Channel Thermal Hydraulics Driver (Subroutine TSCL0)

3.2 SAS Channel Approach

SASSYS-1 and SAS4A use of multi-channel treatment. Each channel represents a fuel pin, its associated coolant, and a fraction of the subassembly duct wall, as indicated in Fig. 3.2-1. Usually, a channel is used to represent an average pin in a fuel subassembly or a group of similar subassemblies. A channel can also be used to represent a blanket assembly or a control-rod channel, and the hottest pin in a subassembly can be represented instead of the average pin. Different channels can be used to account for radial and azimuthal power variations within the core, as well as variations in coolant flow orificing and fuel burn-up. In the multiple pin option, more than one channel can be used to represent a subassembly

3.2.1 Axial Mesh Structure

A channel usually represents the whole length of the subassembly, from coolant inlet to coolant outlet. A number of axial zones are used, as indicated in Fig. 3.2-2. One zone represents the fuel-pin section, including the core, axial blankets, and gas plenum. Other zones represent reflector regions above and below the pin section. A maximum of 7 zones can be used in a channel. In general, radial dimensions and thermal properties are constant with a reflector zone. The pin section zone is treated separately in considerably more detail than the reflector zones. The gas plenum can be either above or below the core.

Figure 3.2-3 shows the axial mesh structure used for a channel. The coolant and structure nodes run the whole length of the channel. The coolant nodes are staggered with respect to the fuel, cladding, reflector, and structure nodes. Using coolant temperatures defined at the axial boundaries between cladding and structure nodes makes it easier to calculate accurate coolant temperatures. If non-uniform axial mesh sizes are used, a simple finite differencing of the coolant temperature equation gives accurate coolant temperatures with a staggered mesh, whereas if the coolant nodes were at the middle of the cladding nodes, then obtaining accurate coolant temperatures would require extra terms in the finite differencing of the coolant temperature equation.

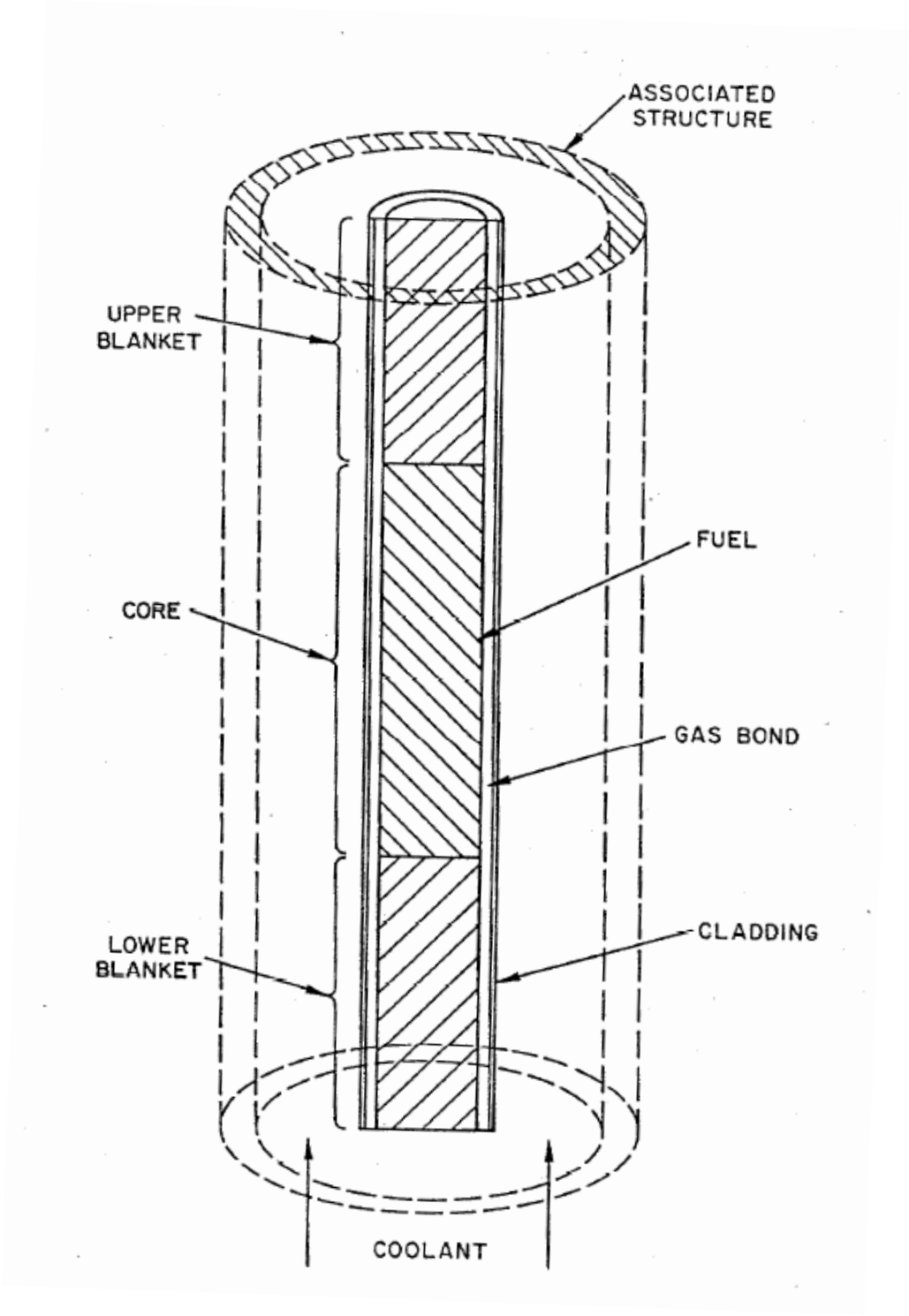

Figure 3.2-1: SAS Channel Treatment

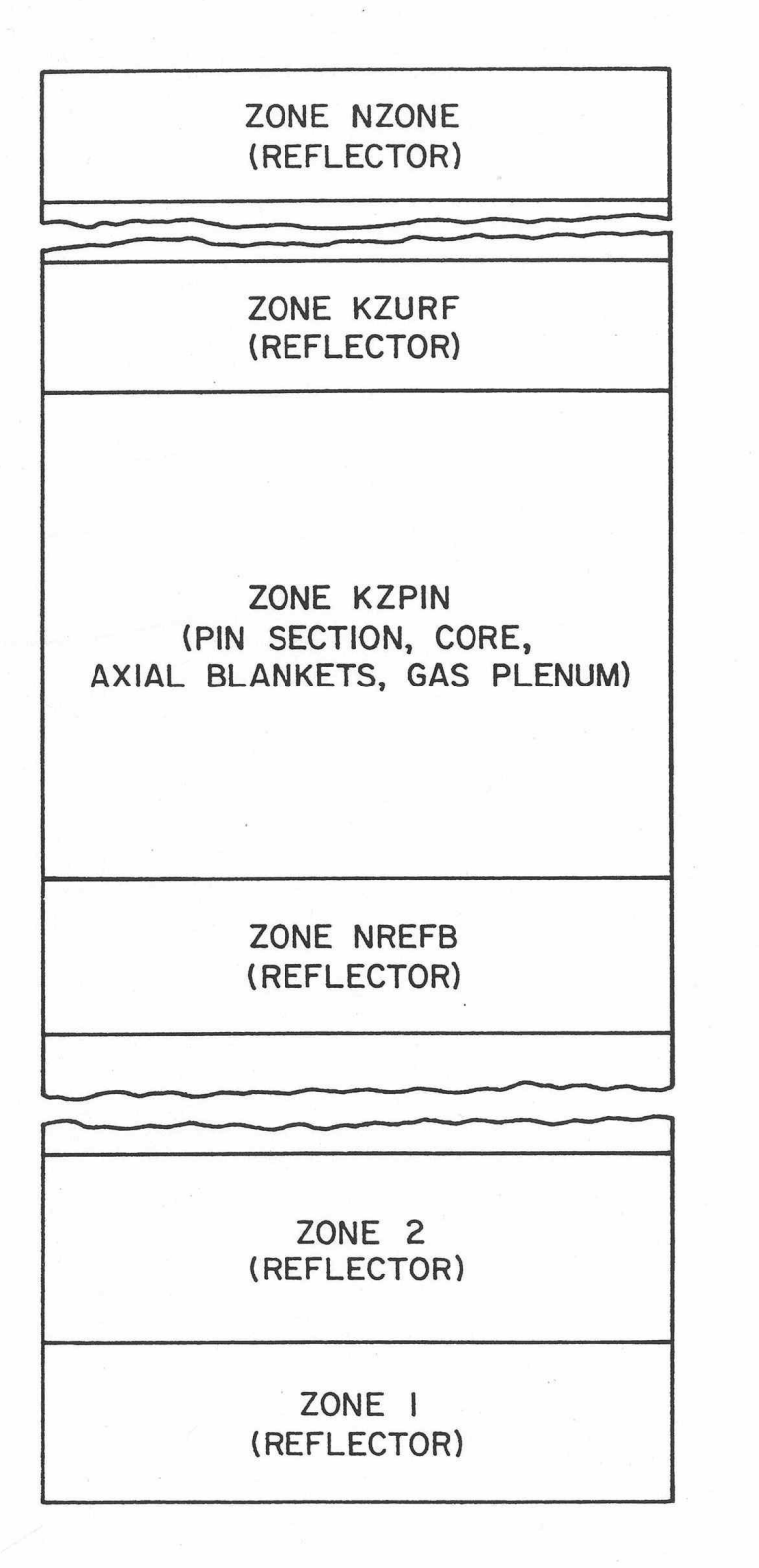

Figure 3.2-2: Axial Zones in a SASSYS-1/SAS4A Channel

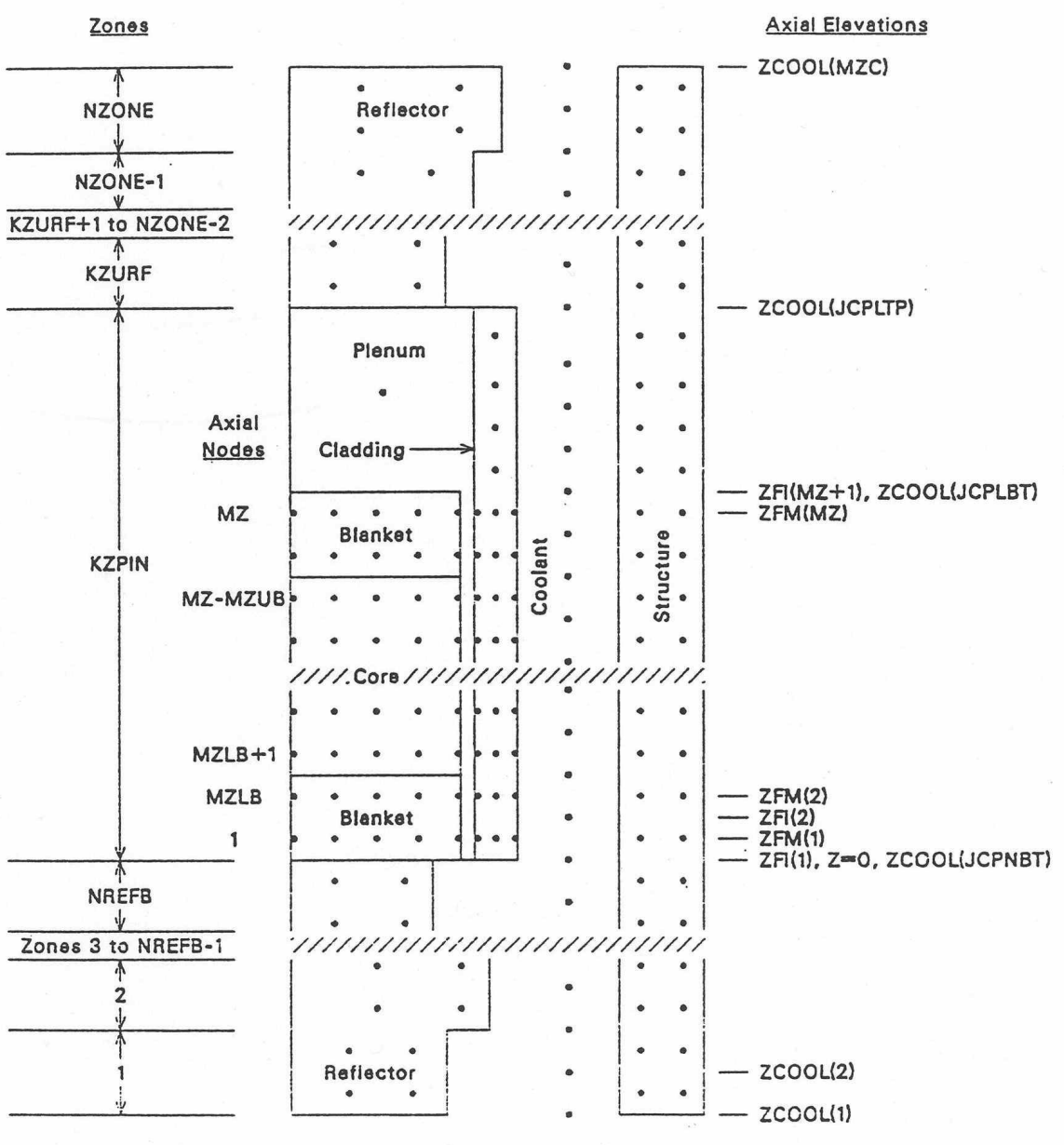

Figure 3.2-3: Schematic of SASSYS-1/SAS4A Channel Discretization

3.2.2 Radial Mesh Structure

3.2.2.1 Core and Blanket Region

Figure 3.2-4 shows the radial mesh structure used for temperature calculations in the core and blanket regions. This figure represents one axial node. Between four and eleven radial nodes are used in the fuel, three in the cladding, one in the coolant, and two in the structure. In the fuel, the nodes can be set up on either an equal radial difference basis or an equal mass basis. In either case, the first and last nodes are half-size. For a given number of nodes, an equal radial difference mesh will usually give more accurate center-line temperatures, but equal mass nodes are sometimes used to get more nodes in the outer part of the fuel, where temperature gradients are steeper. Steady-state fuel restructuring can change the node sizes. Also, during the transient calculation, the radii will move with the fuel as it expands or contracts due to temperature changes. After the steady-state initialization, the mass of fuel associated with a radial node is constant, at least until fuel-pin disruption and coupling is made to PLUTO2, PINACLE, or LEVITATE in SAS4A.

The inner fuel node is at $r = 0$ if there is no central void. Otherwise, it is at the fuel inner surface. The outer fuel node is at the fuel outer surface.

The "structure" represents each pin's share of the duct wall. A wrapper wire can be lumped in with either the cladding or the structure.

3.2.2.2 Gas Plenum Region

The radial mesh structure used in the gas plenum region is shown in Fig. 3.2-5. The plenum gas is represented by a single axial and radial node. This gas is in contact with a number of axial cladding nodes. At each axial node, there is one radial node in the cladding, one in the coolant, and two in the structure.

3.2.2.3 Reflector Regions

The radial mesh structure in an axial node in a reflector region is shown in Fig. 3.2-6. Two nodes are used in the reflector, one in the coolant, and two in the structure.

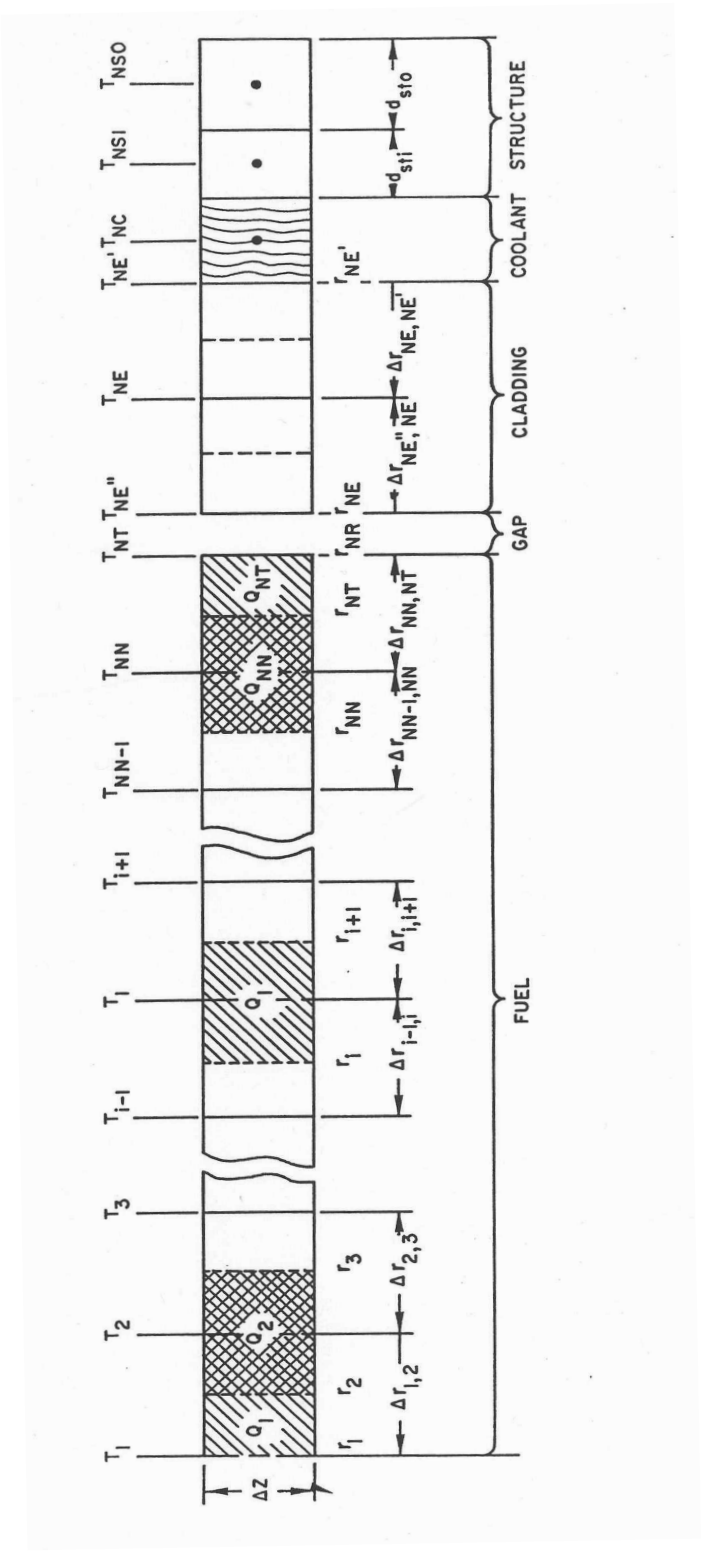

Figure 3.2-4: Radial Temperature Nodes, Core and Axial Blanket Regions

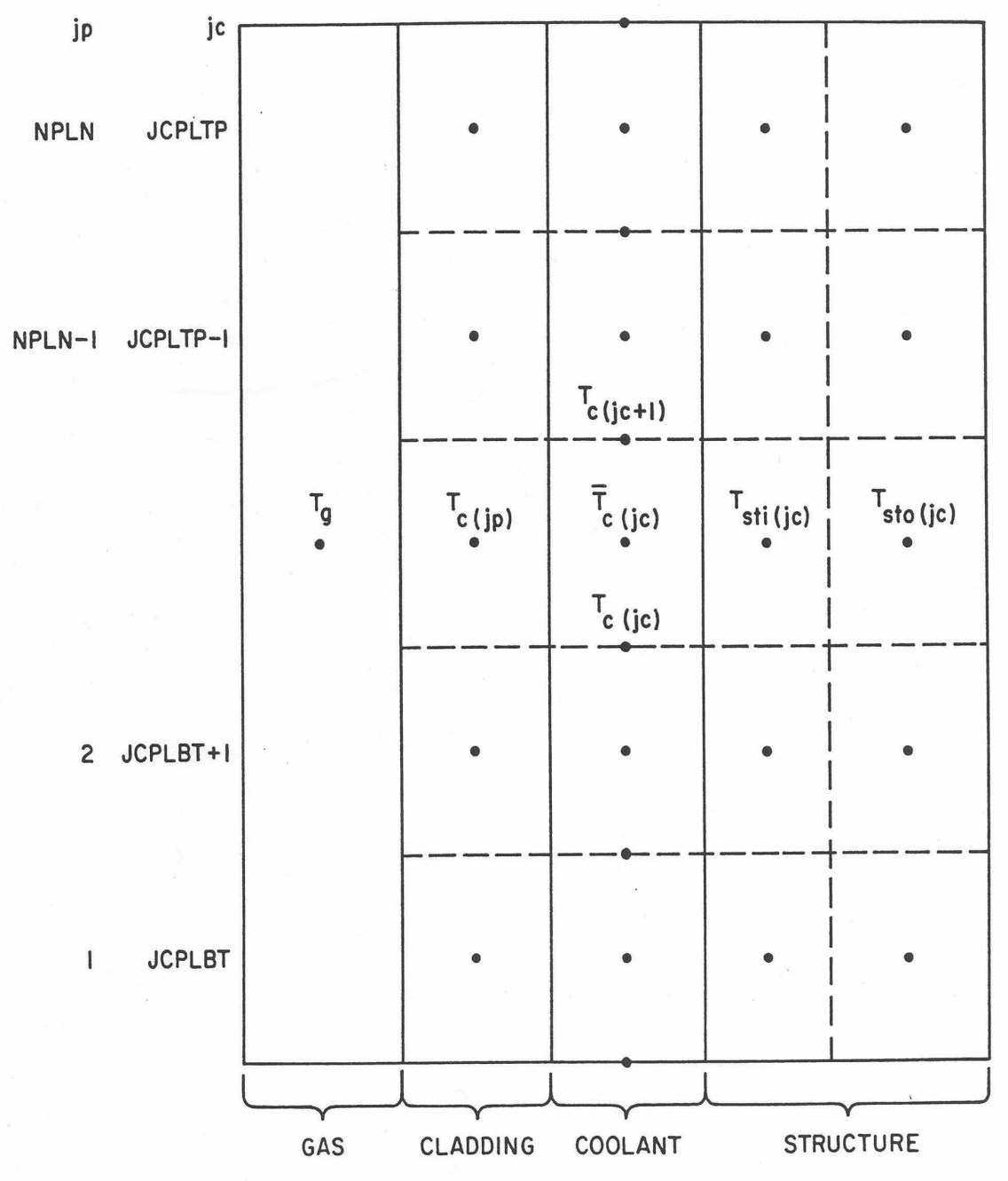

Figure 3.2-5: Radial Temperature Nodes, Gas Plenum Region

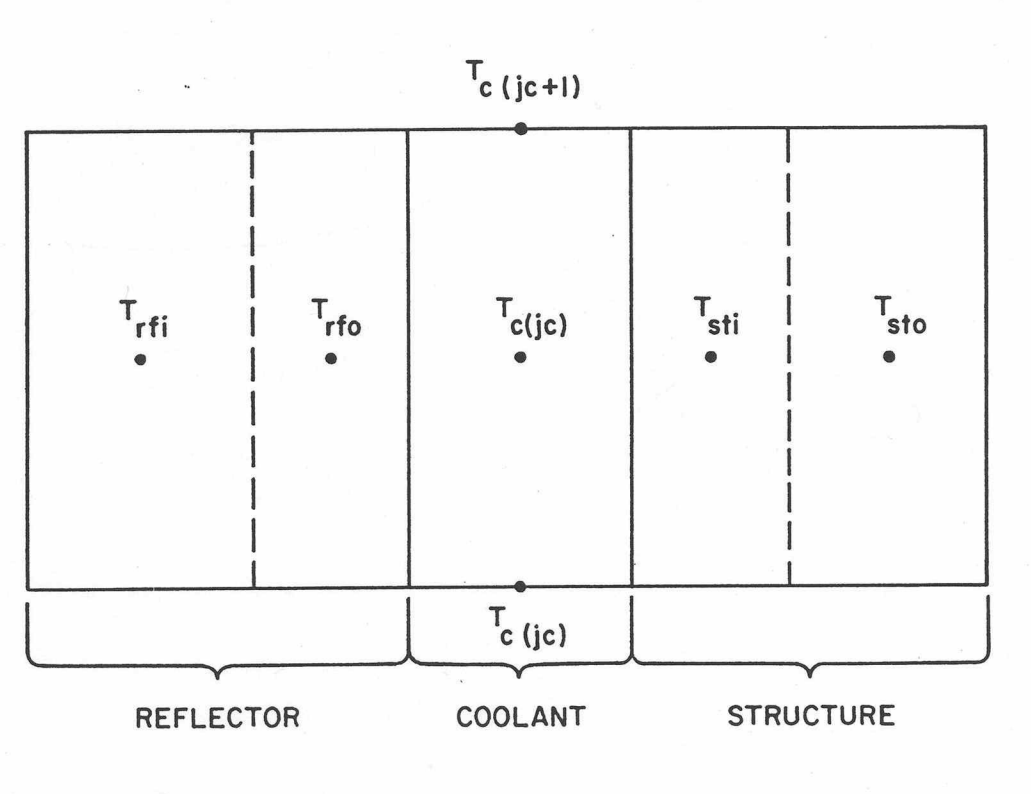

Figure 3.2-6: Radial Temperature Nodes, Reflector Region

3.3 Pre-boiling Transient Heat Transfer, Single Pin Model

The transient fuel-pin temperature calculations in SASSYS-1 and SAS4A are similar to the Crank-Nickolson scheme [3-1] used in SAS2A [3-2] and SAS3D [3-3], but there are a number of significant differences. One reason for these differences is to allow the use of larger heat-transfer time steps with less computing time per step. Another reason is to obtain greater accuracy and more precise energy balance.

In order to use very long heat-transfer time steps on one second or more in the pre-voiding phase of a very slow transient, the fuel, cladding, coolant, and structure temperatures at an axial node are computed simultaneously in non-voiding cases. Therefore, coolant temperatures are computed in the fuel-pin heat-transfer routine in the non-voiding situation.

The coupling between TSHTRN and the pre-voiding coolant dynamics routines is different from the coupling between TSHTRV and the voiding routines, although in both cases the coolant dynamics or voiding calculations are done before the fuel-pin heat-transfer calculations. In the non-voiding case, extrapolated coolant temperatures are used to obtain the temperature-dependent sodium properties used in the calculation of the coolant flow rates and heat-transfer coefficients. Then, TSHTRN uses these values to compute the coolant temperatures, and these new coolant temperatures are used in the next extrapolation. In the voiding routines, extrapolated cladding temperatures are used in the implicit calculation of the heat flux from cladding to coolant to obtain new

coolant temperatures. The voiding routines then sum the integrated heat flux from cladding to coolant at each axial node, and this integrated heat flux at the cladding surface is used as a boundary condition in TSHTRV.

TSHTRN and TSHTRV are somewhat simpler than the corresponding TSHTR in SAS3A and SAS3D. In SAS3D, TSHTR contains extraneous material related to other modules, such as initiating cladding and fuel motion; this material is not included in the SASSYS-1 and SAS4A heat-transfer routines. Also, in SAS3D, the fuel mass for each radial node of each axial node is recomputed every time step from the temperature-dependent fuel density and the node radii. In SASSYS-1 and SAS4A the node mass is computed in the steady-state module and then stored for used in the transient. This node mass is held constant until fuel relocation starts.

Another difference between the SAS3D and SASSYS-1 heat-transfer routines is in the amount of vectorization of the algorithms and the coding. Some of the calculations in the SAS3D routines happen to vectorize, but a special effort was made to vectorize many more of the calculations in the SAS4A and SASSYS-1 heat-transfer routines. On a vector machine, such as CRAY-1, vectorized coding usually runs much faster than scalar coding. Even on the IBM 3033 or the CDC 6700 computers, which are normally considered to be scalar machines, vectorizable coding tends to run faster than unvectorizable coding. In general, vectorizing involves setting up arrays so that all elements in the array are processed in the same way and so that the results of a given calculation for one element in the array do not depend on the results for any other element in the array. Vectorization is partly just a coding matter, but it also involves choosing vectorizable algorithms or adapting algorithms for vectorization.

To some extent, the descriptions in Sections 3.3.1.2 to 3.3.1.3 below reflect the emphasis on vectorization. Intermediate quantities used in the solution are usually defined as elements in arrays, and, where possible, the array elements are defined so that all of the elements in an array can be treated in the same manner in the calculations. In order to emphasize the array nature of the solution, when a new array is introduced, all of the elements in the array are defined in the same section, even though many of the elements are often not used until later sections.

As indicated above in Section 3.2.2, three different radial mesh structures are used in the heat-transfer calculations: one for the core and blanket region, one for the gas plenum region, and one for the reflector regions. Different heat-transfer calculations are done for each of these three regions.

3.3.1 Core and Axial Blankets

3.3.1.1 Basic Equations

The basic transient heat-transfer equation within the fuel and within the cladding is

$$\rho c \frac{\partial T}{\partial t} = \frac{1}{r} \frac{\partial}{\partial r} \left(kr \frac{\partial T}{\partial r} \right) + Q \qquad (3.3\text{-}1)$$

where

T = temperature

ρ = density

c = specific heat

r = radius

k = thermal conductivity

t = time

and

Q = heat source per unit volume

Melting of fuel and cladding is treated using a melting range, bounded by solidus and liquidus temperatures, T_{sol} and T_{liq}, respectively, and a heat of fusion, U_{melt}. Separate values of T_{sol}, T_{liq}, and U_{melt} are used for the fuel and cladding. In the melting range, Eq. 3.3-1 is modified and becomes

$$\rho c_m \frac{\partial T}{\partial t} = \frac{1}{r}\frac{\partial}{\partial r}\left(kr\frac{\partial T}{\partial r}\right) + Q \tag{3.3-2}$$

where

$$c_m = \frac{U_{melt}}{T_{liq} - T_{sol}} \tag{3.3-3}$$

In the actual solution of Eq. 3.3-2 for a time step, c is used instead of c_m in the calculation of the temperature change for the step. Then, if the temperatures are in the melting range, the computed temperature change is modified to account for the heat of fusion, as described in Section 3.3.5.

The heat flux, q_{fe}, from the fuel outer surface to the cladding inner surface contains both a bond gap conductance term, h_b, and a radiation term:

$$q_{fe} = h_b[T(\text{NT}) - T(\text{NT}")] + \varepsilon\sigma[T(\text{NT})^4 - T(\text{NT}")^4] \tag{3.3-4}$$

where

ϵ = thermal emissivity of the fuel

σ = Stefan=Boltzman constant

$T(\text{NT})$ = fuel outer surface temperature

and

$T(\mathrm{NE}'') =$ cladding inner surface temperature

For the coolant, the basic heat-transfer equation is

$$\rho c\ A_c \frac{\partial T}{\partial r} + \frac{\partial}{\partial r}(wcT) = (Q_c + Q_{ec} + Q_{sc})A_c \tag{3.3-5}$$

where A_c = coolant flow area. The heat, Q_c, produced directly in the coolant is computed from the fraction, γ_c, of the total energy production that goes into neutron and gamma heating of the coolant:

$$Q_c = \frac{\gamma_c \bar{P}(j)}{A_c \Delta z(j)} \tag{3.3-6}$$

where

$\bar{P}(j) =$ total heat production rate in axial node j

and

$\Delta z(j) =$ axial node height

The heat flow from the cladding to the coolant, Q_{ec} is calculated as

$$Q_{ec} = h_c\left[T(\mathrm{NE}') - T(\mathrm{NC})\right]\frac{2\pi r(\mathrm{NE}')}{A_c} \tag{3.3-7}$$

and the heat flow from structure to coolant, Q_{sc}, is calculated as

$$Q_{sc} = h_c[T(\mathrm{NSI}) - T(\mathrm{NC})]\frac{S_{st}}{A_c} \tag{3.3-8}$$

where S_{st} is the perimeter of the structure. The coolant heat-transfer coefficient, h_c, is calculated using

$$\frac{h_c D_h}{k} = c_1\left[\frac{D_h\ w\ c}{k\ A_c}\right]^{c_2} + c_3 \tag{3.3-9}$$

which is a form used in correlations for convective heat-transfer coefficients for low Prandtl number fluids, such as liquid metal [3-4]. The user supplied constants c_1, c_2, and c_3 depend on the particular correlation used.

The structure is treated with a one-dimensional heat conduction equation:

$$\rho c \frac{\partial T}{\partial t} = \frac{\partial}{\partial x}\left[k \frac{\partial T}{\partial x}\right] + Q \tag{3.3-10}$$

The treatment of the heat source, Q, in the structure is discussed in Section 3.3.1.2.8.

3.3.1.2 Finite Difference Equations

Finite differencing in both space and time is used for the transient heat-transfer calculations. The radial mesh structure is described in Section 3.2.2 above. In the equations below, the time t represents the beginning of the temp step, and Δt is the step size. The parameters θ_1 and θ_2 determine the degree of implications. For an explicit scheme, θ_1 = 1.0 and θ_2 = 0.0. For a fully implicit scheme, θ_1 = 0.0 and θ_2 = 1.0. For a semi-implicit scheme θ_1 – 0.5 and θ_2 = 0.5. The degree of implicitness is calculated by the code, based on the ratio of the time-step size, Δt, to a user-supplied time constant for fuel-pin heat transfer, τ_{ht}. As explained in Appendix 3.1, the expression used for θ_1 and θ_2 in TSHTRN are

$$\theta_2 = \frac{1.65 + x}{3.3 + x} \tag{3.3-11a}$$

where

$$x = \Delta t / \tau_{ht} \tag{3.3-11b}$$

and

$$\theta_1 = 1.0 - \theta_2 \tag{3.3-12}$$

Also, large relative changes in coolant flow rate, w, during a long heat transfer time step can lead to anomalous coolant temperature changes if the value of θ_1 is too large; therefore, θ_2 is calculated as

$$\theta_2 = \frac{|w_1|}{|w_1| + |w_2|} \tag{3.3-13}$$

if Eq. 3.3-13 gives a larger value than Eq. 3.3-11. In Eq. 3.3.13, w_1 and w_2 are the coolant flow rates at the beginning and end of the heat-transfer time step, respectively. In any case, Eq. 3.3-12 is used for θ_1.

The heat transfer time step size is limited to a relatively small value (0.02 s or less) after the onset of boiling, and so TSHTRV used $\theta_1 = \theta_2 = 0.5$.

The finite difference equations used for the fuel and for the two inner cladding nodes are the same in TSHTRN and TSHTRV. The differences between these routines start at the outer cladding node.

In general, the time derivative of a variable *y* is approximated as

$$\frac{\partial y}{\partial t} = \frac{y(t+\Delta t) - y(t)}{\Delta t} \tag{3.3-14}$$

and the spatial derivative is approximated as

$$\frac{\partial y}{\partial t} \simeq \theta_1 \left[\frac{y(t, z+\Delta z) - y(t,z)}{\Delta z}\right] + \theta_2 \left[\frac{y(t+\Delta t, z+\Delta z) - y(t+\Delta t, z)}{\Delta z}\right] \tag{3.3-15}$$

In the following sections, it will be useful to refer to Fig. 3.2-4 for the radial node structure and the definitions of the radial node indexes.

3.3.1.2.1 Fuel Inner Surface, Node 1

There is an adiabatic boundary at the fuel inner surface; so the node 1, Eq. 3.3-1 becomes

$$\begin{aligned} & m_f(1)\,\bar{c}_f(1)\left[\frac{T_2(1) - T_1(1)}{\Delta t}\right] \\ & = \frac{2\pi r(2)\Delta z(j)\bar{k}_{1,2}}{\Delta r_{1,2}}\{\theta_1[T_1(2) - T_1(1)] + \theta_2[T_2(2) - T_2(1)]\} + Q(1) \end{aligned} \tag{3.3-16}$$

where

$m_f(i)$ = fuel mass at node i

$\bar{c}(i)$ = fuel heat capacity at radial node i at $t = t_1 + \theta_2 \Delta y$

$T_2(i)$ = temperature at $t + \Delta t$

$T_1(i)$ = temperature at time t

$\Delta z(j)$ = axial mesh height

$$\Delta r(1) = 2\left[r(2) - r(1)\right] \tag{3.3-17}$$

$$\Delta r(i) = r(i+1) - r(i) \quad 2 \le i \le \mathrm{NN} \tag{3.3-18}$$

$$\Delta r(\mathrm{NT}) = 2\left[r(\mathrm{NR}) - r(\mathrm{NT})\right] \tag{3.3-19}$$

$$\Delta r(i) = \frac{[r(NE') - r(NE)]}{2} \quad i = NE'', NE, NE' \tag{3.3-20}$$

(note: NE" = NR)

$$\Delta r_{i,i+1} = \frac{\Delta r(i) + \Delta r(i+1)}{2} \; 1 \le i \le NE \tag{3.3-21}$$

$$Q(i) = \frac{\overline{P}(j)\,(1-\gamma_e-\gamma_c-\gamma_s)\,P_r(i)\,m_f(i)}{\sum_{ii=1}^{NT} P_r(ii)\,m_f(ii)} \; 1 \le i \le NT \tag{3.3-22}$$

$$Q(NE'') = \frac{\overline{P}(j)\gamma_e}{4} \tag{3.3-23}$$

$$Q(NE) = \frac{\overline{P}(j)\gamma_e}{2} \tag{3.3-24}$$

$$Q(NE') = \frac{\overline{P}(j)\gamma_e}{4} = Q(NE'') \tag{3.3-25}$$

where

$\overline{P}(j)$ = total power (watts) in axial node *j*

$P_r(i)$ = radial power shape per unit mass

and

$\gamma_e, \gamma_c, \gamma_s$ = fraction of power in direct heating of clad, coolant, and structure, respectively.

The thermal conductivity, $\overline{k}_{1,2}$ used in Eq. 3.3-16 is a weighted average of the values for the two adjacent nodes. It is calculated as

$$\overline{k}_{i,i+1} = \frac{k(i)k(i+1)\left[\Delta r(i) + \Delta r(i+1)\right]}{k(i)\Delta r(i+1) + k(i+1)\Delta r(i)} \tag{3.3-26}$$

where

$k(i)$ = thermal conductivity for radial node i, evaluated using the fuel temperature extrapolated to $t + \theta_2 \Delta t$

Equation 3.3-26 is carried over from SAS3D. The fuel restructuring algorithm used in SAS3D uses up to three different fuel types (columnar, equiaxed, and unrestructured) for the fuel at each axial node. Sharp boundaries between fuel types are used. The radial mesh is adjusted, if necessary, so that fuel-type boundaries fall on radial node boundaries. One consequence of the sharp fuel-type boundaries in SAS3D is that the fuel thermal conductivity can change significantly from one node to the next at a fuel-type boundary. The average thermal conductivity of Eq. 3.3-26 will give accurate steady-state fuel temperatures even if the thermal conductivity has large jumps at node boundaries. The fuel restructuring provided by DEFORM-IV in SAS4A is somewhat smoother than that used in SAS3D, and the node-to-node changes in thermal conductivity in SAS4A are usually smaller than the corresponding changes at fuel-type boundaries in SAS3D, so the need for special weighting of the fuel thermal conductivities in SAS4A Lis less than in SAS3D, but Eq. 3.3-26 still provides more accurate fuel temperatures than simpler weighting schemes.

Note that even though most of the variables in Eqs. 3.3-16 to 3.3-26 vary with axial node j, the subscript j has only been included for some of these variables.

3.3.1.2.2 Inner Fuel Nodes, Nodes 2 to NN

For fuel radial node I, Eq. 3.3-1 becomes

$$\begin{aligned} & m_f(i)\bar{c}_f(i)\frac{\left[T_2(i)-T_1(i)\right]}{\Delta t} \\ & = \frac{2\pi r(i+1)\Delta z(j)\bar{k}_{i,i=1}}{\Delta r_{i,i+1}}\left\{\theta_1\left[T_1(i+1)-T_1(i)\right]+\theta_2\left[T_2(i+1)-T_2(i)\right]\right\} \\ & -\frac{2\pi r(i)\Delta z(j)\bar{k}_{i-1,i}}{\Delta r_{i-1,i}}\left\{\theta_1\left[T_1(i)-T_1(i-1)\right]+\theta_2\left[T_2(i)-T_2(i-1)\right]\right\}+Q(i) \end{aligned} \qquad (3.3\text{-}27)$$

Note that the left-hand side of Eq. 3.3-27 represents the change in internal energy as node i, whereas the terms on the right-hand side represent heat conduction into node i from nodes i+1 and i-1, as well as the heat source in node i.

3.3.1.2.3 Fuel Outer Surface Node, Node NT

The heat flux q_{fc}, from the fuel outer surface to the cladding inner surface contains both a bond gap conductance and a radiation term.

$$q_{fc} = h_b\left[\,T(\mathrm{NT})-T(\mathrm{NE}'')\,\right]+\varepsilon\sigma\left[\,T(\mathrm{NT})^4-T(\mathrm{NE}'')^4\,\right] \qquad (3.3\text{-}28)$$

where

h_b = bond conductance

ε = thermal emissivity of the fuel

and

σ = Stefan-Boltzmann constant.

The T^4 terms are rewritten as

$$T(\mathrm{NT})^4 - T(\mathrm{NE}'')^4 = h_r \left[T(\mathrm{NT}) - T(\mathrm{NE}'')\right] \tag{3.3-29}$$

where

$$h_r = \frac{T_1(\mathrm{NT})^4 - T_1(\mathrm{NE}'')^4}{T_1(\mathrm{NT}) - T_1(\mathrm{NE}'')} = [T_1(\mathrm{NT}) + T_1(\mathrm{NE}'')][T_1(\mathrm{NT})^2 + T_1(\mathrm{NE}'')^2] \tag{3.3-30}$$

The approximation is then made that h_r is a constant for a time step, and the equation for node NT becomes

$$\begin{aligned} m_f(\mathrm{NT})\bar{c}_f(\mathrm{NT})\ & \frac{T_2(\mathrm{NT}) - T_1(\mathrm{NT})}{\Delta t} \\ &= \frac{2\pi r(\mathrm{NT})\Delta z(j)\bar{k}_{\mathrm{NN,NT}}}{\Delta r_{\mathrm{NN,NT}}}\{\theta_1[T_1(\mathrm{NN}) - T_1(\mathrm{NT})] \\ &+ \theta_2[T_2(\mathrm{NN}) - T_2(\mathrm{NT})]\}\, 2\pi r(\mathrm{NR})\Delta z(j)[h_b \\ &+ \epsilon\sigma h_r]\,\{\theta_1[T_1(\mathrm{NE}'') - T_1(\mathrm{NT})] + \theta_2[T_2(\mathrm{NE}'') \\ &- T_2(\mathrm{NT})]\} + Q(\mathrm{NT}) \end{aligned} \tag{3.3-31}$$

3.3.1.2.4 Cladding Inner Node, Node NE″

For the cladding inner node, Eq. 3.3-1 becomes

$$\frac{m_e c_e}{4}\frac{T_2(\mathrm{NE}'')-T_1(\mathrm{NE}'')}{\Delta t} = \frac{2\pi\Delta z(j)\bar{r}_{NE}\,k_{NE'',NE}}{\Delta r_{NE'',NE}}\left\{\theta_1\left[T_1(\mathrm{NE})-T_1(\mathrm{NE}'')\right]+\theta_2\left[T_2(\mathrm{NE})-T_2(\mathrm{NE}'')\right]\right\} - 2\pi r(\mathrm{NR})\Delta z(j)\left(h_b+\varepsilon\sigma h_r\right)\left\{\theta_1\left[T_1(\mathrm{NE}'')-T_1(\mathrm{NT})\right] + \theta_2\left[T_2(\mathrm{NE}'')-T_2(\mathrm{NT})\right]\right\}+Q(\mathrm{NE}'') \tag{3.3-32}$$

where

c_e = cladding heat capacity

$\mathrm{m_e}$ = cladding mass $= 2\pi\rho_e[r(\mathrm{NE}')^2 - r(\mathrm{NE})^2]\Delta z(j)$ (3.3-33)

ρ_e = cladding density

and

$$\bar{r}_{NE} = r(\mathrm{NE})+\tfrac{1}{4}\left[r(\mathrm{NE}')-r(\mathrm{NE})\right] \tag{3.3-34}$$

Note that the factors of 4 in Eqs. 3.3-32 and 3.3-34 come about because the inner cladding node represents one fourth of the thickness of the cladding.

3.3.1.2.5 Cladding Mid-point, Node NE

For the cladding mid-point node, Eq. 3.3-1 becomes

$$\frac{n_e c_e}{2}\frac{T_2(\mathrm{NE})-T_1(\mathrm{NE})}{\Delta t} = \frac{2\pi\bar{r}_{\mathrm{NE}'}\Delta z(j)\bar{k}_{\mathrm{NE,NE}'}}{\Delta r_{\mathrm{NE,NE}'}}\{\theta_1[T_1(\mathrm{NE}')-T_1(\mathrm{NE})]+\theta_2[T_2(\mathrm{NE}') - T_2(\mathrm{NE})]\} - \frac{2\pi\bar{r}_{\mathrm{NE}}\Delta z(j)\bar{k}_{\mathrm{NE'',NE}}}{\Delta r_{\mathrm{NE'',NE}}}\{\theta_1[T_1(\mathrm{NE})-T_1(\mathrm{NE}'')] + \theta_2[T_2(\mathrm{NE})-T_2(NE'')]\}+Q(\mathrm{NE}) \tag{3.3-35}$$

where

$$\bar{r}_{NE'} = r(\mathrm{NE}) + \tfrac{3}{4}\left[r(\mathrm{NE}') - r(\mathrm{NE})\right] \tag{3.3-36}$$

3.3.1.2.6 Cladding Outer Node, Node NE′

The out cladding node transfers heat to both the cladding mid-point node and the coolant node, so the equation for the outer cladding node temperature is

$$\begin{aligned}
&\frac{m_e c_e}{4}\frac{T_2(\mathrm{NE}') - T_1(\mathrm{NE}')}{\Delta t} \\
&\quad = -\frac{2\pi \bar{r}_{\mathrm{NE}'}\Delta z(j)\bar{k}_{\mathrm{NE,NE}'}}{\bar{r}_{\mathrm{NE,NE}'}}\left\{\theta_1\left[T_1(\mathrm{NE}') - T_1(\mathrm{NE})\right]\right. \\
&\quad + \left.\theta_2\left[T_2(\mathrm{NE}') - T_2(\mathrm{NE})\right]\right\} \\
&\quad + 2\pi r(\mathrm{NE}')\Delta z(j)\left\{\theta_1 h_{c1}(j)[T_1(\mathrm{NC}) - T_1(\mathrm{NE}')]\right. \\
&\quad + \left.\theta_2 h_{c2}(j)[T_2(\mathrm{NC}) - T_2(\mathrm{NE}')]\right\} + Q(\mathrm{NE}')
\end{aligned} \tag{3.3-37}$$

Note that $T(\mathrm{NC}) = \bar{T}_c(jc)$. Also, hc_1 and hc_2 are the coolant heat-transfer coefficients at t and $t + \Delta t$ as calculated from Eq. 3.3-9,

3.3.1.2.7 Coolant, Node NC

Coolant temperatures are calculated for the whole length of the subassembly, whereas fuel temperatures are computed in the core and blankets only. Therefore, the axial coolant node mesh extends beyond the fuel mesh; and the coolant axial node index, *jc*, is related to the fuel axial node index, *j*, by

$$jc = j + j_{cblbt} - 1 \tag{3.3-38}$$

where j_{cblbt} is the coolant node at the bottom of the lower blanket. In the $T_1(i,j)$ and $T_2(i,j)$ arrays, the coolant node corresponds to

$$T_2(\mathrm{NC}, j) = \bar{T}_c(jc) \tag{3.3-39}$$

In the non-voiding case, the coolant flow is usually upward. In such a situation, the transient calculation for a time step starts at the subassembly inlet and works upward through the lower reflector zones, through the pin section, and finally through the

upper reflector zones. The codes can also handle downward coolant flow during the transient, although the initial steady-state coolant flows must all be upward. In the downward situation, the calculation starts at the top of the subassembly and works down to the inlet.

In the core and blanket regions, Eq. 3.3-5 becomes

$$\begin{aligned}
&\bar{\rho}_c(jc)\bar{c}_c(jc)\frac{T_2(\mathrm{NC})-T_1(\mathrm{NC})}{\Delta t}+\frac{2\bar{c}_c(jc)}{\Delta z(j)A_c(jc)}\Big\{\theta_1|w_1|\left[T_1(\mathrm{NC})-T_1'\right]\\
&\quad+\theta_2|w_2|\left[T_2(\mathrm{NC})-T_2'\right]\Big\}=\frac{Q(\mathrm{NC})}{A_c(jc)\Delta z(j)}+\frac{2\pi r(\mathrm{NE'})}{A_c(jc)}\\
&\quad\Big\{\theta_1 h_{c1}(j)\left[T_1(\mathrm{NE'})-T_1(\mathrm{NC})\right]+\theta_2 h_{c2}(j)\ \left[T_2(\mathrm{NE'})-T_2(\mathrm{NE})\right]\Big\}\\
&\quad+\frac{S_{pr}}{A_c(jc)}\Big\{\theta_1 H_{sic1}(jc)\ \left[T_1(\mathrm{NSI})-T_1(\mathrm{NC})\right]\\
&\quad+\theta_2 H_{sic2}(jc)\left[T_2(\mathrm{NSI})-T_2(\mathrm{NC})\right]\Big\}
\end{aligned}\tag{3.3-40}$$

where

S_{pr} = structure perimeter

w_1 and w_2 = the coolant mass flow rates (kg/s) at t and $t+\Delta t$

NSI = the inner structure node

$$T_1'=\begin{cases}T_{c1}(jc) & \text{if } w_1\geq 0\\ T_c(jc+1) & \text{if } \mathrm{w}_1<0\end{cases}\tag{3.3-41a-b}$$

$$T_2'=\begin{cases}T_{c2}(jc) & \text{if } w_2\geq 0\\ T_{c2}(jc+1) & \text{if } \mathrm{w}_2<0\end{cases}\tag{3.3-42a-b}$$

and

$\mathrm{H_{sic}}$ = the heat-transfer coefficient from the structure inner node to the coolant

$$H_{sic}=\frac{2h_c\ k_{si}}{2k_{si}+h_c d_{sti}}\tag{3.3-43}$$

Note that Eq. 3.3-43 is obtained by adding thermal resistance in series:

$$\frac{1}{H_{sic}} = \frac{1}{h_c} + \frac{d_{sti}}{2k_{si}} \tag{3.3-44}$$

3.3.1.2.8 Structure Inner Node, Node NSI

In the core and blanket regions,

$$\begin{aligned}(\rho c)_{sti}\, d_{sti} \frac{T_2(\mathrm{NSI}) - T_1(\mathrm{NSI})}{\Delta t} &= \theta_1 H_{sic1}(jc)\left[T_1(\mathrm{NC}) - T_1(\mathrm{NSI})\right] \\ &+ \theta_2 H_{sic2}(jc)\left[T_2(\mathrm{NC}) - T_2(\mathrm{NSI})\right] \\ &+ H_{stio}(jc)\{\ \theta_1\ \left[T_1(\mathrm{NSO}) - T_1(\mathrm{NSI})\right] \\ &+ \theta_2\left[T_2(\mathrm{NSO}) - T_2(\mathrm{NSI})\right]\} + Q_{st}\frac{d_{sti}}{d_{sti} + d_{sto}}\end{aligned} \tag{3.3-45}$$

where

NSO = outer structure node

d_{sti} = thickness of inner structure node

d_{sto} = thickness of outer structure node

$$H_{stio} = \frac{2k_{si}k_{so}}{d_{sti}k_{so} + d_{sto}k_{si}} \tag{3.3-46}$$

k_{si} = thermal conductivity of the inner structure node

k_{so} = thermal conductivity of the outer structure node

and

Q_{st} = direct heating source in the structure.

The left-hand side of Eq. 3.3-45 represents the change in internal energy in the node. The terms on the right-hand side represent heat flow from the coolant and the outer structure node, as well as direct heating of the structure by neutrons and gamma rays. It is assumed that the direct heating source is divided between the inner and outer nodes in proportion to their thicknesses.

3.3.1.2.9 Structure Outer Node, Node NSO

In the core and blankets,

$$(\rho c)_{sto} d_{sto} \frac{T_2(\text{NSO}) - T_1(\text{NSO})}{\Delta t}$$

$$= H_{stio}(jc)\{\theta_1[T_1(\text{NSI}) - T_1(\text{NSO})]$$

$$+ \theta_2[T_2(\text{NSI}) - T_2(\text{NSO})]\} + Q_{st}(jc)\frac{d_{sto}}{d_{sti} + d_{sto}} \qquad (3.3\text{-}47)$$

$$+ Q_{chch}(jc)$$

where

$Q_{chch} =$ subassembly-to-subassembly heat transfer heat flux

The values used for Q_{chch} are discussed in Section 3.11.

3.3.1.2.10 Solution of Finite Difference Equations

Equations 3.3-16, 3.3-27, 3.3-31, 3.3-32, 3.3-35, 3.3-37, 3.3-40, 3.3-45, and 3.3-47 can be written in matrix form, yielding a tri-diagonal matrix of the form

$$\begin{bmatrix} \alpha_1+\beta_1 & -\beta_1 & 0 & 0 & \cdots \\ -\beta_1 & \alpha_2+\beta_1+\beta_2 & -\beta_2 & 0 & \cdots \\ 0 & -\beta_2 & \alpha_3+\beta_2+\beta_3 & -\beta_2 & \cdots \\ & \ddots & & & \\ & & & & \\ & & & & \\ & & & & \\ & & & & \\ & & & & \\ 0 & \cdots 0 & -\beta_{\text{NC}} & \alpha_{\text{NSI}}+\beta_{\text{NC}}+\beta_{\text{NSI}} & -\beta_{\text{NSI}} \\ 0 & \cdots & 0 & -\beta_{\text{NSI}} & \alpha_{\text{NSO}}+\beta_{\text{NSI}}+\beta_{\text{NSO}} \end{bmatrix} \begin{bmatrix} T_2(1) \\ T_2(2) \\ T_2(3) \\ \\ \\ \\ \\ \\ \\ T_2(\text{NSI}) \\ T_2(\text{NSO}) \end{bmatrix} = \begin{bmatrix} D_1 \\ D_2 \\ D_3 \\ \\ \\ \\ \\ \\ \\ D_{\text{NSI}} \\ D_{\text{NSO}} \end{bmatrix}$$

(3.3-48)

where

$$\alpha_1 = \frac{\text{M}_\text{f}(i)\bar{c}_f(i)}{2\pi\Delta z(j)} \quad \text{for } i = 1,\ldots NT \qquad (3.3\text{-}49a)$$

$$\alpha_{NE''} = \frac{\text{M}_\text{e}c_e}{8\pi\Delta z(j)} \qquad (3.3\text{-}49b)$$

$$\alpha_{NE} = \frac{\mathrm{M_e} c_e}{4\pi\Delta z(j)} = 2\alpha_{NE''} \tag{3.3-49c}$$

$$\alpha_{NE'} = \alpha_{NE''} \tag{3.3-49d}$$

$$\alpha_{NC} = \frac{\bar{\rho}_c(\mathrm{jc})\bar{\mathrm{c}}_c(\mathrm{jc})\mathrm{A_c(jc)}}{2\pi} + \frac{\bar{c}_c(jc)}{\pi\Delta z(jc)}\,\theta_2\,|w_2|\,\Delta t \tag{3.3-49e}$$

$$\alpha_{NSI} = \frac{(\rho\mathrm{c})_{\mathrm{sti}}\,\mathrm{d_{sti}S_{pr}}}{2\pi} \tag{3.3-49f}$$

$$\alpha_{NSO} = \frac{(\rho\mathrm{c})_{\mathrm{sto}}\,\mathrm{d_{sto}S_{pr}}}{2\pi} \tag{3.3-49g}$$

$$\beta_i = \frac{r(i+1)\bar{k}_{i,i+1}}{\Delta r_{i,i+1}}\,\theta_2\,\Delta t \quad \text{for } i = 1,\ldots NN \tag{3.3-50a}$$

$$\beta_{NT} = r(NR)\,\theta_2\left[h_b + \varepsilon\sigma h_r\right]\Delta t \tag{3.3-50b}$$

$$\beta_{NE''} = \frac{\bar{r}_{\mathrm{NE}}\,\bar{k}_{\mathrm{NE''},\mathrm{NE}}}{\Delta r_{\mathrm{NE''},\mathrm{NE}}}\theta_2\Delta t \tag{3.3-50c}$$

$$\beta_{NE} = \frac{\bar{r}_{\mathrm{NE'}}\,\bar{k}_{\mathrm{NE},\mathrm{NE'}}}{\Delta r_{\mathrm{NE},\mathrm{NE'}}}\theta_2\Delta t \tag{3.3-50d}$$

$$\beta_{\mathrm{NE'}} = r_{\mathrm{NE'}}\,h_{c2}(j)\theta_2\Delta t \tag{3.3-50e}$$

$$\beta_{\mathrm{NC}} = \frac{S_{pr}}{2\,\pi}H_{\mathrm{sic2}}(jc)\;\theta_2\Delta t \tag{3.3-50f}$$

$$\beta_{\mathrm{NSI}} = \frac{S_{pr}}{2\,\pi}H_{\mathrm{stio}}(jc)\;\theta_2\Delta t \tag{3.3-50g}$$

$$\beta_{\mathrm{NSO}} = 0 \tag{3.3-50h}$$

$$D_1 = T_1(1)\left[\alpha_1 - \frac{\theta_1}{\theta_2}\beta_1\right] + \frac{\theta_1}{\theta_2}\beta_1 T_1(2) + \psi_1 \tag{3.3-51a}$$

$$\begin{aligned} D_i = {} & \frac{\theta_1}{\theta_2}\beta_{i-1}T_1(i-1) + T_1(i)\left[\alpha_1 - \frac{\theta_1}{\theta_2}(\beta_{i-1}+\beta_i)\right] \\ & + \frac{\theta_1}{\theta_2}\beta_i T_1(i+1) + \psi_1 \quad \text{for } i = 2,\ldots,NSI \end{aligned} \tag{3.3-51b}$$

$$D_{\mathrm{NSO}} = \frac{\theta_1}{\theta_2}\beta_{NSI}T_1(\mathrm{NSI}) + T_1(\mathrm{NSO})\left[\alpha_{\mathrm{NSO}} - \frac{\theta_1}{\theta_2}(\beta_{\mathrm{NSI}} + \beta_{\mathrm{NSO}})\right] + \psi_{\mathrm{NSO}} \tag{3.3-51c}$$

$$\psi_i = \frac{\mathrm{Q(i)}\Delta\mathrm{t}}{2\pi\Delta z(j)} \text{ for } i = 1,\ldots,\mathrm{NE'} \tag{3.3-52a}$$

$$\psi_{NC} = \frac{\mathrm{Q(NC)}\Delta t}{2\pi\Delta z(j)} + \frac{\bar{c}_c(jc)\Delta t}{\pi\Delta z(j)}\left[\theta_1|w_1|T_1' + \theta_2|w_2|T_2'\right] \tag{3.3-52b}$$

$$\psi_{NSI} = \frac{Q(\mathrm{NSI})\Delta t}{2\pi\Delta z(j)} \tag{3.3-52c}$$

and

$$\psi_{NSO} = \frac{\mathrm{Q(NSO)}\Delta t}{2\pi\Delta z(j)} + \frac{S_{pr}}{2\pi}\mathrm{Q_{chch}}\Delta\mathrm{T} \tag{3.3-52d}$$

In these equations the α array is related to heat capacity, the β array is related to heat transfer between adjacent nodes, and the ψ array is related to the heat source.

The matrix equations 3.3-49 are solved by Gaussian elimination. First arrays A_i and S_i are defined:

$$A_1 = \alpha_1 + \beta_1 \tag{3.3-53a}$$

$$A_i = \alpha_i + \beta_i + \beta_{i=1} - \frac{\beta_{i-1}^2}{A_{i-1}} \quad \text{for } i = 2,..., \text{NSO} \tag{3.3-53b}$$

$$S_1 = D_1 \tag{3.3-54a}$$

and

$$S_i = D_i + \frac{\beta_{i-1} S_{i-1}}{A_{i-1}} \quad \text{for } i = 2,..., \text{NSO} \tag{3.3-54b}$$

Then,

$$T_2(\text{NSO}) = \frac{S_{\text{NSO}}}{A_{\text{NSO}}} \tag{3.3-55a}$$

and

$$T_2(i) = S_i + \frac{\beta_i}{A_i} T_2(i+1) \quad \text{for } i = \text{NSI, NC},..., 1 \tag{3.3-55b}$$

3.3.2 Reflector Zones

In reflector zones, a two-node slab geometry treatment is used at each axial node for heat transfer to the "reflector". The reflector represents any material in the subassembly outside the pin section.

Typically, this material includes shield orifice blocks near the subassembly inlet, and instrumentation in the upper part of the subassembly. Usually, this material does not come to the form of either pure slabs or pure cylinders, and so any simple geometrical treatment of it will be only an approximation. The best that one is likely to do with a simple heat-transfer calculation is to use a slab calculation with parameters chosen to match total heat capacity, total heat-transfer surface area, and the approximate effective thickness of the material.

3.3.2.1 Basic Equations

The basic equations used for coolant and structure temperatures in reflector zones are the same as Eqs. 3.3-5 and 3.3-10 used in the core and blanket regions, except that no heat generation is considered in the reflector zones. Therefore, the Q_c, term of Eq. 3.3-5 and the Q term of Eq. 3.3-10 are eliminated in the reflector zones. The reflector is treated with a one-dimensional heat conduction equation that is the same as the one used for the structure, except that the thermal properties ρ, c, and k used for the reflector can be different from those used for the structure.

3.3.2.2 Finite Difference Equations

Figure 3.2-6 shows the radial mesh structures used for an axial node in a reflector region.

3.3.2.2.1 Reflector Inner Node

Equation 3.3-10 becomes

$$(\rho c)_r d_{ri} \frac{T_{ri2}(jc) - T_{ri1}(jc)}{\Delta t} = H_{rio}(jc)\{\theta_1[T_{ro1}(jc) - T_{ri1}(jc)] + \theta_2[T_{ro2}(jc) - T_{ri2}(jc)]\} \quad (3.3\text{-}56)$$

where

$(\rho c)_r$ = density times specific heat of the reflector

d_{ri} = thickness of inner node

T_{ri1}, T_{ri2} = reflector inner node temperature at the beginning and end of the time step

T_{ro1}, T_{ro2} = reflector outer node temperature at the beginning and end of the time step

d_{ro} = thickness of outer reflector node

and

$$H_{rio} = \frac{2k_r}{d_{ri} + d_{ro}} \quad (3.3\text{-}57)$$

Equation 3.3-57 is obtained by adding thermal resistances in series:

$$\frac{1}{H_{rio}} = \frac{d_{ri}}{2k_r} + \frac{d_{ro}}{2k_r} \quad (3.3\text{-}58)$$

Equation 3.3-56 is similar to Eq. 3.3-47 for the outer structure node, except there is no direct heating source in the reflectors.

3.3.2.2.2 Reflector Outer Node

The equation for the reflector outer node temperature is similar to Eq. 3.3-45 for the structure inner node:

$$
\begin{aligned}
&(\rho c)_r\, d_{ro}\, \frac{T_{ro2}(jc)-T_{ro1}(jc)}{\Delta t} \\
&\quad = \theta_1 H_{erc1}(jc)\left[\bar{T}_{c1}(jc)-T_{r01}(jc)\right]+\theta_2 H_{erc2}(jc)\left[\bar{T}_{c2}(jc)-T_{r02}(jc)\right] \\
&\quad + H_{rio}(jc)\left\{\theta_1\left[T_{ri1}(jc)-T_{ro1}(jc)\right]+\theta_2\left[T_{ri2}(jc)-T_{ro2}(jc)\right]\right\}
\end{aligned}
\tag{3.3-59}
$$

where

$$
H_{erc} = \frac{h_c k_r}{k_r + \frac{h_c d_{ro}}{2}} \tag{3.3-60}
$$

Note that

$$
\bar{T}_c(jc) = \left[T_c(jc) + T_c(jc+1)\right]/2 \tag{3.3-61}
$$

3.3.2.2.3 Coolant Node

In the reflector zones and in the gas plenum, Eq. 3.3-5 becomes

$$
\begin{aligned}
&\bar{\rho}_c(jc)\bar{c}_c(jc)\frac{\bar{T}_{c2}(jc)-T_{c1}(jc)}{\Delta t}+\frac{2\bar{c}_c(jc)}{\Delta z(jc)A_c(jc)}\left\{\theta_1|w_1|\left[\bar{T}_c(jc)-T_1'\right]\right. \\
&\quad \left.+\theta_2|w_2|\left[\bar{T}_{c2}(jc)-T_2'\right]\right\} \\
&\quad = \frac{S_{er}(KZ)}{A_c(jc)}\left\{\theta_1 H_{erc1}\left[T_{er1}(jc)-T_{c1}(jc)\right]\right. \\
&\quad \left.+\theta_2 H_{erc2}\left[T_{er2}(jc)-\bar{T}_{c2}(jc)\right]\right\}+\frac{S_{pr}}{A_c(jc)}\left\{\theta_1 H_{sic1}\left[T_{ri1}(jc)\right.\right. \\
&\quad \left.\left.-T_{c1}(jc)\right]+\theta_2\, H_{sci2}(jc)\left[T_{sti2}(jc)-\bar{T}_{c2}(jc)\right]\right\}
\end{aligned}
\tag{3.3-62}
$$

where, in reflector zones,

T_{er1} = T_{rol}

T_{er2} = T_{ro2}

S_{er} = Sr = reflector perimeter

S_{pr} = structure perimeter

and

T_{sti} = structure inner node temperature

3.3.2.2.4 Structure Nodes

The finite difference approximation to Eq. 3.3-10 for the structure nodes is the same as in the core and blanket regions. Equations 3.3-45 and 3.3-47 are used, except that Q_{st} is zero outside the core and blankets.

3.3.2.3 Solution of Finite Difference Equations

$$\begin{bmatrix} \alpha_1+\beta_1 & -\beta_1 & 0 & 0 & 0 \\ -\beta_1 & \alpha_2+\beta_1+\beta_2 & -\beta_2 & 0 & 0 \\ 0 & -\beta_2 & \alpha_3+\beta_2+\beta_3 & -\beta_3 & 0 \\ 0 & 0 & -\beta_3 & \alpha_4+\beta_3+\beta_4 & -\beta_4 \\ 0 & 0 & 0 & -\beta_4 & \alpha_5+\beta_4+\beta_5 \end{bmatrix} \begin{bmatrix} T_{ri2} \\ T_{ro2} \\ \overline{T}_{c2} \\ T_{Sti2} \\ T_{St02} \end{bmatrix} = \begin{bmatrix} D_1 \\ D_2 \\ D_3 \\ D_4 \\ D_5 \end{bmatrix} \tag{3.3-63}$$

where

$$\alpha_1 = (\rho c)_r \, d_{ri} S_{er}(\mathrm{KZ}) \tag{3.3-64a}$$

$$\alpha_2 = (\rho c)_r \, d_{ro} S_{er}(\mathrm{KZ}) \tag{3.3-64b}$$

$$\alpha_3 = \overline{\rho}_c \, \overline{c}_e \, A_c + 2 \, \overline{c}_c \, \theta_2 |w_2| \Delta t \tag{3.3-64c}$$

$$\alpha_4 = (\rho c)_{sti} \, d_{sti} S_{pr} \tag{3.3-64d}$$

$$\alpha_5 = (\rho c)_{sto} \, d_{sto} S_{pr} \tag{3.3-64e}$$

$$\beta_1 = \theta_2 H_{rio}(jc) S_{er} \Delta t \tag{3.3-65a}$$

$$\beta_2 = \theta_2 H_{erc2}(jc) S_{er} \Delta t \tag{3.3-65b}$$

$$\beta_3 = \theta_2 H_{sic2}(jc) S_{pr} \Delta t \tag{3.3-65c}$$

$$\beta_4 = \theta_2 H_{stio}(jc) S_{pr} \Delta t \tag{3.3-65d}$$

$$\beta_5 = \theta \tag{3.3-65e}$$

$$D_1 = T_{ri1}\left[\alpha_1 - \frac{\theta_1}{\theta_2}\beta_1\right] + \frac{\theta_1}{\theta_2}\beta_1\, T_{ro1} \tag{3.3-66a}$$

$$D_i = \frac{\theta_1}{\theta_2}\beta_{i-1}\, T_1''(i-1) + T_1''(i)\left[\alpha_1 - \frac{\theta_1}{\theta_2}(\beta_{i-1} + \beta_1)\right] + \frac{\theta_1}{\theta_2}\beta_i\, T_1''(i+1) \quad \text{for } i = 2, 4 \tag{3.3-66b}$$

$$D_3 = \frac{\theta_1}{\theta_2}\beta_2\, T_1''(2) + T_1''(3)\left[\alpha_3 - \frac{\theta_1}{\theta_2}(\beta_2 + \beta_3)\right] + \frac{\theta_1}{\theta_2}\beta_3\, T_1''(4) + 2\frac{\bar{c}_c \Delta t}{\Delta z}\left[\theta_1 |w_1|\, T_1' + \theta_2 |w_2| T_2'\right] \tag{3.3-66c}$$

$$D_5 = \frac{\theta_1}{\theta_2}\beta_4\, T_1''(4) + T_1''(5)\left[\alpha_5 - \frac{\theta_1}{\theta_2}(\beta_4 + \beta_5)\right] + S_{pr}\, Q_{chch}\Delta t \tag{3.3-66d}$$

$$T_1''(1) = T_{ri1}(jc) \tag{3.3-67a}$$

$$T_1''(2) = T_{ro1}(jc) \tag{3.3-67b}$$

$$T_1''(3) = \bar{T}_{c1}(jc) \tag{3.3-67c}$$

$$T_1''(4) = T_{sti1}(jc) \tag{3.3-67d}$$

and

$$T_1''(5) = T_{sto1}(jc) \tag{3.3-67e}$$

This tri-diagonal matrix is solved in the same manner as in Section 3.3.1.3 above.

3.3.3 Gas Plenum Region

In the gas plenum region, a single gas node is in contact with all axial cladding nodes. A single radial node is used in the cladding, as indicated in Fig. 3.2-5.

3.3.3.1 Basic Equations

The basic equations used in the cladding, coolant, and structure in the gas plenum region are the same as those used in the core and blankets, except that there is no heat source term outside of the core and blankets. The gas is assumed to transfer heat only to the cladding, and the basic equation used for the gas temperature is

$$\left(z_{pt}-z_{pb}\right)\left(\rho c\right)_g A_g \frac{dT_g}{dt} = 2\pi r_{brp} H_{eg} \int_{z_{pb}}^{z_{pt}} \left(T_e - T_g\right) dz \tag{3.3-68}$$

where

z_{pb} = elevation at the bottom of the gas plenum

z_{pt} = elevation at the top of the gas plenum

$(\rho c)_g$ = density times specific heat for the plenum gas

A_g = cross sectional area of the gas plenum

$$A_g = \pi\, r^2_{brp} \tag{3.3-69}$$

r_{brp} = cladding inner radius in the gas plenum region

T_g = gas temperature

H_{eg} = heat-transfer coefficient from the plenum gas to the cladding node

T_e = cladding temperature

3.3.3.2 Finite Difference Equations

3.3.3.2.1 Gas Plenum

Equation 3.3-69 becomes

$$\left(\rho c\right)_g A_g \frac{\left(T_{g2}-T_{g1}\right)}{\Delta t} = 2\pi r_{brp} H_{eg} \frac{\sum_{jp}\left\{\theta_1\left[T_{e1}(jp)-T_{g1}\right]+\theta_2\left[T_{e2}(jp)-T_{g2}\right]\right\}\Delta z(jp)}{\sum_{jp}\Delta z(jp)} \tag{3.3-70}$$

where

jp = plenum node

T_{g1} = plenum gas temperature at the beginning of the time step

T_{g2} = plenum gas temperature at the end of the time step

$$H_{eg} = \frac{1}{R_g + \frac{r_{erp} - r_{brp}}{2k_{ep}}} = \frac{2k_{ep}}{r_{erp} - r_{brp} + 2k_{ep}R_g} \tag{3.3-71}$$

k_{ep} = cladding thermal conductivity in the gas plenum

and

R_g = thermal resistance of the gas.

3.3.3.2.2 Cladding Node

The equation for the cladding node is

$$\begin{aligned} &\rho_e c_e A_{ep} \frac{T_{e2}(jp) - T_{e1}(jp)}{\Delta t} \\ &= 2\pi r_{erp} \left\{ \theta_1 H_{erc1} \left[\overline{T}_{c1}(jc) - T_{e1}(jp) \right] \right. \\ &\left. + \theta_2 H_{erc2} \left[\overline{T}_{c2}(jc) - T_{e2}(jp) \right] \right\} + 2\pi r_{brp} H_{eg} \left\{ \theta_1 \left[T_{g1} - T_{e1}(jp) \right] \right. \\ &\left. + \theta_2 \left[T_{g2} - T_{e2}(jp) \right] \right\} \end{aligned} \tag{3.3-72}$$

where

ρ_e = cladding density

c_e = cladding specific heat

$$A_{ep} = \pi \left[r_{erp}^2 - r_{brp}^2 \right] \tag{3.3-73}$$

and

r_{erp} = cladding outer radius in the gas plenum region

3.3.3.2.3 Coolant Node

The equation for the coolant node in the gas plenum region is the same as Eq. 3.3-62 for reflector zones, except that in the gas plenum

$$H_{erc} = \frac{h_e k_e}{k_e + \frac{h_c \left(r_{erp} - r_{brp}\right)}{2}} \tag{3.3-74}$$

$$S_{cr} = 2\pi r_{erp} \tag{3.3-75}$$

and

k_e = cladding thermal conductivity.

3.3.3.2.4 Structure Nodes

The finite difference approximations used for the structure in the gas plenum region are the same as those used in the core and blankets. Equations 3.3-45 and 3.3-47 are used, except that Q_{st} is zero.

3.3.3.3 Solution of Finite Difference Equations

A direct solution of the finite difference equations would be complicated, since Eq. 3.3-70 connects a number of axial nodes, each containing a number of radial nodes. Instead, an approximate solution method is used. This method uses the assumption that the total heat capacity of the gas is much less than the total heat capacity of the cladding in the gas plenum region, or

$$\left(\rho c\right)_g A_g << \rho_e c_e A_{ep} \tag{3.3-76}$$

which should always be the case.

The solution method contains five steps:

1. Set $T_{g2} = T_{g1}$.
2. Solve Eqs. 3.3-72, 3.3-62, 3.3-45, and 3.3-47 for all axial nodes in the gas plenum to get new cladding, coolant, and structure temperatures.
3. Use Eq. 3.3-70 to obtain a new computed value for T_{g2}.
4. For each axial node, calculate the heat flow error, ΔE, due to the assumption in step 1:

$$\Delta E = \left(\rho c\right)_g A_g \left(T_{g2} - T_{g1}\right) \tag{3.3-77}$$

5. Add this heat flow to the cladding, changing the cladding temperature:

$$T_{e2} = T_{c2} + \frac{\Delta E}{\rho_e c_e A_{ep}} \tag{3.3-78}$$

In step 2, the equations for each axial node give a matrix equation of the form

$$\begin{bmatrix} \alpha_1+\beta_1 & -\beta_1 & 0 & 0 \\ -\beta_1 & \alpha_1+\beta_1+\beta_2 & -\beta_2 & 0 \\ 0 & -\beta_2 & \alpha_3+\beta_2+\beta_3 & -\beta_3 \\ 0 & 0 & -\beta_3 & \alpha_4+\beta_3+\beta_4 \end{bmatrix} \begin{bmatrix} T_2''(1) \\ T_2''(2) \\ T_2''(3) \\ T_2''(4) \end{bmatrix} = \begin{bmatrix} D_1 \\ D_2 \\ D_3 \\ D_4 \end{bmatrix} \tag{3.3-79}$$

where

$$T_2''(1) = T_{e2}(jp) \tag{3.3-80a}$$

$$T_2''(2) = \bar{T}_{c2}(jc) \tag{3.3-80b}$$

$$T_2''(3) = T_{sti2}(jc) \tag{3.3-80c}$$

$$T_2''(4) = T_{st02}(jc) \tag{3.3-80d}$$

$$\alpha_1 = \rho_e c_e A_{ep} + 2\pi r_{brp} \Delta t \ \theta_2 H_{eg} \tag{3.3-81a}$$

$$\alpha_2 = \bar{\rho}_e \bar{c}_e A_e + 2\bar{c}_c \ \theta_2 |w_2| \Delta t \tag{3.3-81b}$$

$$\alpha_3 = (\rho c)_{sti} \, d_{sti} \, S_{pr} \tag{3.3-81c}$$

$$\alpha_4 = (\rho c)_{sto} \, d_{sto} \, S_{pr} \tag{3.3-81d}$$

$$\beta_1 = 2\pi r_{erp} \ \theta_2 H_{erc2}(jc) \Delta t \tag{3.3-82a}$$

$$\beta_2 = \theta_2 H_{sic2}(jc) S_{pr} \Delta t \tag{3.3-82b}$$

$$\beta_3 = \theta_2 H_{stio2}(jc) S_{pr} \Delta t \tag{3.3-82c}$$

$$\beta_4 = 0 \tag{3.3-82d}$$

$$D_1 = T_1''(1)\left[\alpha_1 - \frac{\theta_1}{\theta_2}\beta_1\right] + \frac{\theta_1}{\theta_2}\beta_1 T_1''(2) + 2\pi r_{brp}\Delta t H_{eg}\left[T_{g1} - T_{e1}(jp)\right] \tag{3.3-83a}$$

$$D_2 = \frac{\theta_1}{\theta_2}\beta_1 T_1''(1) + T_1''(2)\left[\alpha_2 - \frac{\theta_1}{\theta_2}(\beta_1 + \beta_2)\right] + \frac{\theta_1}{\theta_2}\beta_2 T_1''(3) + 2\frac{\overline{c}_c \Delta t}{\Delta z}\left[\theta_1 |w_1| T_1' + \theta_2 |w_2| T_2'\right] \tag{3.3-83b}$$

$$D_3 = \frac{\theta_1}{\theta_2}\beta_2 T_1''(2) + T_1''(3)\left[\alpha_1 - \frac{\theta_1}{\theta_2}(\beta_2 + \beta_3)\right] + \frac{\theta_1}{\theta_2}\beta_3 T_1''(4) \tag{3.3-83c}$$

$$D_4 = \frac{\theta_1}{\theta_2}\beta_3 T_1''(3) + T_1''(4)\left[\alpha_4 - \frac{\theta_1}{\theta_2}(\beta_3 + \beta_4)\right] + S_{pr} Q_{chch} \Delta t \tag{3.3-83d}$$

$$T_1''(1) = T_{e1}(jp) \tag{3.3-84a}$$

$$T_1''(2) = \overline{T}_{c1}(jc) \tag{3.3-84b}$$

$$T_1''(3) = T_{sti1}(jc) \tag{3.3-84c}$$

and

$$T_1''(4) = T_{sto1}(jc) \tag{3.3-84d}$$

This tri-diagonal matrix equation is solved in the same manner as in Section 3.3.1.3 above. For step 3, Eq. 3.3-70 is rewritten as

$$T_{g2} = \frac{T_{g1} + d' s'}{1 + d' \theta_2} \tag{3.3-85}$$

where

$$d' = \frac{2\pi r_{brp} H_{eg} \Delta t}{(\rho c)_g A_g} \tag{3.3-86}$$

and

$$s' = \frac{\sum_{jp} \left\{\theta_1 \left(T_{c1}(jp) - T_{g1}\right) + \theta_2 T_{e2}(jp)\right\} \Delta z(jp)}{\sum_{jp} \Delta z(jp)} \tag{3.3-87}$$

3.3.4 Order of Solution

For a time step, the coolant flow rates are calculated before any temperatures are calculated. Extrapolated coolant temperatures are used to obtain temperature-dependent coolant properties for the flow-rate calculations. Section 3.9 describes the pre-voiding coolant flow-rate calculations.

The order in which the temperature calculations are carried out depends on whether the coolant flow is up or down. In either case, the calculation goes in the direction of the flow. For upward flow, the calculation starts at the subassembly inlet. The coolant temperature at the first coolant node is set equal to the inlet temperatures, T_{in}:

$$T_{c2}(1) = T_{in} \tag{3.3-88}$$

The inlet temperature is supplied by the primary loop calculation, as discussed in Chapter 5. For each axial coolant node, *jc*, the coolant temperature, $T_{c2}(jc)$, at the bottom of the node is used as input for the simultaneous calculation of temperatures at all radial nodes. The solutions in Sections 3.3.1, 3.3.2, and 3.3.3 provide $\overline{T}_{c2}(jc)$, the average coolant temperature for the axial node. The T_{c2} (*jc* + 1) is obtained from

$$T_{c2}(jc+1) = 2\overline{T}_{c2}(jc) - T_{c2}(jc) \tag{3.3-89}$$

This coolant temperature at the top of the node *jc* is the coolant inlet temperature used as input for the calculation at node *jc* + 1.

If the flow is downward, the process is the same, except that the calculation starts at the top of the subassembly and works down. The coolant reentry temperatures, $T_{up\ell}$, described in Section 3.3.6 is used as the starting point for the last coolant node MZC:

$$T_{c2}(\mathrm{MZC}) = T_{up\ell} \tag{3.3-90}$$

For each coolant node, *jc*, T_{c2} (*jc* + 1) is used as input to the calculation of all radial nodes. The solutions in Sections 3.3.1, 3.3.2, and 3.3.3 again provide $\overline{T}_{c2}(jc)$. Then T_{c2} (*jc*) is obtained from

$$T_{c2}(jc) = 2\overline{T}_{c2}(jc) - T_{c2}(jc+1) \tag{3.3-91}$$

3.3.5 Melting of Fuel or Cladding

As discussed in Section 3.3.1.1, melting of both fuel and cladding is treated with a melting range form a solidus temperature, T_{sol}, to a liquidus temperature, T_{liq}, rather than using a sharp melting temperature. Between the solidus and the liquidus, an effective specific heat, c_m, based on the heat of fusion is used, as in Eq. 3.3-3. In the actual temperature calculations for a time step, the heat of fusion is neglected. Then, at the end of the step the temperatures are modified to account for the heat of fusion at any radial node that is going through the melting range. A number of different cases are considered, depending on the relationships between T_1, the temperature at the beginning of the step, and T_2, the temperature calculated for the end of the step, ignoring melting, T_{sol} and T_{liq}. In all cases, T_2'' is the final adjusted temperature at the end of the step, and T_2' would be the final adjusted temperature if it did not go beyond the melting range.

Case 1: $T_1 < T_{\text{sol}}, T_2 > T_{\text{sol}}$

In this case, an adjusted temperature, T_2', is calculated as

$$T_2' = T_{sol} + \left(T_2 - T_{sol}\right)\frac{c}{c_m} \tag{3.3-92}$$

where c is the normal specific heat that was used in the calculation of T_2. Then,

$$T_2'' = \begin{cases} T_{liq} + \left(T_2' - T_{liq}\right)\dfrac{c_m}{c} & \text{if } T_2' > T_{liq} \\ T_2' & \text{otherwise} \end{cases} \tag{3.3-93a-b}$$

In essence, Eq. 3.3-92 divides the energy above the solidus by c_m to get the temperature above the solidus; and Eq. 3.3-93 divides any energy above the liquidus by c to get the temperature above the liquidus.

Case 2: $T_1 > T_{\text{liq}}, T_2 < T_{\text{liq}}$

In this case,

$$T_2' = T_{liq} + \left(T_2 - T_{liq}\right)\frac{c}{c_m} \tag{3.3-94}$$

$$T_2'' = \begin{cases} T_{sol} + \left(T_2' - T_{sol}\right)\dfrac{c_m}{c} & \text{if} \quad T_2' > T_{sol} \\ T_2' & \text{otherwise} \end{cases} \tag{3.3-95a-b}$$

Case 3: $T_{\text{liq}} \geq T_1 \geq T_{\text{sol}}$

In this case

$$T_2' = T_1 + \left(T_2 - T_1\right)\frac{c}{c_m} \tag{3.3-96}$$

$$T_2' = \begin{cases} T_{liq} + \left(T_2' - T_{liq}\right)\dfrac{c_m}{c} & \text{if } T_2' > T_{liq} \\ T_{sol} + \left(T_2' - T_{sol}\right)\dfrac{c_m}{c} & \text{if } T_2' < T_{sol} \\ T_2' & \text{otherwise} \end{cases} \tag{3.3-97a-b-c}$$

3.3.6 Coolant Inlet and Re-entry Temperature

The coolant inlet temperature at the subassembly inlet and the re-entry temperature at the subassembly outlet are determined mainly by the coolant plenum temperatures calculated in PRIMAR-4; but, in addition, mixing zones are modeled at the inlet and outlet of each channel. Therefore, the temperature of coolant entering a subassembly is based on the temperature in the part of the plenum in the immediate vicinity of the end of the subassembly, and the reentry temperature soon after an expulsion is based on both the bulk plenum temperature and the temperature of the coolant that was recently expelled.

The mixing mode uses a mass, M_{mix}, of the coolant in the mixing volume, a specific heat, C_{mix}, of the coolant, and a time constant, τ_{mix}, for heat transfer or mixing between the mixing volume and the bulk plenum coolant. If all temperatures and flows are constant, then the mixing volume temperature, T_{mix}, is assumed to approach an equilibrium value asymptotically with an exponential decay. Figure 3.3-1 shows the model for the outlet mixing volume.

If T_{mix1} is the mixing volume temperature at the beginning of a time step, the T_{mix2} is the value at the end, then

$$T_{\text{mix2}} = T_{eq} + \left(T_{mix1} - T_{eq}\right) e^{-\frac{\Delta t}{\tau}} \tag{3.3-98}$$

For the outlet plenum,

$$\frac{1}{\tau} = \frac{1}{\tau_{\text{mix}}} + \frac{|\bar{w}|}{M_{\text{mix}}} \tag{3.3-99}$$

where $\bar{w}$ is the average coolant flow rate at the subassembly outlet. The equilibrium temperature is

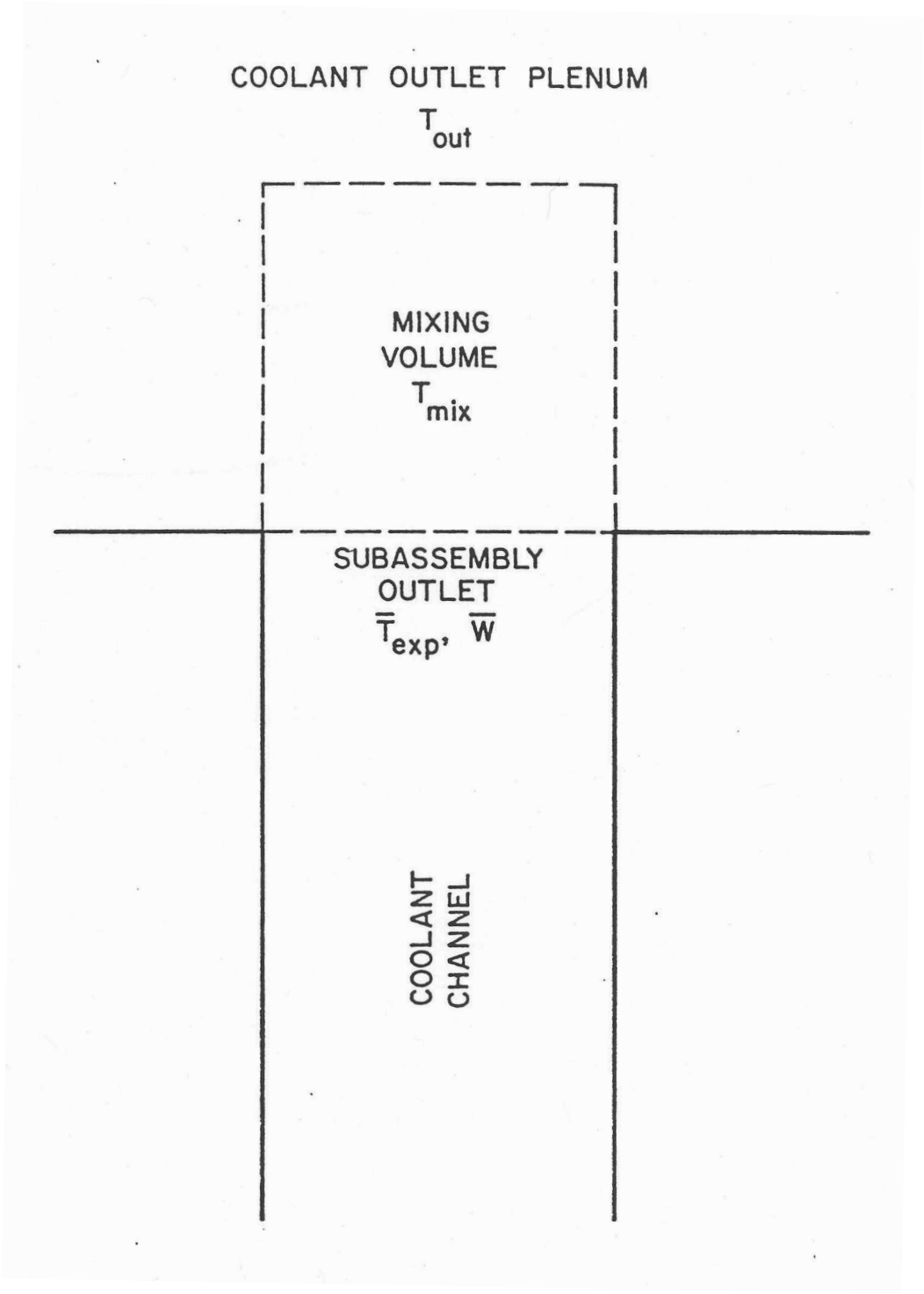

Figure 3.3-1: Coolant Re-entry Temperature Model

$$T_{eq} = \begin{cases} T_{\text{out}} & \text{if } \bar{w} \le 0 \\ \left(\dfrac{T_{\text{out}}}{\tau_{\text{mix}}} + \dfrac{\bar{w}\bar{T}_{\text{exp}}}{M_{\text{mix}}} \right) \tau & \text{if } \bar{w} > 0 \end{cases} \qquad \text{(3.3-100a-b)}$$

where $\bar{T}_{\text{exp}}$ is the average temperature of the sodium expelled from the top of the subassembly into the mixing volume during the time step. T_{out} is the bulk temperature in the outlet plenum. For the inlet plenum, the same equations are used except that $\bar{w}$ changes sign because positive flow results in flow from the inlet mixing volume into the subassembly inlet. For the inlet, Eqs. 3.3-100a and 3.3-100b become

$$T_{\text{eq}} = \begin{cases} T_{\text{in}} & \text{if } \bar{w} \ge 0 \\ \left(\dfrac{T_{\text{in}}}{\tau_{\text{mix}}} - \dfrac{\bar{w}\bar{T}_{\text{exp}}}{M_{\text{mix}}} \right) \tau & \text{if } \bar{w} < 0 \end{cases} \qquad \text{(3.3-101a-b)}$$

where T_{in} is the bulk temperature in the inlet plenum.

The coolant inlet and reentry temperature calculations described above are used in both the pre-voiding module and the boiling module except when a vapor bubble has blown out of the top of the channel. In this case, the condensation of vapor in the outlet plenum raises the temperature in the mixing volume. A two-step process is used for each time step. In the first step, vapor condensation raises the mixing volume temperature. In the second step, heat transfer or mixing with the bulk plenum coolant is accounted for. For the first step, a condensation heat-transfer time constant, τ_c, is calculated as

$$\tau_c = \frac{M_{\text{mix}} C_{\text{mix}}}{h_{\text{cond}} \Delta Z_v p_{er}} \qquad \text{(3.3-102)}$$

where h_{cond} is the vapor condensation heat-transfer coefficient, ΔZ_v is the length of the vapor bubble beyond the subassembly outlet, and p_{er} is the bubble perimeter or surface area per unit length. The value of p_{er} is taken from the coolant channel dimensions in the top node below the subassembly outlet. For step 1, the new mixing volume temperature, T_{new}, is calculated as

$$T_{\text{new}} = \bar{T}_v + \left(T_{\text{mix1}} - \bar{T}_v \right) e^{-\frac{\Delta t}{\tau_c}} \qquad \text{(3.3-103)}$$

where $\bar{T}_v$ is the average vapor temperature in the part of the bubble above the subassembly outlet. In the second step, the final mixing volume temperature is calculated as

$$T_{\text{mix2}} = T_{\text{new}} + \left(T_{\text{out}} - T_{\text{new}}\right)\left(1 - e^{-\frac{\Delta t}{\tau_{\text{mix}}}}\right) \tag{3.3-104}$$

3.4 Steady-State Thermal Hydraulics

The steady-state thermal hydraulics calculations for a channel using the single pin per subassembly option consist of direct solutions of the relevant steady-state equations, rather than running the transient calculations until they converge to a steady-state solution.

For the steady-sate calculations, the user specifies the coolant flow rate for each channel, the coolant inlet temperature and exit pressure, and the power in each node of each channel. The code then calculates the remaining coolant temperatures and pressures, as well as the temperatures in the fuel, cladding, structure, and reflectors. First, the coolant temperatures in a channel are calculated, starting at the inlet and working upward. The steady-state coolant temperature calculation requires only the coolant flow rate, the total power in each axial node, and the coolant heat capacity; so coolant temperatures can be calculated before the fuel and cladding temperatures are known. The second step is to calculate the coolant pressures, starting at the subassembly outlet and working down. Inlet orifice coefficients are adjusted so that all channels have the same total pressure drop. The pressure calculations are described in Section 3.9. The third step is to set the structure and reflector temperatures equal to the coolant temperatures everywhere except in the core and axial blankets. The gas plenum temperatures are also set equal to the coolant temperature in this region, and the cladding temperature in the gas plenum region is also set equal to the coolant temperature. Fourth, the fuel-pin temperatures are calculated for each axial node in the core and axial blankets, starting at the cladding outer surface and working inward. Last, the structure temperatures in the core and axial blankets are calculated.

3.4.1 Basic Equations

The basic heat-transfer equations used in the steady-state calculations are the same as those used for the transient solution, except that all of the time derivatives are dropped in the steady-state solution. These equations include Eq. 3.3-1 and Eqs. 3.4-4 to 3.3-10. Also, the spatial finite differencing used in the steady-state is the same as that used in the transient.

For the steady-state calculations, eq. 3.3-5 becomes

$$\frac{d}{dz}\left(wc_c T\right) = Q_{ct} A_c \tag{3.4-1}$$

where the total heat source per unit volume, Q_{ct}, at node *jc* is

$$Q_{ct}(jc) = Q_c(jc) + Q_{ec}(jc) + Q_{sc}(jc) = \frac{\overline{P}(jc)}{A_c \Delta z(jc)} \tag{3.4-2}$$

and $\overline{P}(jc)$ is the total steady-state power (watts) in the node. For this equation, it is assumed that all heat generated in the fuel, cladding, and structure ends up in the coolant. Note that outside the core and axial blankets $\overline{P}(jc)$ and $Q_{ct}(jc)$ are zero.

For the steady-state fuel and cladding calculations, Eq. 3.3-1 is multiplied by $2\pi r$ and integrated from the fuel inner surface, r_{if}, to give

$$2\pi k r \frac{dT}{dr} = -2\pi \int_{r_{if}}^{r} r' Q(r') dr' \tag{3.4-3}$$

where the adiabatic boundary condition at r_{if} has been used.

3.4.2 Coolant Temperatures

The finite difference form for Eq. 3.4-1 may be written as

$$w\bar{c}_c(j) \frac{\left[T_c(jc+1) - T_c(jc)\right]}{\Delta z(jc)} = \frac{\overline{P}(jc)}{\Delta z(jc)} \tag{3.4-4}$$

or

$$T_c(jc+1) = T_c(jc) + \frac{\overline{P}(jc)}{w\bar{c}_c(jc)} \tag{3.4-5}$$

where $\bar{c}_c(jc)$ is the specific heat evaluated at the average temperature, $\overline{T}_c(jc)$, given by

$$\overline{T}_c(jc) = \frac{T_c(jc) + T_c(jc+1)}{2} \tag{3.4-6}$$

Also, $T_c(1)$ is equal to the inlet temperature:

$$T_c(1) = T_{in} \tag{3.4-7}$$

Starting from *jc* = 1, Eq. 3.4-5 is used to match up the channel. An iteration is used to obtain consistency between $\bar{c}_c(jc)$ and $\overline{T}_c(jc)$.

3.4.3 Fuel and Cladding Temperatures in the Core and Axial Blankets

At each axial node, the radial node powers, $Q(i)$, are calculated using Eqs. 3.3-22 to

3.3-25. Note that the Q in Eq. 3.4-3 is a power per unit volume, whereas $Q(i)$ is an integral value for a node:

$$Q(i) = \int_{z(j)}^{z(j+1)} \int_{r_i}^{r_{i+1}} 2\pi r\, Q\, dr\, dz \tag{3.4-8}$$

The sums, $Q_{sm}(i)$, are calculated as

$$Q_{sm}(i) = \sum_{ii=1}^{i} Q(ii) \tag{3.4-9}$$

Equation 3.4-3 becomes

$$2\pi \bar{k}_{i,i+1} \frac{r(i+1)\left[T(i+1) - T(i)\right]}{\Delta r_{i,i+1}} = \frac{Q_{sm}(i)}{\Delta z} \tag{3.4-10}$$

or

$$T(i) = T(i+1) + \frac{\Delta r_{i,i+1}\, Q_{sm}(i)}{2\pi k_{i,i+1}\, r(i+1)\Delta z} \tag{3.4-11}$$

where $\Delta r_{i,i+1}$ and $\bar{k}_{i,i+1}$ are given by Eqs. 3.3-21 and 3.3-26.

The calculations for an axial node start with the coolant temperature that has already been calculated, as in the section above:

$$T(\mathrm{NC}, j) = \bar{T}(jc) \tag{3.4-12}$$

Then the cladding surface temperature is given by

$$T(\mathrm{NE}') = T(\mathrm{NC}) + \frac{Q_{sm}(\mathrm{NE}')}{2\pi r(\mathrm{NE}')\Delta z h_c} \tag{3.4-13}$$

Cladding temperatures at nodes NE and NE″ are calculated using Eq. 3.4-11. Since $\bar{k}_{i,i+1}$ can be a function of T_i, a simple iteration between Eq. 3.4-11 and Eq. 3.3-26 is used.

The equation used for the fuel surface temperature is

$$2\pi r(\mathrm{NR})\left\{h_b\left[T(\mathrm{NT}) - T(\mathrm{NE}'')\right] + \varepsilon\sigma\left[T(\mathrm{NT})^4 - T(\mathrm{NE}'')^4\right]\right\} = \frac{Q_{sm}(\mathrm{NT})}{\Delta z} \tag{3.4-14}$$

or

$$T(\mathrm{NT}) = d_1 - d_2\,T(\mathrm{NT})^4 \tag{3.4-15}$$

where

$$d_1 = T(\mathrm{NE}") + \frac{Q_{sm}(\mathrm{NT})}{2\pi r(\mathrm{NR})\Delta z h_b} + \frac{\varepsilon\sigma T(\mathrm{NE}")^4}{h_b} \tag{3.4-16}$$

and

$$d_2 = \frac{\varepsilon\sigma}{h_b} \tag{3.4-17}$$

Equation 3.4-15 is solved by iteration.

After the fuel surface temperature has been calculated, the inner fuel node temperatures are calculated one at a time, starting at the outside and working inward, by iterating between Eqs. 3.4-11 and 3.3-26. In this procedure, $T(i)$ is to be found after $T(i+1)$ is known. First, $T(i)$ is set equal to $T(i+1)$. Second, $k(i)$ is to be found after $T(i+1)$ is known. First, $T(i)$ is set equal to $T(i+1)$. Second, $k(i)$ is calculated as a function of the temperature, $T(i)$. Third, $\bar{k}_{i,i+1}$ is calculated using Eq. 3.3-26. Fourth, a new value for $T(i)$ is calculated, using Eq. 3.4-11. Fifth, the new $T(i)$ from the fourth step is compared with old value used in the second step. If the two values differ by less than a user-specified convergence criterion, then the iteration is finished, and the code goes on to the next node. Otherwise, the code goes back to the second step, using the new value of $T(i)$, and repeats the process.

3.4.4 Structure Temperatures in the Core Axial Blankets

The inner structure node temperature is calculated using

$$\Delta z\,S_{pr}\,H_{sic}\left[T(\mathrm{NSI}) - T(\mathrm{NC})\right] = \gamma_s \bar{P}(j) \tag{3.4-18}$$

or

$$T(\mathrm{NSI}) = T(\mathrm{NC}) + \frac{\gamma_s \bar{P}(j)}{\Delta z S_{pr} H_{sic}} \tag{3.4-19}$$

The outer structure node is then calculated using

$$T(\mathrm{NSO}) = T(\mathrm{NSI}) + \frac{\gamma_s \bar{P}(j) d_{sto}}{\Delta z S_{pr} H_{stio}\left(d_{sti} + d_{sto}\right)} \tag{3.4-20}$$

3.4.5 Reflector, Structure, Cladding, and Gas Plenum Temperature Outside the Core and Axial Blankets

Outside the core and axial blankets no power sources are considered, so the reflector and structure temperatures at an axial node are the same as the coolant temperature for the steady-state. The coolant temperatures are the same at all axial nodes in the gas plenum region, and the cladding and gas temperatures in this region are equal to the coolant temperatures.

3.5 Transient Heat Transfer after the Start of Boiling

After the start of boiling, the coolant temperatures are calculated in the coolant routines, rather than being calculated simultaneously with fuel, cladding, and structure temperatures. Coupling between the boiling calculations and the non-coolant heat-transfer calculation takes place in two parts for each time step. First, the boiling routines us extrapolated cladding and structure temperatures to calculate the heat fluxes to the coolant for the boiling calculation. Then the heat fluxes actually used in the coolant routines are passed to the heat-transfer routines to be used as boundary conditions at the cladding, structure, and reflector surfaces. The net results of this procedure are that energy is conserved, and a fully implicit boiling calculation can be made without requiring a direct simultaneous solution of all of the fuel-pin temperatures in the boiling model. The coupling through extrapolated cladding and structure temperatures and heat fluxes at the cladding and structure surfaces imposes numerical stability limitations on the heat-transfer time-step sizes. Currently, fuel-pin temperatures are calculated at the end of the fuel-pin heat-transfer time step, whereas structure and reflector temperatures are calculated at every coolant time step. The coolant time step can be no longer than the heat-transfer step, and the coolant step is often much shorter. For typical fuel pins, the stability limit for the heat-transfer time step is of the order of .02 s. With a thin structure, the stability limit for structure temperature calculations could be less than .02 s, although for typical duct wall thicknesses (.12 in. or .003 m) the stability limit would be closer to one second. Should timing studies indicate that the structure and reflector temperature calculations account for a significant fraction of the total computing time, then the code will be modified so as to do these calculations less often than once every coolant time step.

3.5.1 Fuel and Cladding Temperatures in the Core and Axial Blanket

The equations used for fuel and cladding temperatures after the switch to the boiling module are the same as those used in the non-voiding module, except that in the boiling module the fuel-pin heat-transfer calculations stop at the cladding outer surface rather than carrying through to the structure outer node. The finite difference equations for radial nodes 1-NE are the same as Eqs. 3.3-16 to 3.3-36. For node NE', the cladding outer node, the heat flux to the coolant at the cladding surface must be accounted for. Also, in a boiling region, a film of liquid sodium can be left on the cladding. Since the film is in intimate contact with the cladding, the heat capacity of the film is added to the heat capacity of the cladding outer node, rather than being accounted for in the boiling calculation. Thus, the finite difference equation for node NE' becomes

$$\left[\frac{m_e c_e}{4}+2\pi r(\mathrm{NE'})\rho_c c_c w_{fe}\Delta z(j)\right]\cdot\left[\frac{T_2(\mathrm{NE'})-T_1(\mathrm{NE'})}{\Delta t}\right]$$
$$=-\frac{2\pi\bar{r}_{\mathrm{NE'}}\Delta z(j)\bar{k}_{\mathrm{NE,\,NE'}}}{\Delta r_{\mathrm{NE,\,NE'}}}\left\{\theta_{21}\left[T_1(\mathrm{NE'})-T_1(\mathrm{NE})\right]\right.$$
$$\left.+\theta_2\left[T_2(\mathrm{NE'})-T_2(\mathrm{NE})\right]\right\}-2\pi r(\mathrm{NE'})\Delta z(j)\frac{E_{ec}(j)}{\Delta t}$$
$$+Q(\mathrm{NE'}) \tag{3.5-1}$$

where w_{fe} is the thickness of liquid sodium film left on the cladding after voiding occurs, and E_{ec} is the integrated heat flux from cladding to coolant.

The value of E_{ec} is computed in the coolant routines as

$$E_{ec}(jc)=\int_t^{t+\Delta t}\frac{T_{eex}(jc)-\bar{T}_c(jc)}{R_{ec}(jc)}dt' \tag{3.5-2}$$

where

T_{eex} = extrapolated cladding temperature at a point ¼ of the way from the outer cladding surface to the inner cladding surface:

$$T_{eex}(j,t')=f_1\frac{\left[T(\mathrm{NE},j,t_1)+T(\mathrm{NEP},j,t_1)\right]}{2}$$
$$+f_2\frac{\left[T(\mathrm{NE},j,t_2)+T(\mathrm{NEP},j,t_2)\right]}{2} \tag{3.5-3}$$

$$f_1=\frac{t_2-t'}{t_2-t_1} \tag{3.5-4}$$

$$f_1=1-f_1 \tag{3.5-5}$$

$$R_{ec}=\frac{1}{h_c}+R_{ehf} \tag{3.5-6}$$

and

$$R_{ehf} = \frac{\left[r(\mathrm{NE'}) - r(\mathrm{NE}) \right]}{k_e} \left\{ \frac{r(\mathrm{NE'}) \left[1 - \frac{\gamma_e}{4(1-\gamma_c-\gamma_s)} \right]}{r(\mathrm{NE}) + 3r(\mathrm{NE'})} \right\} \tag{3.5-7}$$

If a node is partly voided, then E_{ec} is averaged over the length of the node as well as integrated over time.

The $\rho_c c_c w_{fe}$ term is supplied by the boiling routines. It represents the heat capacity of any liquid film left on the cladding after voiding occurs. This term is zero unless voiding has occurred at this axial node. Since the film temperature tends to follow the cladding surface temperature more closely than it follows the vapor temperature, the film heat capacity is lumped with the cladding outer node, and film temperatures are not explicitly calculated in the boiling routines.

The finite difference equations are again put in a matrix form like Eq. 3.3-48, except that in the voiding case there are only NE′ elements. The definitions of α, β, and D are the same as in Eqs. 3.3-49 to 3.3-51 for nodes 1-NE. For node NE′, α is still given by Eq.

$$\beta_{\mathrm{NE'}} = 0 \tag{3.5-8}$$

3.3-49d or 3.3-49b, except that the $\rho_c c_c w_{fe}$ term is added to it. Also,

and

$$D_{\mathrm{NE'}} = \frac{\theta_1}{\theta_2} \beta_{\mathrm{NE}} T_1(\mathrm{NE}) + T_1(\mathrm{NE'}) \left[\alpha_{\mathrm{NE'}} - \frac{\theta_1}{\theta_2} \beta_{\mathrm{NE}} \right] + \psi_{\mathrm{NE'}} - r(\mathrm{NE'}) E_{ec}(j) \tag{3.5-9}$$

The equations are solved in the same manner as in the non-voiding case.

3.5.2 Structure Temperatures

The basic equations used for the two structure radial nodes at an axial node are

$$(\rho c)_{sto} \, d_{sto} \frac{dT_{sto}}{dt} = H_{stio} (T_{sti} - T_{sto}) + Q_{st} f_o \tag{3.5-10}$$

and

$$\left[(\rho c)_{sti} \, d_{sti} + \rho_c c_c w_{fst} \right] \frac{dT_{sti}}{dt} = H_{stio} (T_{sto} - T_{sti}) + Q_{st} f_i + \frac{(T_c - T_{sti})}{R_{sc}} \tag{3.5-11}$$

where

$$f_i = \frac{d_{sti}}{d_{sti} + d_{sto}} \tag{3.5-12}$$

$$f_o = \frac{d_{sto}}{d_{sti} + d_{sto}} \tag{3.5-13}$$

and w_{fst} = thickness of the liquid-sodium film left on the structure after voiding occurs.

The heat capacity of the film in the boiling region, as represented by the $p_c c_c w_{fst}$ term, is supplied by the boiling routines to be added to the inner structure node.

The structure temperature calculation is either a semi-implicit or a fully implicit calculation, depending on the time-step in relation to an inner structure node heat-transfer time constant, τ_{sti}, calculated as

$$\tau_{sti} = \frac{(\rho c)_{sti} d_{sti}^2}{2k_{sti}} \tag{3.5-14}$$

If Δt is less than τ_{sti} then the semi-implicit calculation is used. Otherwise the fully implicit calculation is used.

3.5.2.1 Semi-Implicit Calculations

For the semi-implicit calculation, finite differencing of Eqs. 3.5-10 and 3.5-11 gives

$$(\rho c)_{sto}\, d_{sto}\, \frac{(T_{sto2} - T_{sto1})}{\Delta t} = \frac{H_{stio}}{2}\left[T_{sti2} - T_{sto2} + T_{sti1} - T_{sto1}\right] + Q_{st}\, f_0 \tag{3.5-15}$$

and

$$\left[(\rho c)_{sti}\, d_{sti} + \rho_c c_c w_{fst}\right]\frac{(T_{sti2} - T_{sti1})}{\Delta t} = \frac{H_{stio}}{2}\left[T_{sto2} - T_{sti2} + T_{sto1} - T_{sti1}\right] + Q_{st}\, f_i - \frac{E_{sc}}{\Delta t} \tag{3.5-16}$$

where

$$E_{sc}(jc) = \int_t^{t+\Delta t} \frac{T_{stex}(jc) - \overline{T}_c(jc)}{R_{sc}(jc)}\, dt' \tag{3.5-17}$$

The value of E_{sc} is computed in the boiling routines. T_{stex} is the extrapolated structure inner node temperature, and

$$R_{sc} = \frac{1}{h_c} + \frac{d_{sti}}{2k_{sti}} \tag{3.5-18}$$

Equations 3.5-15 and 3.5-16 are put in the form

$$a_{11}T_{sto2} + a_{12}T_{sti2} = b_1 \tag{3.5-19}$$

$$a_{21}T_{sto2} + a_{22}T_{sti2} = b_2 \tag{3.5-20}$$

with the solutions

$$T_{sto2} = \frac{a_{22}b_1 - a_{12}b_2}{a_{11}a_{22} - a_{12}a_{21}} \tag{3.5-21}$$

and

$$T_{sti2} = \frac{a_{11}b_2 - a_{21}b_2}{a_{11}a_{22} - a_{12}a_{21}} \tag{3.5-22}$$

where

$$a_{11} = (\rho c)_{sto}\, d_{sto} + \frac{\Delta t}{2} H_{stio} \tag{3.5-23}$$

$$a_{12} = -\frac{\Delta t}{2} H_{stio} \tag{3.5-24}$$

$$a_{21} = a_{12} \tag{3.5-25}$$

$$a_{22} = (\rho c)_{sti}\, d_{sti} + \frac{\Delta t}{2} H_{stio} + \rho_c c_c w_{fst} \tag{3.5-26}$$

$$b_1 = \left[(\rho c)_{sto}\, d_{sto} - \frac{\Delta t}{2} H_{stio} \right] T_{sto1} + Q_{st} f_o \Delta t - a_{12}\, T_{sti1} \tag{3.5-27}$$

and

$$b_2 = \left[(\rho c)_{sti} d_{stio} - \frac{\Delta t}{2} H_{stio} + \rho_c c_c w_{fst} \right] T_{sti1} - a_{12} T_{sto1} + Q_{st} f_i \Delta t - \Delta t Q_{sc} \quad (3.5\text{-}28)$$

3.5.2.2 Fully Implicit Calculations

Since the inner structure node may represent only a small fraction of the total structure thickness, τ_{sti} can be small. If the time-step size is appreciably larger than τ_{sti} then the semi-implicit calculation can become numerically unstable. Therefore, a different algorithm is used for larger time-step sizes. This algorithm uses two steps. First, a fully implicit calculation is made, using a coolant temperature and thermal resistance to the coolant as structure surface boundary conditions, rather than using the integrated heat flux. In this first step, the heat flux from the coolant to the structure will, in general, not match the heat flux form structure to coolant used in the coolant calculations. Therefore, in the second step, the inner node and outer node structure temperatures are both adjusted by the same amount so that the integrated heat flux from structure to coolant is matched.

For the first step the finite difference equations used for the two structure node temperatures are

$$(\rho c)_{sto} d_{sto} \frac{(T_{sto2} - T_{sto1})}{\Delta t} = H_{stio} (T_{sti2} - T_{sto2}) + Q_{st} f_o \quad (3.5\text{-}29)$$

and

$$\left[(\rho c)_{sti} d_{sti} + \rho_c c_c w_{fst} \right] \frac{(T_{sti2} - T_{sti1})}{\Delta t} = H_{stio} (T_{sto2} - T_{sti2}) + \frac{T_c - T_{sti2}}{R_{sc}} + Q_{st} f_i \quad (3.5\text{-}30)$$

where the values for T_c and R_{sc} are supplied by the coolant routines. The solutions for these two equations again have the same form as Eqs. 3.5-21 and 3.5-22 except that in this case the coefficients are defined as

$$a_{11} = (\rho c)_{sto} d_{sto} + \Delta t H_{stio} \quad (3.5\text{-}31)$$

$$a_{12} = a_{21} = -\Delta t H_{stio} \quad (3.5\text{-}32)$$

and

$$a_{22} = (\rho c)_{sti} d_{sti} + \rho_c c_c w_{fst} + \Delta t H_{stio} + \frac{\Delta t}{R_{sc}} \quad (3.5\text{-}33)$$

The temperature difference, ΔT_{st}, between the outer and inner nodes is then defined as

$$\Delta T_{st} = T_{sto2} - T_{sti2} \tag{3.5-34}$$

In the second step, ΔT_{st} is preserved but the temperatures are adjusted so as to match the value of E_{sc} supplied by the coolant routines:

$$\begin{aligned}\left[(\rho c)_{sti} d_{sti} + \rho_c c_c w_{fst}\right](T_{sci2} - T_{sti1}) + (\rho c)_{sto} d_{sto}(T_{sto2} - T_{sto1}) \\ = Q_{st} - E_{sc}\end{aligned} \tag{3.5-35}$$

The solution to Eqs. 3.5-34 and 3.5-35 is

$$\begin{aligned}T_{sto2} = \{&Q_{st}\Delta t - E_{sc} + (\rho c)_{sto} d_{sto} T_{sto1} \\ &+ \left[(\rho c)_{sti} d_{sti} + \rho_c c_c w_{fst}\right] \cdot (T_{sti1} + \Delta T_{st})\} \\ &/\left[(\rho c)_{sto} d_{sto} + (\rho c)_{sti} d_{sti} + \rho_c c_c w_{fst}\right]\end{aligned} \tag{3.5-36}$$

and

$$T_{sti2} = T_{sto2} - \Delta T_{st} \tag{3.5-37}$$

Note that the second step can still cause numerical instabilities if the time-step size is too large or the total structure thickness is too small, but in the fully implicit scheme the stability limit is based on the total structure thickness, whereas in the semi-implicit scheme the stability is based mainly on the inner node thickness.

3.5.3 Reflector Temperatures

In the boiling module the treatment of reflector temperatures is almost identical to the structure temperature treatment. The main difference is that in the reflector, the outer node is in contact with the coolant, whereas in the structure, the inner code is in contact with the coolant. Also, in the reflector the density, specific heat, and thermal conductivity are the same for both nodes, whereas in the structure these properties can vary from inner node to outer node.

The basic equations are

$$(\rho c)_r d_{ri} \frac{dT_{ri}}{dt} = H_{rio}(T_{ro} - T_{ri}) \tag{3.5-38}$$

and

$$\left[(\rho c)_r\, d_{ro} + \rho_c c_c w_{fr}\right]\frac{dT_{ro}}{dt} = H_{rio}\left(T_{ri} - T_{ro}\right) + \left(T_c - T_{ro}\right)H_{erc} \tag{3.5-39}$$

where

w_{fr} = thickness of the liquid-sodium film left on the reflector after voiding occurs.

An outer reflector node heat-transfer time constant, τ_{ro}, is calculated as

$$\tau_{ro} = \frac{(\rho c)_r\, d_{ro}^2}{2k_r} \tag{3.5-40}$$

and a fully implicit calculation is used if the time-step size is greater than τ_{ro}. Otherwise a semi-implicit calculation is used.

3.5.3.1 Semi-Implicit Calculations

Finite differencing of Eqs. 3.5-38 and 3.5-39 gives

$$(\rho c)_r\, d_{ri}\,\frac{\left(T_{ri2} - T_{ri1}\right)}{\Delta t} = \frac{H_{rio}}{2}\left(T_{ro2} - T_{ri2} + T_{ro1} - T_{ri1}\right) \tag{3.5-41}$$

$$\left[(\rho c)_r\, d_{ro} + \rho_c c_c w_{fr}\right]\frac{\left(T_{ri2} - T_{ri1}\right)}{\Delta t} = \frac{H_{rio}}{2}\left(T_{ri2} - T_{ro2} + T_{ri1} - T_{ro1}\right) - \frac{E_{rc}}{\Delta t} \tag{3.5-42}$$

where

$$E_{rc} = \int_t^{t+\Delta t}\left(T_{rex} - \overline{T}_c\right)H_{erc}\, dt' \tag{3.5-43}$$

These equations are put in the form

$$a_{11}T_{ri2} + a_{12}T_{ro2} = b_1 \tag{3.5-44}$$

$$a_{21}T_{ri2} + a_{22}T_{ro2} = b_2 \tag{3.5-45}$$

with the solution

$$T_{ri2} = \frac{a_{22}b_1 - a_{12}b_2}{a_{11}a_{22} - a_{12}a_{21}} \tag{3.5-46}$$

and

$$T_{ro2} = \frac{a_{11}b_2 - a_{21}b_1}{a_{11}a_{22} - a_{12}a_{21}} \tag{3.5-47}$$

The coefficients are

$$a_{11} = (\rho c)_r \, d_{ri} + \frac{\Delta t}{2} H_{rio} \tag{3.5-48}$$

$$a_{12} = -\frac{\Delta t}{2} H_{rio} \tag{3.5-49}$$

$$a_{21} = a_{12} \tag{3.5-50}$$

$$a_{22} = (\rho c)_r \, d_{ro} + \frac{\Delta t}{2} H_{rio} + \rho_c c_c w_{fr} \tag{3.5-51}$$

$$b_1 = \left[(\rho c)_r \, d_{ri} - \frac{\Delta t}{2} H_{rio} \right] T_{ri1} + \frac{\Delta t}{2} H_{rio} \, T_{ro1} \tag{3.5-52}$$

and

$$b_2 = \left[(\rho c)_r \, d_{ro} + \rho_c c_c w_{fr} - \frac{\Delta t}{2} H_{rio} \right] T_{ro1} + \frac{\Delta t}{2} H_{rio} \, T_{ri1} - E_{rc} \tag{3.5-53}$$

3.5.3.2 Fully Implicit Calculations

As in the structure temperature case, a two-step process is used. In the first step, the finite difference equations used are

$$(\rho c)_r \, d_{ri} \frac{(T_{ri2} - T_{ri1})}{\Delta t} = H_{rio} (T_{ro2} - T_{ri2}) \tag{3.5-54}$$

and

$$\left[(\rho c)_r \, d_{ro} + \rho_c c_c w_{fr} \right] \frac{(T_{ro2} - T_{ro1})}{\Delta t} = H_{rio} (T_{ri2} - T_{ro2}) + (\overline{T}_c - T_{ro2}) H_{erc} \tag{3.5-55}$$

The solutions again have the same form as Eqs. 3.5-46 and 3.5-47, with the coefficients

given by

$$a_{11} = (\rho c)_r d_{ri} + \Delta t\, H_{rio} \tag{3.5-56}$$

$$a_{12} = -\Delta t\, H_{rio} \tag{3.5-57}$$

$$a_{21} = a_{12} \tag{3.5-58}$$

$$a_{22} = (\rho c)_r d_{ro} + \Delta t\ H_{rio} + \rho_c c_c w_{fr} \tag{3.5-59}$$

$$b_1 = (\rho c)_r d_{ri} T_{ri1} \tag{3.5-60}$$

and

$$b_2 = \left[(\rho c)_r d_{ro} + \rho_c c_c w_{fr}\right] T_{rol} + \bar{T}_c \Delta t\, H_{erc} \tag{3.5-61}$$

The temperature difference between nodes, ΔT_r, is defined as

$$\Delta T_r = T_{ri2} - T_{ro2} \tag{3.5-62}$$

In the second step, ΔT_r is preserved and E_{rc} is matched. The energy conservation equation is

$$(\rho c)_r d_{ri}(T_{ri2} - T_{ri1}) + \left[(\rho c)_r d_{ro} + \rho_c c_c w_{fr}\right](T_{ro2} - T_{ro1}) = -E_{rc} \tag{3.5-63}$$

The solution to Eq. 3.5-62 and 3.5-63 is

$$T_{ri2} = \frac{\left\{-E_{rc} + (\rho c)_r d_{ri} T_{ri1} + \left[(\rho c)_r d_{ro} + p_c c_c w_{fr}\right] \cdot (T_{rol} + \Delta T_r)\right\}}{\left[(\rho c)_r (d_{ri} + d_{ro}) + p_c c_c w_{fr}\right]} \tag{3.5-64}$$

and

$$T_{ro2} = T_{ri2} - \Delta T_r \tag{3.5-65}$$

3.5.4 Gas Plenum Region

The basic equations used for the cladding and gas temperatures in the gas plenum region are Eq. 3.3-68 and the following equation:

$$\rho_e c_e A_{ep} \frac{dT_e(jp)}{dt} = 2\pi r_{erp} H_{erc} \left[\bar{T}_c(jc) - T_e(jp) \right] + 2\pi r_{brp} H_{eg} \left[T_g - T_e(jp) \right] \tag{3.5-66}$$

Since Eq. 3.3-68 links all of the cladding nodes in the gas plenum, a direct semi-implicit or implicit solution of Eqs. 3.3-68 and 3.5-66 would require a simultaneous solution for the gas temperature and all of the cladding node temperatures. Instead, the cladding temperatures are calculateed first, using the gas temperature at the beginning of the time step. Then the gas temperature is calculated using the newly computed cladding temperatures.

Finite differencing of Eq. 3.5-66 gives

$$\rho_e c_e A_{ep} \frac{(T_{e2} - T_{e1})}{\Delta t} = -2\pi r_{erp} \frac{E_{ec}}{\Delta t} + \pi r_{brp} H_{eg} (2T_{g1} - T_{e2} - T_{e1}) \tag{3.5-67}$$

where E_{ec} is calculated in the coolant routines in the same manner as indicated in Eq. 3.5-2, except that in the gas plenum only one radial node is used in the cladding, and R_{ehf} becomes

$$R_{ehf} = \frac{r_{erp} - r_{brp}}{2k_e} \tag{3.5-68}$$

The solution of Eq. 3.5-67 for T_{e2} gives

$$T_{e2} = \frac{\{(\rho_e c_e A_{ep} - \pi r_{brp} H_{eg} \Delta t) T_{el} - 2\pi r_{erp} E_{cc} + 2\pi r_{brp} H_{eg} \Delta t \, T_{g1}\}}{(\rho_e c_e A_{ep} + \pi r_{brp} H_{eg} \Delta t)} \tag{3.5-69}$$

In the second step, Eq. 3.3-70 is used with $\theta_1 = \theta_2 = 1/2$. The solution for T_{g2} is

$$T_{g2} = \frac{\left[(\rho c)_g A_g - \pi r_{brp} H_{eg} \Delta t \right] T_{g1} + \pi r_{brp} H_{eg} \Delta t \, s_1 / s_2}{(\rho c)_g A_g + \pi r_{brp} H_{eg} \Delta t} \tag{3.5-70}$$

where

$$s_1 = \sum_{jp} \left[T_{e1}(jp) + T_{e2}(jp) \right] \Delta z(jp) \tag{3.5-71}$$

and

$$s_2 = \sum_{jp} \Delta z(jp) \tag{3.5-72}$$

3.5.5 Coolant Temperatures in Liquid Slugs

Before the onset of coolant voiding, coolant temperatures are calculated at all node boundaries, as indicated in Fig. 3.2-3. After the start of boiling, liquid coolant temperatures are calculated at all node boundaries outside vapor regions, as well as at moving nodes near the bubble interfaces. Two different types of calculations are made. Eulerian temperature calculations are made for fixed coolant nodes in the inlet and outlet liquid slugs. Lagrangian temperature calculations are made for the moving interface nodes and for any fixed nodes in liquid slugs between bubbles. There is also an option to use Lagrangian temperature calculations for all nodes, both fixed and moving.

The Eulerian calculation is probably more accurate for the fixed nodes. The main disadvantage of this method is that a sudden jump in inlet temperature can lead to a sawtooth temperature pattern, with the temperature high at one node, low at the next, and high again at the third node. The Lagrangian calculation does not exhibit this behavior. This sawtooth behavior is not unstable: the perturbation at any node is no larger than the jump in the inlet temperature, and the perturbations tend to die out in later time steps. Also, the coolant inlet and reentry temperature calculations described in Section 3.3.6 tend to eliminate sudden jumps in inlet and reentry temperatures.

3.5.5.1 Eulerian Temperature Calculation

The basic equation used in this calculation is again E. 3.3-5. The heat fluxes Q_{ec} and Q_{sc} are calculated as

$$Q_{ec} = \frac{\left(T_e - \bar{T}_c\right)}{R_{ec}} \frac{2\pi r\left(\mathrm{NE'}\right)}{A_c} \tag{3.5-73}$$

and

$$Q_{sc} = \frac{\left(T_{si} - \bar{T}_c\right)}{R_{sc}} \frac{S_{st}}{A_c} \tag{3.5-74}$$

where R_{ec} and R_{sc} are given by Eqs. 3.5-6 and 3.5-18, T_e is the average of T(NE) and T(NE′), and T_{si} is the inner structure node temperature. In reflector zones, T_e is replaced by the reflector outer node temperature; and in the gas plenum region, the one radial cladding node temperature is used. In the boiling module, the coolant temperatures are calculated before the cladding and structure temperatures are, so linear extrapolation in time is used to obtain values of T_e and T_{si} at the end of a time step.

A semi-implicit finite differencing of Eq. 3.3-5 gives

$$\begin{aligned}
&\bar{p}(jc)\bar{c}_c(jc)A_c(jc)\frac{\left[T_{c2}(jc+1)+T_{c2}(jc)-T_{c1}(jc+1)+T_{c1}(jc)\right]}{2\Delta t}\\
&\quad+\bar{c}_c(jc)w_1\frac{\left[T_{c1}(jc+1)+T_{c1}(jc)\right]}{2\Delta z(jc)}+\bar{c}_c(jc)w_2\frac{\left[T_{c2}(jc+1)-T_{c2}(jc)\right]}{2\Delta z(jc)}\\
&\quad=Q_c(jc)A_c(jc)+\frac{k_5(jc)A_c(jc)}{4}\left\{\frac{2T_{e2}(jc)-T_{e2}(jc)-T_{c2}(jc+1)}{R_{ec2}(jc)}\right.\\
&\quad+\frac{2T_{e1}(jc)-T_{e1}(jc)-T_{c1}(jc+1)}{R_{ec1}(jc)}+\gamma_2(jc)\left[\frac{2T_{si2}(jc)-T_{c2}(jc)-T_{c2}(jc+1)}{R_{sc2}(jc)}\right.\\
&\quad\left.\left.+\frac{2T_{si1}(jc)-T_{c1}(jc)-T_{c1}(jc+1)}{R_{sc1}(jc)}\right]\right\}
\end{aligned}\tag{3.5-75}$$

where

$$k_5(jc)=\begin{cases}\dfrac{2\pi r(\mathrm{NE}',jc)}{A_c(jc)} & \text{in the core and blankets}\\[2ex] \dfrac{s_{er}(kz)}{A_c(jc)} & \text{in a reflector region}\\[2ex] \dfrac{2\pi r_{erp}}{A_c(jc)} & \text{in the gas plenum region}\end{cases}\tag{3.5-76a-c}$$

and

$$\gamma_2(jc)=\frac{S_{st}(jc)}{k_5(jc)A_c(jc)}\tag{3.5-77}$$

Solving for $T_{c2}(jc+1)$ gives

$$
\begin{aligned}
T_{c2}(jc+1) = \Bigg\{ & T_{c1}(jc+1)\left[\overline{\rho}_c(jc) - \frac{\Delta t w_1}{\Delta z(jc) A_c(jc)} - \frac{k_5(jc)\Delta t h_{br}(jc)}{2\overline{c}_c(jc)}\right] \\
& + T_{c2}(jc)\left[-\rho(jc) + \frac{\Delta t w_2}{\Delta z(jc) A_c(jc)} - \frac{k_5(jc)\Delta t}{2\overline{c}_c(jc)} h_{b2}(jc)\right] \\
& + T_{c1}(jc)\left[\rho_c(jc) + \frac{\Delta t w_1}{\Delta z(jc) A_c(jc)} - \frac{k_5(jc)\Delta t}{2\overline{c}_c(jc)} h_{b1}(jc)\right] \\
& + \frac{4\Delta t}{2\overline{c}_c(jc)} k_5(jc)\,\phi_1(jc) + \frac{2\Delta t Q_c(jc)}{\overline{c}_c(jc)}\Bigg\} / \Bigg\{\overline{\rho}_c(jc) \\
& + \frac{\Delta t w_2}{\Delta z(jc) A_c(jc)} + \frac{k_5(jc)\Delta t h_{b2}(jc)}{2\overline{c}_c(jc)}\Bigg\}
\end{aligned}
\tag{3.5-78}
$$

with

$$
h_{b1}(jc) = \frac{1}{R_{ec1}(jc)} + \frac{\gamma_2(jc)}{R_{sc1}(jc)} \tag{3.5-79}
$$

$$
h_{b2}(jc) = \frac{1}{R_{ec2}(jc)} + \frac{\gamma_2(jc)}{R_{sc2}(jc)} \tag{3.5-80}
$$

and

$$
\begin{aligned}
\phi_1(jc) = 1/2\Bigg\{ & \frac{T_{e2}(jc)}{R_{ec2}(jc)} + \frac{T_{e1}(jc)}{R_{ec1}(jc)} + \gamma_2(jc)\left[\frac{T_{si2}(jc)}{R_{sc2}(jc)}\right. \\
& \left. + \frac{T_{si1}(jc)}{R_{sc1}(jc)}\right]\Bigg\}
\end{aligned}
\tag{3.5-81}
$$

If the inlet flow is positive, then the coolant temperature at node 1 is determined by the inlet temperature. Equation 3.5-78 is then used to march up the channel through the inlet liquid slug, with $T_{c2}(jc+1)$ being computed after $T_{c2}(jc)$. Similarly, if the flow in the upper liquid slug is downward, then the assembly outlet reentry temperature determines the coolant temperature at the last coolant node. Then an equation similar to Eq. 3.5-79 is used to march down through the upper liquid slug, with $T_{c2}(jc)$ being computed after $T_{c2}(jc+1)$.

The Eulerian calculations always go from node to node in the direction of flow. An

inlet slug expelling downward and an outlet liquid slug going upward are special cases, since in these cases the calculation starts at a liquid vapor interface rather than an end of the subassembly. The interface liquid temperatures are first calculated using the Lagrangian treatment described below. Then Eq. 3.5-78 or the equivalent equation for downward flow is used to calculate the temperatures at the fixed nodes within the liquid slug. For the first fixed node near the interface, some of the terms in Eq. 3.5-78 are modified. The moving interface node is treated as node *jc*. The interface temperature is used for $T_{c2}(jc)$, and an interpolated value is used for $T_{c1}(jc)$. The distance from the fixed node to the interface at the end of the step is used for $\Delta z(jc)$. Interpolated interface cladding and structure temperatures are used in calculating ϕ_1 for the interface node.

3.5.5.2 Lagrangian Calculations for Interface Temperatures

For every liquid-vapor interface a vapor temperature is calculated at or very near the interface. The liquid temperature right at the interface would be close to the vapor temperature, but there can be strong axial temperature gradients in the liquid near the interface. These strong axial gradients would only extend a short distance into the liquid. The heat flow through the interface into a small vapor bubble is accounted for, as described in Chapter 12; but since only one liquid temperature node is used near the interface, the axial temperature distribution neat the interface is not represented. A liquid temperature is calculated for each interface, but axial conduction is neglected in this calculation. Thus, the liquid interface temperature can be considered as either the interface temperature that would occur if there were no axial conduction or the temperature a short distance from the interface where axial conduction is negligible.

A Lagrangian formulation, moving with the liquid, is used for the interface temperature calculation. The basic equation used is

$$\rho c \frac{DT_c}{Dt} = Q_c + Q_{ec} + Q_{sc} \tag{3.5-82}$$

where the Lagrangian total derivative is used. After finite differencing this equation gives

$$\rho_{ci} c_{ci} \frac{T_{\ell i2}(k,L) - T_{\ell i1}(k,L)}{\Delta t} = Q_c(jc) + \frac{k_5(jc)}{2}\left\{\frac{T_{ei1}(k,L) - T_{\ell i1}(k,L)}{R_{eci1}(k,L)} + \frac{T_{ei2}(k,L) - T_{\ell i2}(k,L)}{R_{sci1}(k,L)}\right\} + \gamma_2(jc)\left\{\frac{T_{si1}(k,L) - T_{\ell i1}(k,L)}{R_{sci1}(k,L)} + \frac{T_{si2}(k,L) - T_{\ell i2}(k,L)}{R_{sci2}(k,L)}\right\} \tag{3.5-83}$$

or

$$T_{\ell i2}(k,L) = \left\{T_{\ell i1}(k,L)\left[1 - d_1 h_{bi1}(k,L)\right] + d_1\left[\phi_{1i}(k,L) + 2\,Q_c(jc)/k_5(jc)\right]\right\}/\left[1 + d_1 h_{bi2}(k,L)\right] \tag{3.5-84}$$

where

$$d_1 = \frac{k_5(jc)\Delta t}{2\rho_{ci}\, c_{ci}} \tag{3.5-85}$$

$$h_{bi1}(k,L) = \frac{1}{R_{eci1}(k,L)} + \frac{\gamma_2(jc)}{R_{sci1}(k,L)} \tag{3.5-86}$$

$$h_{bi2}(k,L) = \frac{1}{R_{eci2}(k,L)} + \frac{\gamma_2(jc)}{R_{sci2}(k,L)} \tag{3.5-87}$$

k = bubble number

L = 1 for lower bubble interface, 2 for upper bubble interface

jc = coolant node containing the interface

$$\theta_{1i}(k,L) = \frac{T_{ei2}(k,L)}{R_{eci2}(k,L)} + \frac{T_{ei1}(k,L)}{R_{eci1}(k,L)} + \gamma_2(jc)\left[\frac{T_{si2}(k,L)}{R_{sci2}(k,L)} + \frac{T_{si1}(k,L)}{R_{sci1}(k,L)}\right] \tag{3.5-88}$$

T_{ei2}, T_{si2}=cladding and structure interface temperatures at the end of the step, extrapolated in tir

T_{ei1}, T_{si1} = same at the beginning of the time step.

R_{eci2}, R_{sci2} = values of R_{ec} and R_{sc} at the interface at the end of the time step.

R_{eci1}, R_{sci1} = same at the beginning of the time step.

3.5.5.3 Lagrangian Calculation for Fixed Nodes

The Lagrangian temperature calculations for fixed coolant nodes are similar to those for interface nodes. The fluid particle that ends up at coolant node *jc* at the end of a time step is considered. During the time step, the particle travelled a distance

$$\Delta z' = \frac{(w_1 + w_2)\Delta t}{2\rho_c(jc)A_c(jj)} \tag{3.5-89}$$

where

$$jj = \begin{cases} jc & \text{if } w_1 + w_2 < 0 \\ jc-1 & \text{otherwise} \end{cases} \tag{3.5-90}$$

At the beginning of the time step, the particle was at z', given by

$$z' = z_c(jc) - \Delta z' \tag{3.5-91}$$

The coolant temperature, T'_{c1}, at z' at the beginning of the step is obtained by linear interpolation between the nodes on either side of z'. Also, the cladding and structure temperatures, T'_{e1} and T'_{s1}, at z' at the beginning of the step are obtained by linear interpolation. The cladding and structure temperatures, T'_{e2} and T'_{s2}, at $z_c(jc)$ at the end of the time step are also obtained by linear interpolation between the cladding and structure nodes.

The result of finite differencing of Eq. 3.5-82 for the particle at node *jc* is

$$T_{c2}(jc) = \left\{T'_{c1}\left[1 - d'_1 h_{b1}(jj)\right] + d'_1\left[\theta'_1 + 2Q_c(jj)/k_5(jj)\right]\right\}/\left[1 + d'_1 h_{b2}(jj)\right] \tag{3.5-92}$$

where

$$d'_1 = \frac{k_5(jj)\Delta t}{\rho_c(jc)\bar{c}_c(jj)} \tag{3.5-93}$$

and

$$\phi_1' = \frac{T_{e2}'}{R_{ec2}(jj)} + \frac{T_{e1}'}{R_{ec1}(jj)} + \gamma_2(jj)\left[\frac{T_{s2}'}{R_{sc2}(jj)} + \frac{T_{s1}'}{R_{sc1}(jj)}\right] \tag{3.5-94}$$

Again, h_{b1} and h_{b2} are given by Eqs. 3.5-79 and 3.5-80.

3.6 Fuel-Cladding Bond Gap Conductance

A number of gap-size-dependent bond gap correlations are available in SASSYS-1 and SAS4A. The bond gap conductance depends on two main factors: the gap size or the contact pressure between fuel and cladding after the gap has closed, and the correlation for bond gap conductance as a function of gap size or contact pressure. Since small differences in differential expansion between fuel and cladding can make the difference between an open gap and a closed gap, and since gap conductance correlations are strongly dependent on gap size, the models used for fuel and cladding thermal expansion and swelling might have a much larger impact on computed bond gap conductances than the choice of the particular correlation used for bond gap conductance as function of gap size.

There are a number of options for computing the gap size. One common option for oxide fuel is to use DEFORM-IV to compute the steady-state and transient dimensions. Chapter 8 describes DEFORM-IV and the bond gap conductance correlations that can be used with it. A second option would be to use DEFORM-IV for the steady-state but not for the transient. In this case, the gap size and gap conductance determined in the steady-state calculations would be constant during the transient. A third option is not to use DEFORM-IV at all. In this case the gap size is constant, based on the user-specified pin dimensions, and the bond gap conductance is constant. The fourth option is to use a simple thermal expansion model for the transient bond gap size. For a metal fuel, the DEFORM-5 model described in Chapter 9 can be used to obtain the bond gap conductance.

The simple thermal expansion model applies only to the transient calculation. It can be used either with or without the DEFORM-IV steady-state calculations, but it cannot be used with the transient DEFORM-IV. In this model, it is assumed that the gap size, Δr_g, is determined by simple thermal expansion of the fuel and cladding from their steady-state dimensions:

$$\begin{aligned}\Delta r_g = {} & r_o(\mathrm{NE}) - r_o(\mathrm{NR}) \\ & + \frac{\left[r_o(\mathrm{NE}) + r_o(\mathrm{NE'})\right]}{2}\alpha_e\left[T(\mathrm{NE}) - T_o(\mathrm{NE})\right] \\ & - r_o(\mathrm{NR})\alpha_f\left(\bar{T}_f - \bar{T}_{fo}\right)\end{aligned} \tag{3.6-1}$$

where

r_o = steady-state radii,

$\overline{T}_o$ = steady-state temperature,

$\overline{T}_f$ = average fuel temperature, mass-weighted average,

$\overline{T}_{fo}$ = average steady-state fuel temperature,

α_e = cladding thermal expansion coefficient, and

α_f = fuel thermal expansion coefficient

The bond gap conductance then has the form

$$h_b = \frac{\overline{h}_b}{\Delta r_g} \tag{3.6-2}$$

or

$$h_b = A_g + \frac{1}{B_g + \frac{\Delta r_g + C_g}{\overline{h}_b}} \tag{3.6-3}$$

depending on the correlation chosen. In these correlations $\overline{h}_b$, A_g, B_g, and C_g are user-supplied correlation coefficients. For either correlation, the bond gap conductance is also constrained to lie between user-supplied minimum and maximum values; so if a value outside this range is calculated using Eq. 3.6-2 or 3.6-3, the minimum or the maximum value is used instead.

3.7 Fuel Pin Heat-transfer After Pin Disruption or Relocation of Fuel or Cladding

The preceding sections describe fuel pin heat transfer with intact fuel pins and no relocation of fuel of cladding. After pin disruption or the relocation of fuel or cladding, the heat transfer calculations are modified. The modifications after the start of in-pin fuel relocation in the PINACLE module are described in Chapter 15. The modification after the start of cladding melting and relocation in the CLAP module are described in Chapter 13. The modifications after pin disruption are described in Section 3.7.1 below and in Chapters 14 and 16.

3.7.1 Fuel-pin Heat Transfer After Pin Disruption in PLUTO2 or LEVITATE

When PLUTO2 or LEVITATE is active, the PLHTR subroutine calculates the heat conduction in all solid fuel (including axial blankets) and also in the cladding which is in contact with the lower and upper coolant slugs. The heat conduction calculation of the cladding in the interaction region, which is between the lower and upper coolant slug,

(see Fig. 14.1-4) is performed in the PLUTO2 or LEVITATE modules (see Section 14.5.2 and 16.5.7) using a shorter time step than the PLHTR calculation.

Along the interaction region, the heat flow rate from the cladding inner surface to the fuel outer surface is calculated in PLUTO2 or LEVITATE assuming a constant gap conductance of the value in existence at the time of initiation. The PLUTO2 or LEVITATE calculated heat flow rates are integrated over a PLHTR time step in order to provide PLHTR with the total heat added during a heat-transfer time step. Outside the interacting region the heat flow rate between the liquid sodium flow and the cladding outer surface is calculated in the PLCOOL subroutine of PLUTO2. The latter subroutine mainly determines the liquid sodium temperatures in the coolant slugs. It uses the same time step as the PLHTR subroutine.

The temperature calculations in the molten fuel cavity in the pins are performed by PLUTO2 or LEVITATE and are part of the in-pin fuel motion calculation in these modules. The heat flow rates from each molten cavity node to the surrounding sold fuel are also calculated in PLUTO2 or LEVITATE. Since the time steps of the latter modules are shorter than the PLHTR time steps, the PLUTO2 or LEVITATE heat flow rates have to be integrated over the whole heat-transfer time step, because the total heat transferred to the cavity wall during a heat-transfer time step is required by PLHTR.

The initial configuration of the molten pin cavity at the time of pin failure is determined in the PLUTO2 and LEVITATE initialization routines PLINPT and PLSET (see Section 14.2.2). PLINPT initializes the integer array IXJ(K) for each axial node K with the index of the innermost radial fuel node whose melt fraction has not yet exceeded the input value FNMELT. This array IZJ(K) thus determines the initial molten cavity configuration.

When PLUTO2 or LEDVITATE are active, additional fuel can melt into the cavity and thereby enlarge it. The integer array IZJ(K) is updated for each axial node K whenever another radial node exceeds the input value FNMELT. However, such a radial node is only gradually added to the molten cavity (see Eqs. 14.2-10 to 14.2-12). The heat conduction calculation in PLHTR includes this partial node.

Figure 3.7-1 shows the radial grid used in PLHTR. The heat conduction calculation covers the radial region from I = INDBOT to I = NTHELP. The latter can be the outermost radial fuel node (for axial nodes in the interaction region) or the outer cladding node (for axial nodes outside the interaction region). Temperatures and heat sources are defined at the midpoints of the grid in Fig. 3.7-1.

PLHTR is a modified version of the TSHTRV subroutine that calculates the fuel-pin heat transfer during coolant boiling and the reader is referred to Section 3.5 for a detailed presentation of the equations. One of the main differences is that the conduction calculation is done only in the solid fuel region and in the cladding outside the interaction region. This is achieved by having the calculational loops go from I = INDBOT to I = NTHELP (see Fig. 14.2-1) and by adding or subtracting the integrated heat flux to or from the solid fuel nodes at the boundaries in the form of heat sources or sinks, respectively. The integrated heat flux at the outer pin boundary is obtained from

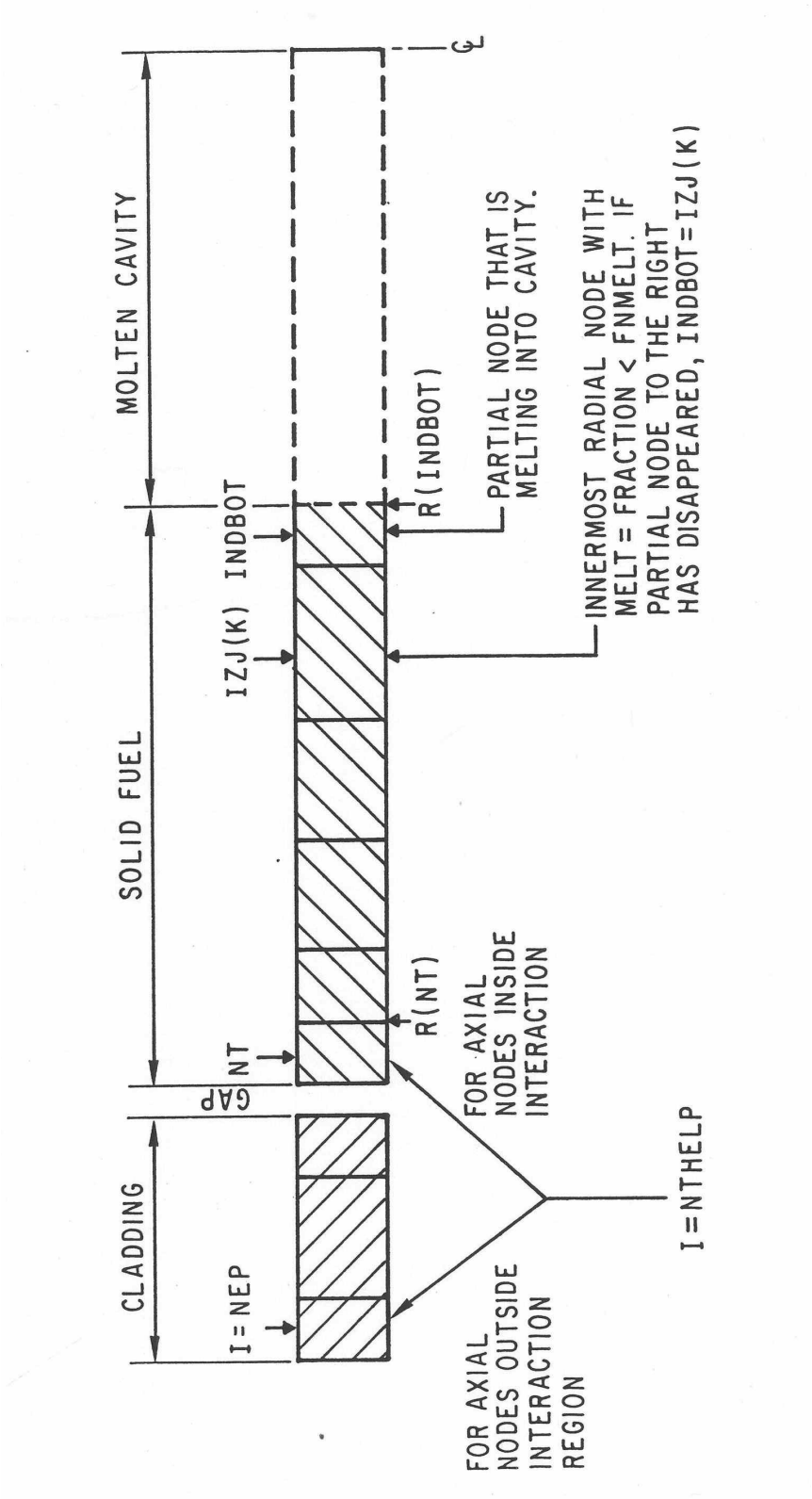

Figure 3.7-1: Radial Grid for the PLHTR Calculation

the array HFPICL, calculated in the PLUTO routine PLMISE or in the LEVITATE routine LESDEN. The integrated heat flux at the cavity boundary is obtained from the array HFCAWA; calculated in the PLUTO routine PC1PIN or the LVITATE routine LE1PIN. Moreover, the heat conduction terms at the fuel surface, which are necessary in the TSHTRV calculation, had to be set to zero. This meant setting the term BETA (NTHELP) in Eq. 3.3-48 to zero and ignoring all equations related to the cladding in Eq. 3.3-48.

3.8 Heat-transfer Time Step Control

Each channel uses its own separate heat-transfer time step size, so that channels in which temperatures are changing rapidly or in which boiling is occurring can use small heat-transfer time steps while other channels use larger steps.

After each heat-transfer time step, the size of the next step is determined, based on number of criteria. Most of these criteria are based on user-supplied values for maximum time step sizes and maximum temperature changes per step. The time step used in the smallest of the various criteria. If not other factor is more limiting, then the next heat-transfer step size is set equal to the initial main time-step size. This is usually in the range of .05-1.0 s. After the onset of boiling in a channel, a maximum boiling heat-transfer time step size, typically .01-.02 s, is used. In addition, a heat-transfer time step cannot go past the end of a main time step. Also, if the channel has not started boiling yet, then an attempt is made to end a heat-transfer time step right at, or very close to, the time when the first bubble is formed. For this purpose, the pre-boiling coolant routines make an estimate of the boiling time at the end of each coolant time step. The boiling time estimate is based on linear extrapolations in time for the coolant temperature and the saturation temperature at each axial node. The other criteria are based on the rate of change of the temperatures. The user supplies values of the maximum change per time step for the fuel and clad temperatures. Typical values are in the range of 30-50K. The rate of change of the fuel center-line temperature, the fuel surface temperature, and the clad mid-point temperature at each axial node are used to determine maximum time step sizes. After the minimum of the various time-step criteria has been found, the time step size is rounded to eight decimal places to minimize differences in results caused by different round-off errors on different computers. These criteria are summarized in Table 3.8-1.

Table 3.8-1: Criteria for Heat-Transfer Time Step Sizes

1.	Initial time step size
2.	Maximum boiling time step size, if boiling
3.	End of a main time step
4.	Initiation of boiling
5.	Maximum fuel center-line temperature change
6.	Maximum fuel surface temperature change
7.	Maximum clad mid-point temperature change

3.9 Steady-State and Single-Phase Transient Hydraulics

3.9.1 Introduction

The core assembly hydraulics treatment in SAS4A and SASSYS-1 includes the calculation of coolant flow rates and pressure distributions within each core channel. Coolant flow rates and pressures are calculated in a number of different places in the codes. They are used in the steady-state thermal hydraulics initialization; the pre-voiding thermal hydraulics module calculates coolant flows and pressures; and after the onset of voiding, they are calculated in the boiling module. This section describes only the steady-state and pre-voiding calculations. Chapter 12 describes the hydraulics calculations after the onset of voiding. Chapters 14 and 16 describe the hydraulics calculations after pin disruption.

The coolant flow provides the heat removal from the fuel pins, and so the main reason for calculating coolant flow rates before the onset of voiding is to provide information for the fuel-pin temperature calculations. Core channel flow rates are also needed for the PRIMAR-4 primary loop thermal hydraulics calculations. The pressure distribution within a channel is calculated mainly to obtain the pressure-dependent coolant saturation temperature used to determine the onset of boiling.

For the steady-state initialization the user specifies the initial coolant flow rate for each channel and the outlet plenum pressure. The code then calculates the pressure distribution in each channel, starting from the outlet and working down to the inlet. The channel with the largest steady-state pressure drop is used to determine the steady-state inlet plenum pressure; and the inlet orifice coefficients in all other channels are adjusted so that all channels have the same total steady-state pressure drop.

In the transient hydraulic calculations, both the coolant flow rates and the pressure distributions are calculated for each channel. Pressure boundary conditions are used for the transient coolant flow rate calculations. The driving pressures for these calculations are the inlet and outlet coolant plenum pressures supplied by the PRIMAR-4 module. Since all channels use the same inlet and outlet pressures, flow redistribution between channels is automatically accounted for as temperatures and flows change. Extrapolated coolant temperatures are used to evaluate coolant properties in the transient hydraulics calculations, since coolant flow rates for a time step are calculated before temperatures are calculated.

Figure 3.1-2 shows the logic flow in subroutine TSCL0, the driver for pre-voiding core channel thermal hydraulics. As indicated previously, a multi-level time step approach is used for the transient calculations in SAS4A and SASSYS-1. In general, the routines in a transient module start with all quantities knows at the beginning of a time step, and a pass through a module results in calculating the values of relevant parameters of the module for one channel at the end of the time step. Different time-step sizes can be used for different phenomena. In particular, the pre-voiding coolant hydraulics time step can be smaller than, but not larger than, the heat-transfer time step or the PRIMAR time step. One pass through TSCL0 calculates one coolant time step

for one channel. If the coolant time step finishes a heat-transfer step, then the temperature calculations for the heat-transfer step are also carried out.

Figure 3.9-1 shows the logic flow in subroutine TSCNV1. This subroutine and the routines called by it carry out the pre-viding coolant flow and pressure calculations. Subroutine TSCNV1 also checks on whether to switch to the boiling model.

As indicated in Fig. 3.9-2, the pre-voiding transient hydraulics module interacts with PRIMAR and TSHTRN. PRIMAR supplies the inlet and outlet pressures that drive the coolant flows in the core channels. In return, TSCL0 supplies PRIMAR with the current channel flow rates, as well as hydraulic parameters to use in estimating future flow rates for the next PRIMAR time step. TSCL0 supplies the coolant flow rates to TSHTRN, and TSHTRN computes the coolant temperatures used by TSCL0.

3.9.2 Basic Equations

Before the onset of voiding, the coolant is treated as incompressible, and the basic equation used for liquid coolant flow in non-voided channels is

$$\frac{1}{A_c}\frac{\partial w}{\partial t}+\frac{\partial p}{\partial z}+\frac{1}{A_c}\frac{\partial (wv)}{\partial z}=-\left(\frac{\partial p}{\partial z}\right)_{fr}-\left(\frac{\partial p}{\partial z}\right)_{K}-\rho_c g \qquad (3.9\text{-}1)$$

with

w = $w(t)$-independent of z

w = coolant flow rate $(kg/s) = \rho_c\, v\, A_c$

Ac = coolant flow area

p = pressure

ρ_c = density

v = coolant velocity (m/s)

z = axial position

t = time

$\left(\frac{\partial p}{\partial z}\right)_{fr}$ = friction pressure drop

$$\left(\frac{\partial p}{\partial z}\right)_{fr}=\mathrm{f}\frac{\mathrm{w}^2}{2\rho_c A_c^2 D_h} \qquad (3.9\text{-}2)$$

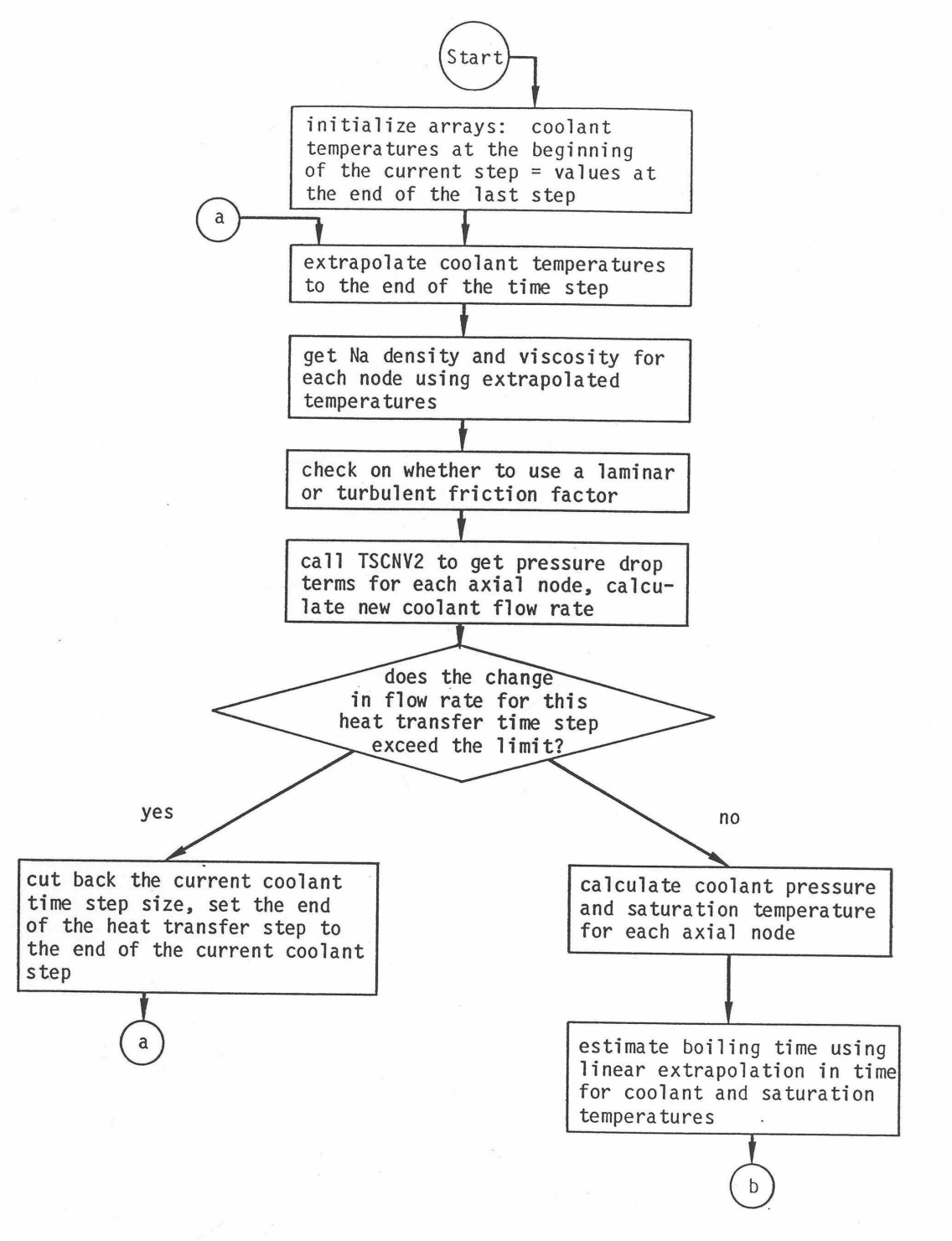

Figure 3.9-1: Subroutine TSCNV1, Pre-Boiling Coolant Flow Rates and Pressure Distribution

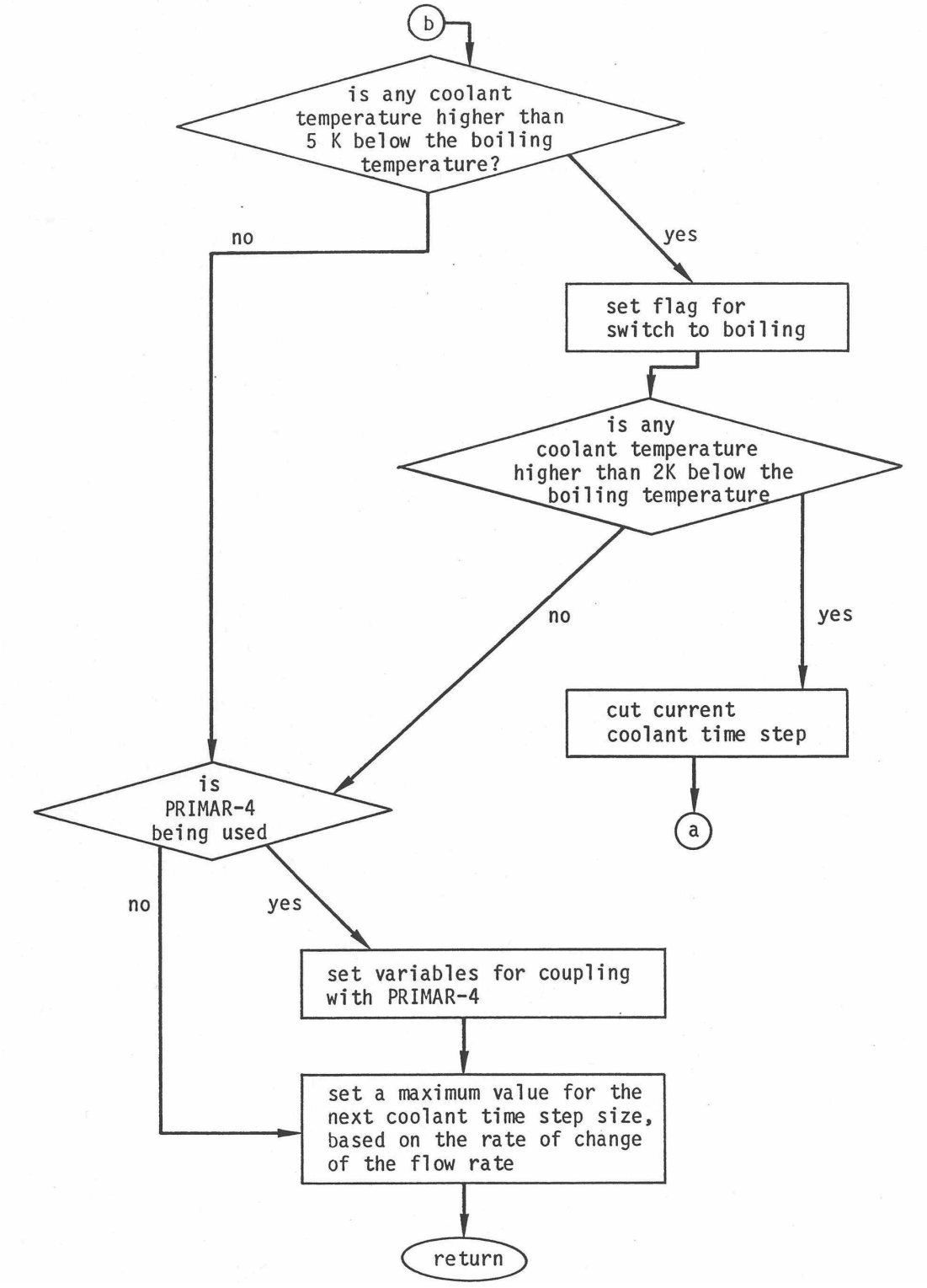

Figure 3.9-1: Subroutine TSCNV1, Pre-Boiling Coolant Flow Rates and Pressure Distribution (Cont'd)

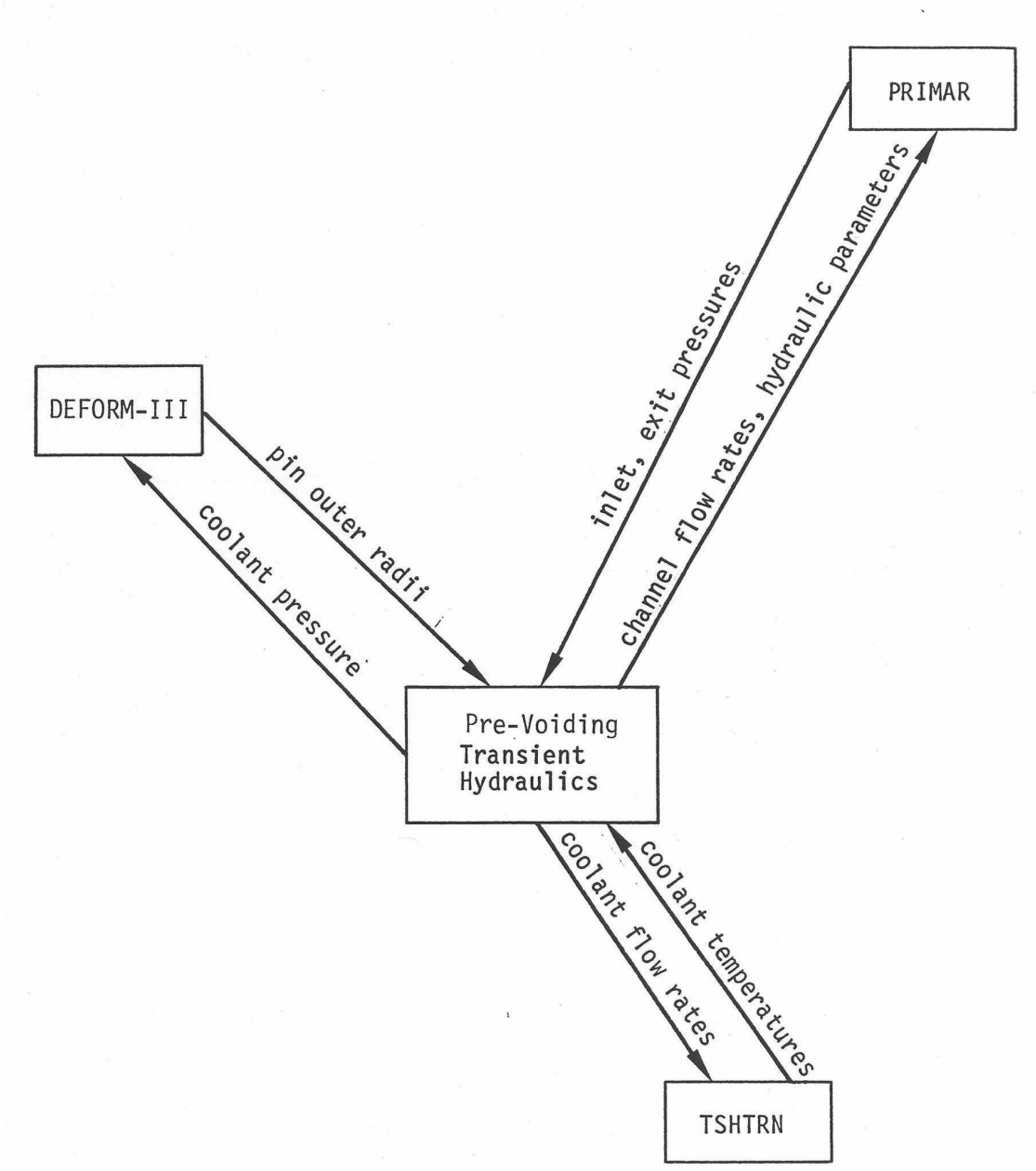

Figure 3.9-2: Interactions Between Pre-Voiding Transient Hydraulics and Other Modules

f= friction factor, approximated either as

$$f = \begin{cases} A_{fr}(\mathrm{Re})^{b_{fr}} \text{ if } \mathrm{Re} \geq R_{eL} \\ A_{fL}/\mathrm{Re} \text{ if } \mathrm{Re} < R_{eL} \end{cases} \quad (3.9\text{-}3a)$$

or as

$$f = A_{fr}(\mathrm{Re})^{b_{fr}} + A_{fL}/\mathrm{Re} \quad (3.9\text{-}3a)$$

where A_{fr} b_{fr}, and A_{fL} are user-supplied correlation coefficients

$$\mathrm{Re} = \frac{D_h w}{\mu A_c} = \text{Reynolds number} \quad (3.9\text{-}4)$$

R_{eL} = Reynolds number for the transition from turbulent to laminar flow

μ = viscosity

D_h = hydraulic diameter

$\left(\frac{\partial p}{\partial z}\right)_K$ = orifice pressure drop

g = acceleration of gravity

ρ = density

The axial node structure shown in Fig. 3.2-3 is used for the coolant. Figure 3.9-3 shows which variables are defined at node boundaries and which are averages or integrals over the length of a node. With this mesh structure, integrating Eq. 3.9-1 over the length of the channel gives

$$I_1 \frac{\partial w}{\partial t} + p_t - p_b + w^2 I_2 + A_{fr} w\,|w|^{l+b_{fr}} I_3 + w|w|\, I_4 + g\, I_5 = 0 \quad (3.9\text{-}5)$$

where

$$I_1 = \int \frac{dz}{A_c} = \left(\frac{\Delta z_i}{A}\right)_b + \left(\frac{\Delta z_i}{A}\right)_t + \sum_{\mathrm{JC}=1}^{\mathrm{MZC}-1} X_{I1}(\mathrm{JC}) \quad (3.9\text{-}6)$$

and

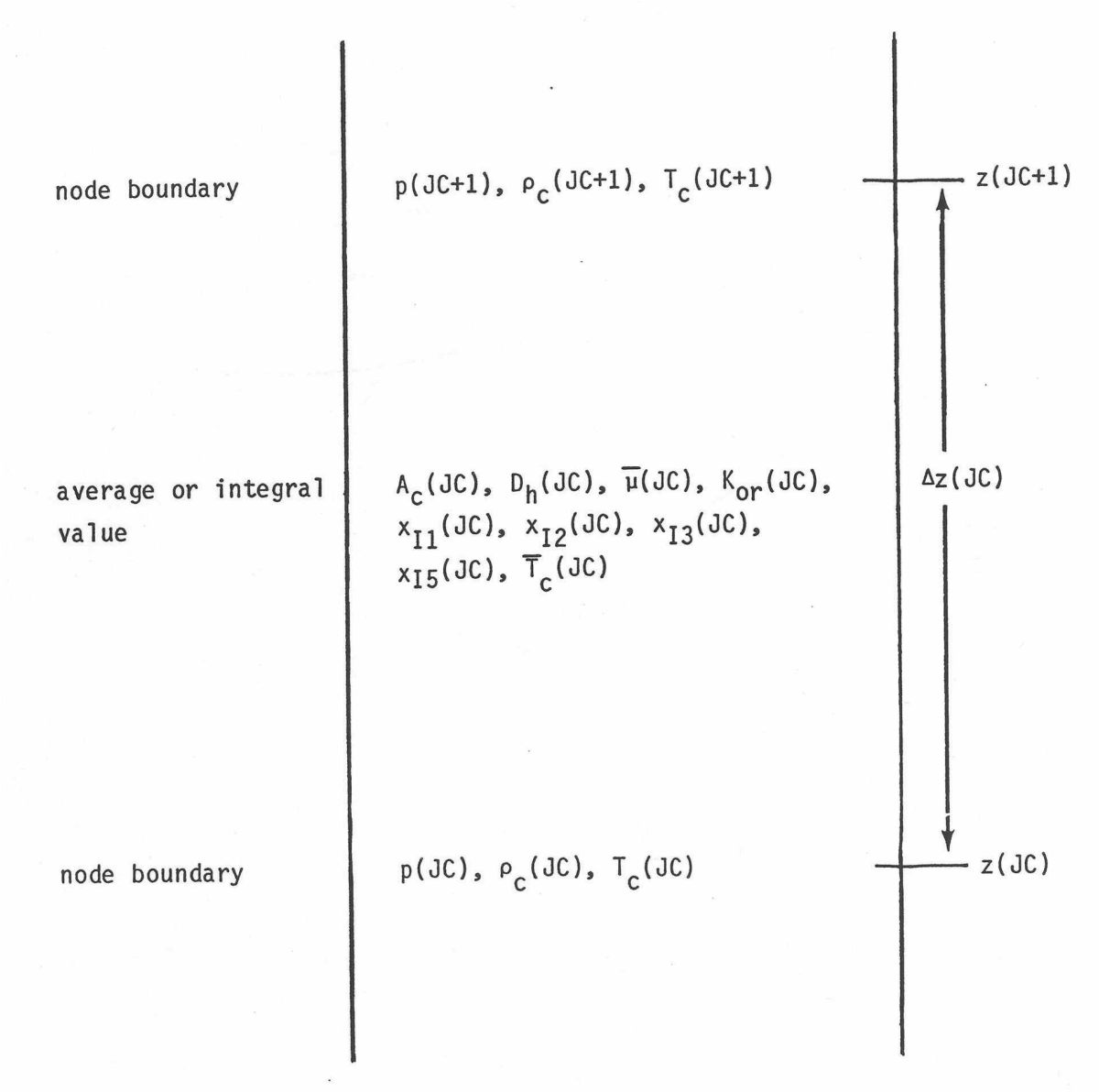

Figure 3.9-3: Interactions Between Pre-Voiding Transient Hydraulics and Other Modules

$$X_{I1}(\mathrm{JC}) = \frac{\Delta z(\mathrm{JC})}{A_c(\mathrm{JC})} \tag{3.9-7}$$

$\left(\frac{\Delta z_i}{A}\right)_b$ and $\left(\frac{\Delta z_i}{A}\right)_t$ are effective inertial terms at the bottom and top of the subassembly.

$$I_2 = \sum_{JC=1}^{\mathrm{MZC-1}} X_{I2}(\mathrm{JC}) \tag{3.9-8}$$

$$X_{I2}(\mathrm{JC}) = \frac{1}{A_c(\mathrm{JC})^2}\left[\frac{1}{\rho_c(\mathrm{JC+1})} - \frac{1}{\rho_c(\mathrm{JC})}\right] \tag{3.9-9}$$

$$I_3 = \int \frac{1}{2\rho_c A_c^2 D_h}\left[\frac{D_h}{\mu A_c}\right]^{b_{fr}} dz = \sum_{JC=1}^{\mathrm{MXC-1}} X_{I3}(\mathrm{JC}) \tag{3.9-10}$$

$$X_{13}(\mathrm{JC}) = \frac{\Delta z(\mathrm{JC})}{[\rho_c(\mathrm{JC}) + \rho_c(\mathrm{JC}+1)]A_c(\mathrm{JC})^2 D_h(\mathrm{JC})}\left[\frac{D_h(\mathrm{JC})}{\bar{\mu}(\mathrm{JC})A_o(\mathrm{JC})}\right]^{b_{fr}} \tag{3.9-11}$$

$$I_4 = \sum_{\mathrm{JC=1}}^{\mathrm{MZC-1}} K_{or}(\mathrm{JC}) \tag{3.9-12}$$

$$I_5 = \int \rho_c \, dz = \sum_{\mathrm{JC=1}}^{\mathrm{MXC-1}} X_{I5}(\mathrm{JC}) \tag{3.9-13}$$

$$X_{I5}(\mathrm{JC}) = .5\left[\rho_c(\mathrm{JC}) + \rho_c(\mathrm{JC+1})\right]\Delta z(\mathrm{JC}) \tag{3.9-14}$$

p_b = pressure at bottom of channel, and p_t – pressure at top of channel.

3.9.3 Flow Orifices

As mentioned in the section on the SAS channel treatment in Section 3.2, the channel is divided axially into a number of zones. One zone represents the fuel-pin region. Other zones represent regions above and below the fuel pins. At the bottom of each zone, a flow direction dependent orifice coefficient can be specified by the user. Another orifice coefficient can be used at the top of the upper zone. These orifices can represent orifice blocks, subassembly inlet and exit losses, and the pin support grid at the bottom of the pins. For each orifice, the user supplies one orifice coefficient for

positive flow and another for negative flow. In addition, in the fuel-pin region, orifice coefficients representing equally spaced grid spacers can be specified. These orifice coefficients are used as the values of $K_{or}(JC)$ in Eq. 3.9-12 for the appropriate axial nodes. The effect of each orifice is spread evenly over an axial node, rather than concentrated at a point.

3.9.4 Finite Difference Equations – Coolant Flow Rates

If $w_1 = w(t), w_2 = w(t + \Delta t), \Delta w = w_2 - w_1$, then we approximate Δw as

$$\Delta w = \left[\theta_1 \left.\frac{\partial w}{\partial t}\right|_t + \theta_2 \left.\frac{\partial w}{\partial t}\right|_{t+\Delta t}\right] \Delta t \tag{3.9-15}$$

and

$$\theta_1 + \theta_2 = 1.0 \tag{3.9-16}$$

in which θ_2 is the degree of implicitness. For small time steps a semi-implicit calculation is used, with $\theta_1 = \theta_2 = .5$. For a fully implicit calculation for large time steps, $\theta_1 = 0$ and $\theta_2 = 1.0$. The value used for θ_2 is

$$\theta_2 = \frac{6.12992 + 2.66054x + x^2}{2x\,6.12992 + 3.56284x + x^2} \tag{3.9-17}$$

where

$$\mathrm{x} = \Delta \mathrm{t}/\tau \tag{3.9-18}$$

and τ is the time constant for flow rate changes given by

$$\tau = I_1/d_1 \tag{3.9-19}$$

The definition of d_1 is given by Eq. 3.9-25 below. This correlation for θ_2 is discussed in Appendix 3.1. The additional approximations are made that

$$(w_1 + \Delta w)^2 \simeq w_1^2 + 2\Delta w\, w_1 \tag{3.9-20}$$

$$(w_1 + \Delta w)\,|w_1 + \Delta w| \simeq w_1\,|w_1| + 2|w_1|\Delta w \tag{3.9-21}$$

$$(w_1 + \Delta w)|w_1 + \Delta w|^{1+b_{fr}} \simeq w_1|w_1|^{1+b_{fr}} + (2 + b_{fr})|w_1|^{1+b_{fr}}\,\Delta w \tag{3.9-22}$$

These equations are combined to give

$$I_1\frac{\Delta w}{\Delta t}+\theta_1(p_{t1}-p_{b1})+\theta_2(p_{t2}-p_{b2})+I_2(w_1^2+2\theta_2 w_1\Delta w)$$
$$+A_{fr}I_3\left[w_1|w_1|^{1+b_{fr}}+\theta_2\left(2+b_{fr}\right)|w_1|^{1+b_{fr}}\Delta w\right] \quad (3.9\text{-}23)$$
$$+I_4(w_1|w_1|+2\theta_2|w_1|\Delta w)+gI_5=0$$

where p_{t1} and p_{t2} are the pressures at the top of the subassembly at the beginning and end of the time step. Similarly, p_{b1} and p_{b2} are the pressures at the bottom of the subassembly at the beginning and end of the time step, respectively.

Solving for the coolant flow rate change, Δw, gives

$$\Delta w=\Delta t\Big[\theta_1\left(p_{b1}-p_{t1}\right)+\theta_2\left(p_{b2}-p_{t2}\right)-I_2w_1^2-A_{fr}I_3w_1\left|w_1\right|^{1+b_{fr}}$$
$$-I_4w_1\left|w_1\right|-g\,I_5\Big]/\left(I_1+\Delta t\,\theta_2 d_1\right) \quad (3.9\text{-}24)$$

where

$$d_1=2\,w_1\,I_2+\left(2+b_{fr}\right)|w_1|^{1+b_{fr}}\,A_{fr}\,I_3+2\,|w_1|\,I_4 \quad (3.9\text{-}25)$$

The temperatures used to evaluate ρ_c and $\bar{\mu}$ in Eqs. 3.9-9, 3.9-11, and 3.9-14 are extrapolated coolant temperatures, extrapolated to the end of the coolant step.

3.9.5 Coolant Pressures

After the flow rate has been calculated, the coolant pressures in a channel at the end of a time step are calculated. First, the pressure at node MZC, the last node at the top of the subassembly, is calculated as

$$p(\mathrm{MXC})=p_{t2}+\left[\frac{\Delta z_i}{A}\right]_t\frac{\partial w}{\partial t} \quad (3.9\text{-}26)$$

where

$$\mathrm{p_{t2}}=p_{x2}+\rho_{cout}\,g\,\left[z_{plu}-z_c(\mathrm{MZC})\right] \quad (3.9\text{-}27)$$

$\mathrm{z_{phi}}$ = outlet plenum elevation

ρ_{cout} = density at outlet

p_{x2} = coolant outlet plenum pressure at the end of the time step

Note that p_{x2}, the outlet plenum pressure supplied by the primary loop module, is defined at an elevation z_{plu}, the elevation of the upper plenum, whereas $p(\mathrm{MZC})$ is calculated at $z(\mathrm{MZC})$, so the gravity head term occurs in Eq. 3.9-27.

After $p(\mathrm{MZC})$ has been calculated, the other pressures are calculated, starting at node MZC-1 working down, using

$$p(\mathrm{JC}) = p(\mathrm{JC}+1) + X_{I1}(\mathrm{JC})\frac{\partial w}{\partial t} + w^2 X_{I2}(\mathrm{JC}) + A_{fr}\, w|w|^{1+b_{fr}} X_{I3}(\mathrm{JC}) + |w| w K_{or}(\mathrm{JC}) + g X_{I5}(\mathrm{JC}) \tag{3.9-28}$$

In Eqs. 3.9-25 and 3.9-28, the value used for $\partial w/\partial t$ is calculated at the end of the time step for the transient calculation as

$$\frac{\partial w}{\partial t} = \left[p_{b2} - p_{t2} - w_2^2 I_2 - A_{fr} w_2 |w_2|^{1+b_{fr}} I_3 - w_2 |w_2| I_4 - g I_5\right] / I_1 \tag{3.9-29}$$

The pressure, p_{b2} at the bottom of the subassembly at the end of the time step is calculated as

$$p_{b2} = p_{in2} - \rho_{cin}\, g\left[z_c(1) - z_{p\ell\ell}\right] \tag{3.9-30}$$

$z_{p\ell\ell}$ = plenum location. Note that p_{in2}, the inlet plenum pressure supplied by he primary loop module, is defined at an elevation $z_{p\ell\ell}$, the elevation of the lower plenum.

The pressure distribution in the steady state is calculated the same as in the transient, except that $\partial w/\partial t$ is zero in the steady-state calculation.

3.10 Multiple-Pin Model

3.10.1 Introduction

The new multiple pin treatment was added to the code to account for pin-to-pin variations within a subassembly. This new multiple pin treatment can be used in at least two different ways. One approach is to use the new treatment to compute nominal or "best estimate" variations within a subassembly. Another approach is to compute hot channel behavior due to postulated deviations in coolant flow rate, coolant flow area, and pin power. When doing a whole-core analysis, one probably would not want the hot channel temperatures used in reactivity feedback calculation or in the core outlet temperatures that feed into the primary loop calculations. Therefore, one would probably use parallel treatments for the same subassembly: a nominal one-pin or multi-pin treatment used for reactivity feedback, plus a hot channel treatment decoupled from the reactivity feedback and from the primary loop calculation. The hot

channel treatment would be de-coupled by setting reactivity feedback coefficients to zero and by setting the number of subassemblies represented by this treatment to zero.

The new multiple pin treatment allows a number of coupled channels to be used to model a single subassembly. Thus a channel can represent a part of a subassembly instead of the whole subassembly. Peaking factors can be mechanistically calculated by reducing coolant flow areas and flow rates or increasing pin power levels in some channels.

As previously mentioned, the multiple pin option is currently only available for steady-state and single phase transient calculations.

3.10.2 Physical Model

In the new multiple pin option, the regions above and below the pin section of a subassembly are still represented by a single channel; but a number of channels can be used to represent the pin section. Each channel in the pin section can represent one or more concentric rows of pins and their associated coolant. It is also possible for channels to represent slices of pins for a subassembly with a strong lateral power skew or for one with a hot subassembly on one side and a cool subassembly on the opposite side. Figure 3.10-1 illustrates one way that a number of channels can be used to model the pin section of a subassembly as concentric rings of pins and coolant subchannels. The thimble flow region in this figure is a feature of the EBR-II XX09 instrumented subassembly and is not found in ordinary subassemblies. This case concentrates on the coolant subchannels and splits the pins. It is also possible to shift the channel boundaries half a pin and use a pin-based representation with intact pins and split coolant subchannels. Currently up to 56 channels can be used to represent a subassembly.

The new option accounts for coolant-to-coolant heat transfer between adjacent channels, including the effects of both conduction and turbulent mixing. It also accounts for subassembly-to-subasembly heat transfer from the duct wall of a subassembly, through the interstitial sodium, to the duct wall of a neighboring subassembly. In addition, axial conduction in the coolant is accounted for.

Figure 3.10-2 illustrates the axial representation of the subassembly flow, with parallel flow paths through the pin section. Each channel used to represent the pin section of subassembly has its own separate time-dependent flow rate, and the flow rates in all channels in a subassembly are driven by common pressures at the inlet and outlet of the pin section. Thus, transient flow redistribution among channels is accounted for. The single flow rate in the regions above and below the pin section is the sum of the pin section flow rates, so the subassembly flow orifice sees the correct total flow rate. Even though the coolant-to-coolant heat transfer coefficient includes a term for turbulent mixing between coolant subchannels, one effect that the flow calculation does not account for is mass flow between channels in the pin section, although cross-flow at the ends of the pin section is allowed. Therefore, if recirculation loops occur within a subassembly at low flows, the model would calculate them; but the recirculation loops would go to the ends of the pin section.

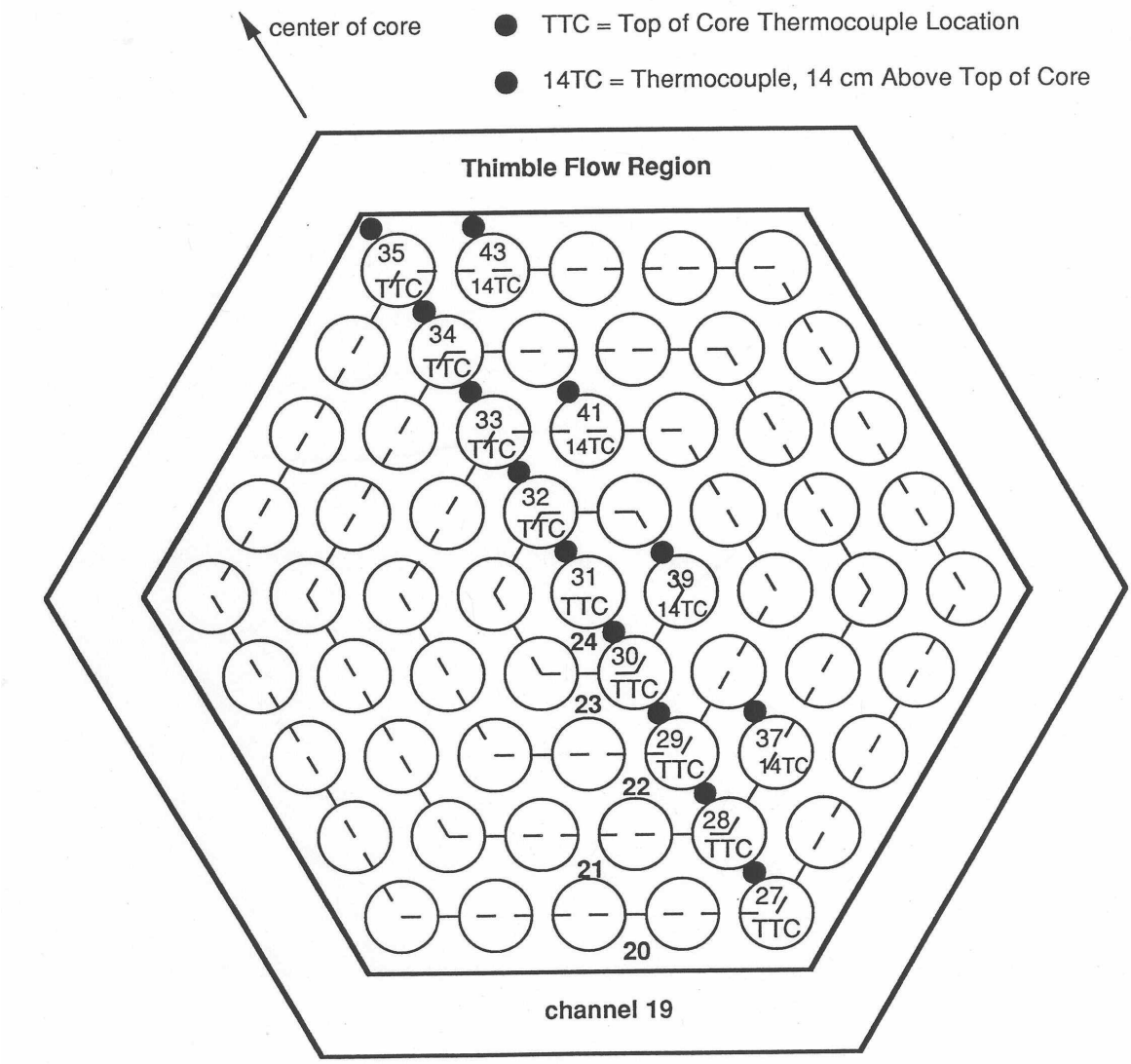

Figure 3.10-1: SASSYS-1 Multiple Pin Representation and Thermocouple Locations for the EBR-II XX09 Instrumented Subassembly

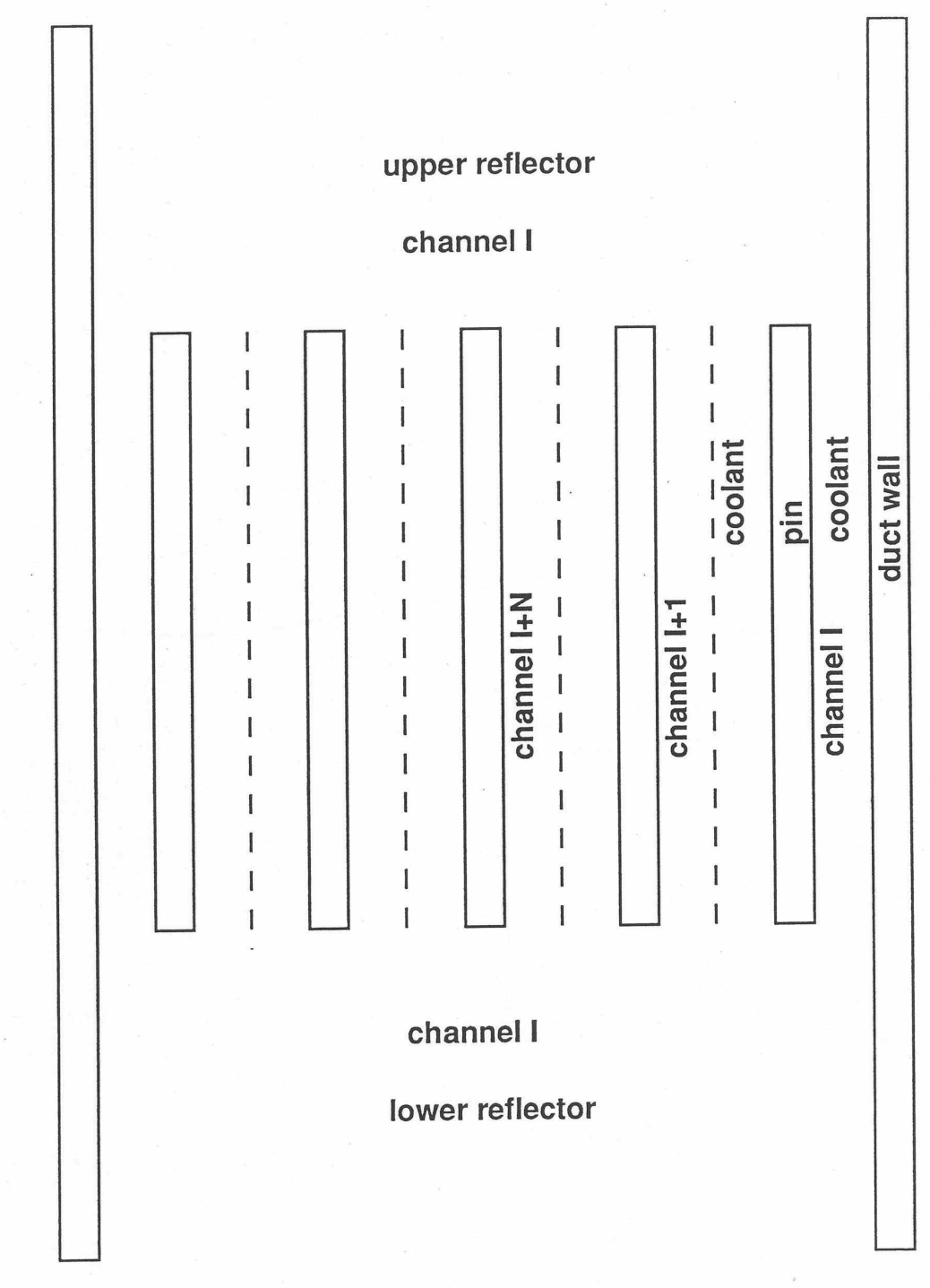

Figure 3.10-2: SASSYS-1 Multiple Pin Treatment of a Subassembly

In the new model the coolant in channel I can transfer heat directly to the coolant in channel I-1 and channel I+1. Using correlations of the same form as those used in THI3D code [3-6] and the HOTCHAN code [3-7], the channel-to-channel heat flow per pin per unit height from channel I to channel I+1 is calculated as:

$$Q_{I,I+1} = \left[U_1 \bar{k} + U_2 \, \bar{C}\left(w_1 + w_{I+1}\right)\right]\left(T_{I-T_{I+1}}\right) \tag{3.10-1}$$

where

$\bar{k}$ = average thermal conductivity of the coolant

$\bar{C}$ = average specific heat

w_i = coolant mass flow per pin (kg/s) in channel I,

and

T_I = coolant temperature

In this equation U_I is a geometry factor for thermal conduction, and U_2 is a product of a turbulent-mixing coefficient and a geometry factor for turbulent mixing between channels. Since a SASSYS-1 channel usually models a group of coolant sub-channels, the values used for U_1 and U_2 must account for a combination of parallel and series heat flow paths between the middle of channel I and the middle of channel $I+1$. Subassembly-to-subssembly heat transfer is handled in a somewhat simpler manner. For heat transfer from the outer surface of the structure in channel I to the outer surface of the structure in channel J, a constant value is used for the produce of the heat transfer coefficient and the heat transfer area per unit height.

3.10.3 Numerical Methods

Most of the transient heat transfer calculations and flow rate calculations in SASSYS-1 use semi-implicit time differencing in order to obtain stable and accurate solutions with reasonably long time steps. Before the onset of coolant boiling or pin disruption, time step sizes of a second or more are commonly used; and the code usually runs significantly faster than real time on a Cray XMP computer.

From a numerical computation point of view, the two main tasks in adding the multiple pin model to the code were the coolant-to-coolant heat transfer calculation and the coolant flow rate calculation with parallel flow paths in the pin section. Both of these calculations use semi-implicit time differencing. In the single-pin model, coolant temperatures for all of the radial temperature nodes in the pin, coolant, and structure at one axial node are solved for simultaneously in order to obtain a semi-implicit time differencing solution without iteration. In the new multiple-pin treatment, this concept is carried one step further. At a given axial node, temperature at all of the radial nodes for all channels representing a subassembly are solved for simultaneously. In the heat transfer calculations, the axial conduction terms, which are small, are treated with explicit forward time differencing so that axial nodes are decoupled and can be treated

separately except for the coolant convection terms. The axial coupling due to the coolant convection terms is handled by starting at one end of the subassembly and solving for axial nodes one at a time in the direction of the flow. If flow has reversed in some channels but not in others, the calculation progresses in the direction of the dominate flow; and explicit forward differencing is used for the coolant convection terms in the non-dominate flow direction channels. The subassembly-to-subassembly heat fluxes are calculated with explicit forward differencing in time, and this does impose a stability limit on the time step size. For typical subassembly duct wall thicknesses, the explicit subassembly-to-subassembly heat flux calculation limits the maximum time step size to a value in the range from .25 to .5 seconds. For the coolant flow rate calculations, the incompressible flow momentum equations are linearized about conditions at the beginning of the time step. Then, flow at the end of the step are calculated for all channels in a subassembly simultaneously.

A null transient is used to obtain steady-state temperatures at the start of the regular transient. First all coolant, pin, structure, and reflector temperatures in all subassemblies are set to the coolant inlet temperature. Then, the power levels and coolant flow rates are held constant while a number of transient heat transfer time steps are made. Since the pin thermal time constant and the coolant transit time through a subassembly are both less than a second, the null transient results converge rapidly if reasonably large time steps are used.

3.10.4 Detailed Mathematical Treatment

The main computational parts of the new multiple pin model are the heat transfer calculations in the pin section of a subassembly, the coolant flow rate calculations for a subassembly, the subassembly-to-subassembly heat transfer, and changes to the driver routines to call the appropriate new routines at the proper times. The pin section heat transfer calculations are done in two new subroutines: TSHTM3 calculates temperatures in the core and axial blankets, and TSHTM2 calculates temperatures in the gas plenum region. The existing TSHTN1 still calculates temperatures in the reflector zones above and below the pin section, but it was modified. TSHTN1 had to be modified slightly to pick up mixed mean outlet temperatures from the multiple channels representing the pin section. Also, axial conduction in the coolant was added to TSHTN1. The new TSCLM1 routine calculates transient coolant flow rates for a subassembly. The subassembly-to-subassembly heat fluxes are calculated in CHCHFL.

3.10.4.1 Heat Transfer Calculations in the Core and Axial Blankets: Subroutine TSHTM3

The multiple pin heat transfer calculations for the core and axial blankets in subroutine TSHTM3 are similar to the single pin calculations in the existing subroutine TSHTN3, as described in Section 3.3.1. One difference is that TSHTN3 does one time step for one channel each time it is called, whereas TSHTM3 solves for temperatures in all pins or channels representing a subassembly when it is called. Also, TSHTM3 adds extra terms for coolant-to-coolant heat transfer; and TSHTM3 includes axial conduction in the coolant.

Within a fuel pin, one-dimensional radial heat transfer is used. The basic heat

transfer equation is Eq. 3.3-1. This part of the calculation in TSHTM3 is identical to the corresponding calculation in TSHTN3.

For the coolant in channel I, the heat transfer calculations are basically one-dimensional in the axial direction, with extra terms for coolant-to-coolant heat transfer from channel I-1 and I+1. The basic heat transfer equation is:

$$\rho c A_c \frac{\partial T}{\partial t} + \frac{\partial}{\partial z}\left(wcT\right) = Q_T A_c \tag{3.10-2}$$

where

A_c = coolant flow area

z = axial position

w = coolant mass flow rate

and

Q_r = total heat source per unit volume

The heat source contains a number of terms:

$$Q_T = Q_c + Q_{ec} + Q_{sc} + Q_{ax} + Q'_{I-1,I} - Q'_{I,I+1} \tag{3.10-3}$$

where

Q_c = source due to direct heating of the coolant by neutrons and gamma rays,

Q_{ec} = heat flow from cladding to coolant,

Q_{sc} = heat flow from structure to coolant,

Q_{ax} = axial conduction source, given by

$$Q_{ax} = \frac{\partial}{\partial z} k \frac{\partial T}{\partial z} \tag{3.10-4}$$

and

$$Q'_{I,I+1} = \frac{Q_{I,I+1}}{A_c} \tag{3.10-5}$$

where $Q'_{I,I+1}$ is given by equation 3.10-1. Note that Eq. 3.10-2 is the same as Eq. 3.3-5, except that additional source terms are included in the multiple pin model.

Finite differencing in space and time is used to solve these heat transfer equations. Figure 3.2-3 shows the axial and radial mesh used for a single channel. In the multiple pin model the pin section mesh is repeated for each channel, but the axial reflector zones are only used in the first channel used to represent a subassembly. At each axial node in the core and axial blankets a number of radial nodes are used for the fuel, three radial nodes are used for the cladding, one node is used in the coolant, and two nodes are used in the structure. All channels, representing a subassembly must use the same axial mesh. Also, all subassemblies connected by subassembly-to-subassembly heat transfer must use the same axial mesh.

For a given time step, Eqs. 3.3-1 and 3.10-2 become linear finite difference equations. The temperatures are known at the beginning of the time step, and the temperature at the end of the step are the unknowns to be solved for. Semi-implicit time differencing is used for all terms except the axial conduction terms Q_{ax}, and the coolant-to-coolant terms $Q_{I-1,I}$ and $Q'_{I,I+1}$. The Q_{ax} axial conduction term is calculated explicitly based on temperatures at the beginning of the time step. The coolant-to-coolant terms are calculated fully implicitly, using the coolant flow rates and temperatures at the end of the step.

After finite differencing for one axial node, one obtains N simultaneous liner equations in N unknowns, where the unknowns are the temperatures at the end of the time step for all radial nodes in all channels representing the subassembly. These equations are solved by Gaussian elimination. The equations are basically tri-diagonal, with extra non-tri-diagonal terms for coolant-to-coolant heat transfer between channels. No full N by N matrix is ever set up by TSHTM3, and a general full matrix solution package is not used. Instead, only non-zero terms are computed and stored; and the Gaussian elimination solution was written specifically for this set of equations. The result is that the storage requirements vary linearly, rather than quadratically, with the maximum allowable value for N; and the computation time varies linearly, rather than quadratically, with the actual value of N.

3.10.4.2 Heat Transfer Calculations in the Gas Plenum Region: Subroutine TSHTM2

Subroutine TSHTM2 does the heat transfer calculations for one time step for all axial nodes in the gas plenum region for all channels representing a subassembly when it is called. TSHTM2 is similar to TSHTM3, but TSHTM2 deals with fewer radial nodes. As shown in Figure 3.2-5, in the plenum region there are still two radial nodes in the structure and one in the coolant; but there is only one in the cladding; and there are no fuel nodes. Instead of fuel temperatures there is one gas temperature common to all of the axial nodes in a pin. As in TSHTM3, for a given axial node TSHTM2 solves simultaneously for temperatures at all radial modes in all channels representing a subassembly.

One special problem in TSHTM2 is the gas temperature, which is common to all axial nodes in the gas plenum region of a pin. Axial nodes are handled one at a time, rather than simultaneously, whereas a semi-implicit time differencing treatment would require solving for all axial nodes simultaneously. The new multiple-pin TSHTM2 routine handles this problem in a simpler manner than the old single-pin TSHTN2. The

way that the gas temperature is handled is TSHTM2 is to calculate a separate gas temperature for each axial node. At the beginning of the time step, the gas temperatures at all axial nodes are set to one common value. Then separate values are calculated for each axial node at the end of the step. Finally, an average of the separate values is calculated for the one common value at the ed of the step.

3.10.4.3 Coolant Flow Rates: Subassembly TSCLM1

The coolant for rate calculation for a subassembly in the multiple-pin routine TSCLM1 is much more complex than the corresponding calculation in the single pin routine TSCNV1. As shown in Figure 3.10-2, the multiple pin calculation involves multiple parallel flow paths in the pin section, in series with single flow paths in the reflector regions. Therefore, the multiple-pin routine TSCLM1 was written from scratch, rather than starting form the single pin TSCNV1 routine.

Figure 3.10-3 illustrates the main variables used in TSCLM1.

Incompressible flow is used for these calculations, so conservation of mass gives

$$N_1 w_r = \sum_k w_{pk} N_k \tag{3.10-6}$$

where

w_r = coolant mass flow rate per pin in the reflector zones,

w_{pk} = pin section coolant mass flow rate per pin in channel k,

N_k = number of pins in channel k,

and

I = channel number of the first channel representing the subassembly.

The momentum equation for the pin section is

$$\frac{L_p}{A_{cpk}} \frac{dw_{pk}}{dt} = p_b - p_c - \Delta p_{pk} \tag{3.10-7}$$

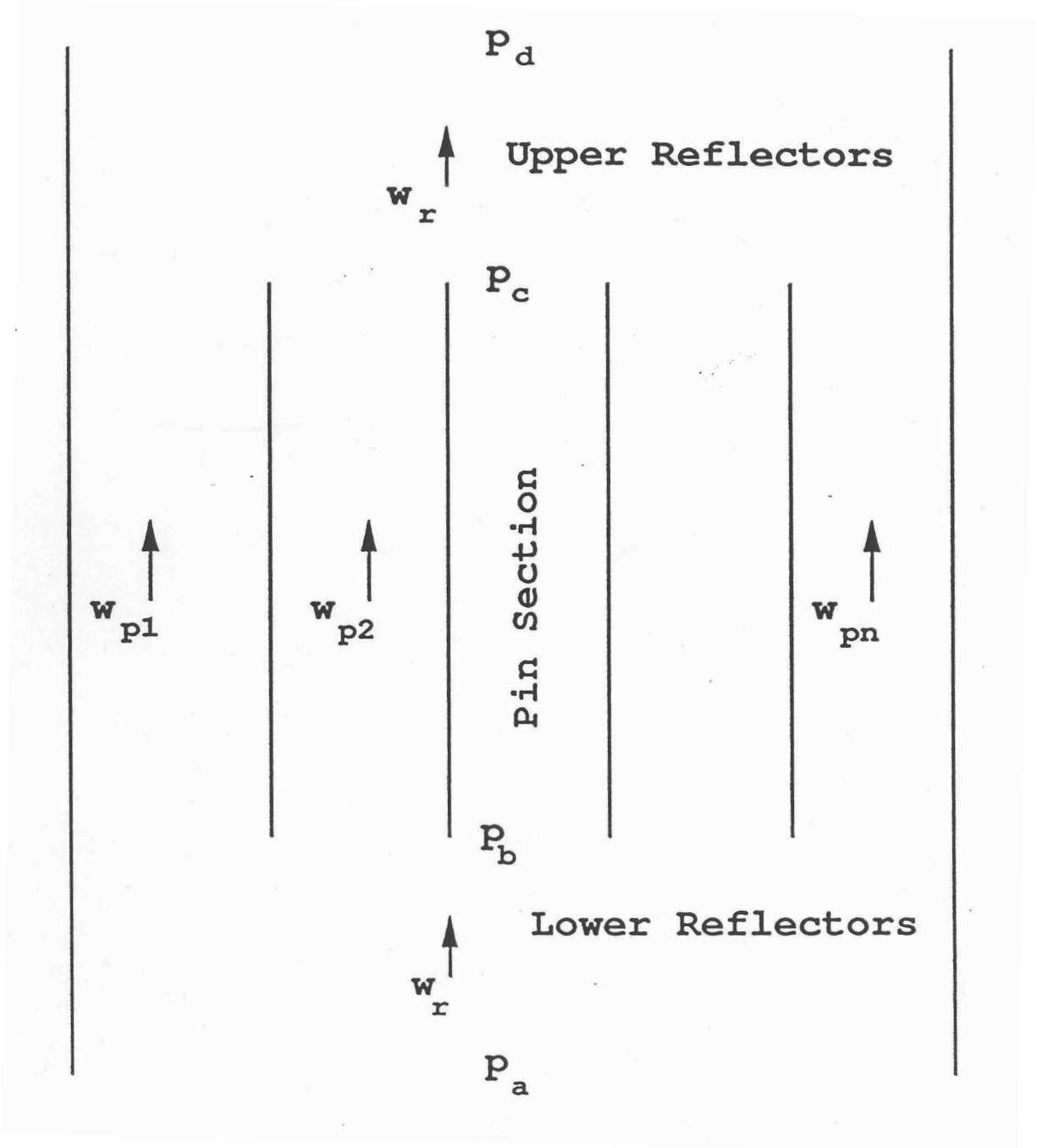

Figure 3.10-3: Subassembly Coolant Flows

where

L_p = length of pins,

A_{cpk} = coolant flow area in channel k in the pin section,

t = time,

p_b = coolant pressure at the bottom of the pins,

p_c = coolant pressure at the top of the pins,

$$\Delta p_{pk} = \text{pressure loss} = \sum_{jv=\text{JCPNBT}}^{\text{JCPNTM}} \Delta p_{kjc} \tag{3.10-8}$$

jc = axial coolant node,

JCPNBT = first axial node in the pin section

JCPNTM = last axial node in the pin section,

and

Δp_{kjc} = pressure loss in axial node jc of channel *k*.

The pressure loss contains a number of terms:

$$\Delta p_{kjc} = \Delta p_{frkjc} + \Delta p_{grkjc} + \Delta p_{orkjc} + \Delta p_{acckjc} \tag{3.10-9}$$

where

$$\Delta p_{frkjc} = \text{friction loss} = \frac{f_{kjc}\,\Delta z_{jc}\,w_{pk}\left|w_{pk}\right|}{2\bar{\rho}_{ckjc}\,A_{cpk}\,D_{hpk}} \tag{3.10-10}$$

$$\Delta p_{grpjc} = \text{gravity head} = g\,\bar{p}_{ckjc}\,\Delta z_{jc} \tag{3.10-11}$$

$$\Delta p_{orfkjc} = \text{orifice loss} = \frac{K_{orkjc}\,w_{pk}\left|w_{ph}\right|}{2\bar{\rho}_{ckjc}\,A_{cpk}^2} \tag{3.10-12}$$

$$\Delta p_{acckjc} = \text{acceleration term} = \frac{w_{pk}^2}{A_{cpm}^2}\left(\frac{1}{\rho_{ckjc+1}} - \frac{1}{\rho_{ckjc}}\right) \tag{3.10-13}$$

Δz_{jc} = axial node length,

f_{kjc} = friction factor in channel k at node *jc*,

ρ_{ckjc} = coolant density at bottom of node *jc* in channel *k*,

$\bar{\rho}_{ckjc}$ = average coolant density in node *jc* in channel *k*,

D_{hpk} = Hydraulic diameter,

and

K_{orkjc} = orifice coefficient in node *jc* of channel *k*

The friction factor is calculated as in Eq. 3.9-3.

using

$$R_e = \text{Reynolds number} = \frac{D_{hpk}\left|w_{pk}\right|}{\mu_{kjc} A_{cpk}} \tag{3.10-14}$$

and

μ_{kjc} = viscosity of the coolant.

After semi-implicit finite differencing in time and linearization of the pressure drop terms, applying Eq. 3.10-7 to a time step from *t* to *t* + Δ*t* gives

$$\frac{L_p}{A_{cpk}}\frac{\Delta w_{pk}}{\Delta t} = p_b(t) + \theta_2 \Delta p_b - p_c(t) - \theta_2 \Delta p_c - \Delta p_{pk}(t) - \theta_2 \Delta w_{pk} K_{wpk} \tag{3.10-15}$$

where

$$\Delta w_{pk} = w_{pk}(t + \Delta t) - w_{pk}(t) \tag{3.10-16}$$

$$\Delta p_b = p_b(t + \Delta t) - p_b(t) \tag{3.10-17}$$

$$\Delta p_c = p_c\left(t+\Delta t\right) - p_c\left(t\right) \tag{3.10-18}$$

θ_2 = degree of implicitness

$$\theta_1 = 1 - \theta_2 \tag{3.10-19}$$

$$K_{wpk} = \sum_{jc=\text{JCPNBT}}^{\text{JCPNTM}} K_{wpkjc} \tag{3.10-20}$$

$$K_{wpkjc} = \frac{\partial \Delta p_{kjc}}{\partial w_{pk}} = K_{frkjc} + K_{wcrkjc} + K_{acckjc} \tag{3.10-21}$$

$$K_{frkjc} = \begin{cases} \left(2+b_{fr}\right)\dfrac{\Delta p_{frkjc}\left(t\right)}{w_{pk}\left(t\right)} & \text{if } R_{ckjc} \geq R_{et} \\ \dfrac{\Delta p_{frkjc}\left(t\right)}{w_{pk}\left(t\right)} & \text{if } R_{ckjc} < R_{et} \end{cases} \tag{3.10-22a}$$

or

$$K_{frkjc} = \left[\left(2+b_{fr}\right)A_{fr}\,A\left(\text{RE}\right)^{b_{fr}} + A_{fL}/\text{RE}\right]\frac{\Delta z_{jc}\left|w_{pk}\left(t\right)\right|}{2p_{ckjc}D_{hpk}A_{cpk}} \tag{3.10-22b}$$

$$K_{wpkjc} = \frac{2\Delta p_{orfkjc}\left(t\right)}{w_{pk}\left(t\right)} \tag{3.10-23}$$

and

$$k_{acckjc} = \frac{2\Delta p_{acckjc}\left(t\right)}{w_{pk}\left(t\right)} \tag{3.10-24}$$

Equation 3.10-15 can then be written as

$$\Delta p_b - \Delta p_c = d_{0\,pk} + d_{0\,pk} + d_{1pk}\Delta w_{pk} \tag{3.10-25}$$

where

$$d_{0pk} = \frac{p_c(t) - p_b(t) + \Delta p_{pk}(t)}{\theta_2} \tag{3.10-26}$$

and

$$d_{1pk} = \frac{L_p / A_{cpk} + \theta_2 \Delta t \, K_{wpk}}{\theta_2 \Delta t} \tag{3.10-27}$$

Applying a similar process to the upper and lower reflector regions gives:

$$\Delta p_b = D_{0\ell} + D_{1\ell} \sum_k \Delta w_{pk} \tag{3.10-28}$$

and

$$\Delta p_c = D_{0u} + D_{1u} \sum_k \Delta w_{pk} \tag{3.10-29}$$

where

$$D_{0\ell} = \frac{\theta_1 p_a(t) + \theta_2 \, p_a(t + \Delta t) - p_b(t) - \Delta p_\ell(t)}{\theta_2} \tag{3.10-30}$$

$$D_{1\ell} = \frac{-\sum_{KA=1}^{KZPIN-1} L_{kz} / A_{cKZ} - \theta_2 \Delta t \, K_{w\ell}}{\theta_2 \Delta t} \tag{3.10-31}$$

$$D_{0u} = \frac{\theta_1 p_d(t) + \theta_2 \, p_d(t + \Delta t) - p_c(t) + \Delta p_u(t)}{\theta_2} \tag{3.10-32}$$

$$D_{1u} = \frac{\sum_{KZ=KZPIN+1}^{KZM} L_{KZ} / A_{cKZ} + \theta_2 \Delta t \, K_{wu}}{\theta_2 \Delta t} \tag{3.10-33}$$

L_{KZ} = length of zone kz

A_{cKZ} = coolant flow area in zone kz

KZPIN = axial zone number of the pin section

KZM = last zone number

$$\Delta p_{\ell} = \sum_{jc=1}^{\text{JCPNBT}-1} \Delta p_{rjc} \tag{3.10-34}$$

$$\Delta p_{u} = \sum_{jc=\text{JCPNTP}}^{\text{MZCM1}} \Delta p_{rjc} \tag{3.10-35}$$

Δp_{rjc} = pressure loss in node *jc* of a reflector zone

JCPNBT = first axial node in pin section

JCPNTP = first axial node above the pin section

MZCM1 = last axial node

$$K_{w\ell} = \frac{\partial \Delta p_{\ell}}{\partial w_r} \tag{3.10-36}$$

and

$$K_{wu} = \frac{\partial \Delta p_{u}}{\partial w_u} \tag{3.10-37}$$

Then, combining Eqs. (3.10-25) and (3.10-28) gives

$$\Delta p_b = B_o + B_1 \Delta p_c \tag{3.10-38}$$

where

$$B_o = \frac{D_{o\ell} - D_{1\ell} S_1}{1 - D_{1f} S_o}, \tag{3.10-39}$$

$$B_1 = \frac{-D_{1l} S_o}{1 - D_{1l} S_o} \tag{3.10-40}$$

$$S_o = \sum_k \frac{1}{d_{1pk}}, \tag{3.10-41}$$

and

$$S_1 = \sum_k \frac{d_{opk}}{d_{1pk}}, \tag{3.10-42}$$

Similarly, combining Eqs. (3.10-25) and (3.10-29) gives

$$\Delta p_c = C_o + C_1 \Delta p_b \tag{3.10-43}$$

where

$$C_o = \frac{D_{ou} - D_{1u} S_1}{1 + D_{1u} S_o}, \tag{3.10-44}$$

and

$$C_1 = \frac{D_{1u} S_o}{1 + D_{1u} S_o}. \tag{3.10-45}$$

Combining Eqs. (3.10-38) and (3.10-43) gives

$$\Delta p_c = \frac{C_o + C_1 B_o}{1 - C_1 B_1} \tag{3.10-46}$$

Then Δp_b can be obtained from Eq. (3.10-38) and Δw_{bk} can be obtained from Eq. (3.10-25) for each channel.

After p_b, p_c, and the coolant flow rates have been calculated for the end of the time step it is possible to calculate the pressures. The pressure is calculated at the axial node boundaries. p_{kjc} is the pressure at the bottom (inlet end) of node *jc* in channel *k*. First, the nodal pressure loss at $t + \Delta t$ is calculated as

$$\Delta p_{pkjc}(t + \Delta t) = \Delta p_{kjc}(t) + K_{wpkjc}\, \Delta w_{pk} \tag{3.10-47}$$

and Δp_{pk} $(t + \Delta t)$ is calculated from Eq. (3.10-8). Then Eq. (3.10-7) is used to obtain $\frac{dw_{pk}(t + \Delta t)}{dt}$.

Integrating the momentum equation over one axial node gives

$$\frac{\Delta z_j}{A_{cpk}} \frac{dw_{pk}}{dt} = p_{pkjc} - p_{pkjc+1} - \Delta p_{kjc} \tag{3.10-48}$$

Starting by setting

$$p_{pkjJCPNTP} = P_c \tag{3.10-49}$$

the code marches down the channel, using Eq. (3.10-48) to obtain p_{pkjc} after p_{pkjc+1} has been calculated. A similar procedure is used for calculating the pressures in the upper and lower reflector zones.

The equation used to compute the degree of implicitness as a function of time step size in TSCMV1 is

$$\theta_2 = \frac{a + bx + x^2}{2a + cx + x^2} \tag{3.10-50}$$

where

$$x=\Delta t/\tau \tag{3.10-51}$$

τ = a time constant

a = 6.12992

b = 2.66054

and

c = 3.56284

The basis for this expression is given in Appendix 3.1. For a single channel treatment, the time constant, τ would be

$$\tau = \frac{\sum_{KZ=1}^{KZM} \frac{L_{KZ}}{A_{cKZ}} + \left(\frac{L_i}{A}\right)_i + \left(\frac{L_i}{A}\right)_x}{K_{wpk}\ K_{w1} + K_{wu}} \tag{3.10-52}$$

where

$\left(\frac{L_i}{A}\right)_i$ =extra coolant inertia term at the subassembly inlet to account for inertia of the coolant in the inlet plenum,

and

$\left(\frac{L_i}{A}\right)_x$ =same for the subassembly outlet.

Since a simultaneous solution of flows in all channels of an assembly plus the lower and upper reflector zones is required, the overall time constant is calculated as

$$\tau = \frac{\dfrac{L_p}{\sum_k A_{cpk}} + \sum_{kZ \neq KZPIN} \dfrac{L_{KZ}}{A_{cKZ}} + \left(\dfrac{L_i}{A}\right)_i + \left(\dfrac{L_i}{A}\right)_x}{K_{w1} + K_{wu} + \dfrac{1}{\sum_k \dfrac{1}{k_{wpk}}}} \qquad (3.10\text{-}53)$$

3.10.4.4 Data Management for the Multiple Pin Option

Implementation of the multiple pin option required modification of the data management philosophy is SASSYS-1. Basically, the data management in SASSYS-1 was based on the idea of treating one channel at a time, and data for only one channel was accessible at any given time. With the multiple pin treatment, it is necessary to deal with a number of channels simultaneously; so the old data management scheme was not sufficient.

The data management scheme in SASSYS-1 goes back many years to the SAS3D code. It was designed for optimum performance and portability on an earlier generation of computers with limited memory, sometimes a two level memory structure, and an ANSI Standard FORTRAN 66 that severely limited the form of expressions that could be used for array subscripts. With current computers, these considerations no longer apply. Memory is plentiful, explicit two level memory structures are not used, and the current ANSI Standard FORTRAN 77 allows much more general subscript expressions. Therefore, it was possible to come up with modifications to the SASSYS-1 data management scheme that make it possible to access data for a number of channels simultaneously without impairing performance or portability.

The SAS3D data management scheme was developed in response to problems with the earlier SAS3A code. SAS3A handled channel-dependent data by adding a channel subscript to all channel-dependent variables. The channel subscript was dimensioned for 10 channels. All data, other than few temporary variables, was stored in COMMON blocks that were available to all subroutines. This scheme had the advantage that all data for all channels was always available. This scheme also had some disadvantages, both obvious and subtle. One disadvantage was that the code required 10 channels worth of memory any time it was run, even if only one channel was actually being used for a particular case. At the time the SAS3A code was in use, most computers did not have enough memory to fit 10 channels worth of data. Even if enough memory was available, using a large amount of memory often required the use of non-standard, system-dependent features that reduced code portability and it difficult to take the code that ran on one computer and get it to run on another computer. Another obvious disadvantage was that SAS3D could not run any case bigger than 10 channels, even if enough memory was available. A subtle disadvantage of the use of a channel subscript on arrays is that many computers use a data cache between the central processor and

main memory. With a dimension of 10 for the channel subscript, about 90% of the data in the cache at any time may be for channels that are not currently being computed. Thus, the effectiveness of the cache is greatly reduced, and the code runs slower. One common way some of these problems are handled is through the use of the standard FORTRAN variable dimensioning capability that allows setting of maximum dimensions at run time, based on the size of the problem being run. The standard variable dimensioning approach is impractical or impossible with the SAS3A/SAS3D/SASSYS-1 codes because they use literally thousands of separate variable names for channel-dependent quantities.

The data management scheme developed for SAS3D and still used in SASSYS-1 and SAS4A uses a working memory and a storage area. All calculations are done with the data in the working memory. Data is stored in the storage area when it is currently not needed. The working memory contains both temporary variables and permanent variables. All permanent variables and most temporary variables are put in COMMON blocks. The permanent variables are saved in the storage area when they are not needed in the working memory, whereas temporary variables are not saved from the time step to time step. Data is moved from the working memory to the storage area and back in large blocks called data packs. Each data pack contains variables for only one channel or maybe for one module for one channel. The working memory is always a part of the central memory, whereas the storage area could in principle be either a dynamically allocated section of main memory or it could be on a disk. With a two level memory architecture, the working memory is in the smaller but faster level, whereas the storage area can be put in the larger but slower level. Data packs are moved between working memory and the storage area by a single subroutine, called DATMOV, which can be optimized for a particular computer. Code portability issues are then limited to the one routine DATMOV.

The modifications to the data management scheme in SASSYS-1 for the multiple pin option are based on the fact that currently the storage area is always in a dynamically allocated section of main memory. Explicit two level memory architectures are not currently used; and putting the storage area on a disk has proved to be impractical, because disk I/O is much too slow to keep up with the central processor speeds for SASSYS-1. Also, memory is now cheap, and plenty of memory is available on all machines where SASSYS-1 is likely to be run. Another aspect of the data management that is taken advantage of in the modifications is that the ordering of variables for a channel in the data storage area is the same as the ordering in the working area of blank common. When more than one channel is used to represent a subassembly, the data packs for the first channel are still moved into the working are by DATMOV, but the data for the rest of the channels stays in the storage area where it is accessed directly by adding the appropriate pointers to array subscripts. Thus, if T2(I,J) is a temperature at radial node I of axial node J, then a multiple-pin routine such as TSHTM3 refers to this variable as T2(I+IPT,J), where IPT is the channel-dependent pointer. For the first channel in the subassembly, IPT is set to 0, since DATMOV has put the data for the first channel into the COMMON block where the FORTRAN compiler expects it to be. For other channels, IPT is set to the offset between the working memory location and the storage area location for the channel. Since data packs are put into blank COMMON in

the working memory in the same order that they are stored in the storage area, the value of the pointer for all floating point variables for a given channel is the same. Also, the pointer for all integers in a channel is the same. The pointer for a floating point variable will be different form the pointer for an integer if the word length of integers is different from the word length of floating point variables. The channel dependent pointers are computed once at the beginning for the run and stored in a labeled COMMON block where they can be used by all routines. The subassembly-to-subassembly heat flux routine CHCHFL accesses temperatures from many different channels. CHCHFL uses only pointers to access different channels. It does not use DATMOV at all.

3.10.5 Relationship Between Single Pin and Multiple Pin Models

The single pin treatment and the multiple pin treatment coexist in the SASSYS-1 and SAS4A codes; it is possible to use single pin treatments for some subassemblies and multiple pin treatments for other subassemblies in the same problem. There are now two separate sets of subroutines in the codes for computing single phase thermal hydraulics: the single pin routines and multiple pin routines. Since the multiple pin model can handle the case of a single pin per subassembly, the single pin single phase thermal hydraulics subroutines are now redundant; and at some point in the future they will probably be removed from the code.

As previously mentioned, currently the multiple pin model is only available for steady state and single phase transient calculations; no multiple pin treatment is available in the codes for coolant boiling, pin disruption, or relocation of fuel or cladding. In the future, the multiple pin treatment will probably be extended to coolant boiling and to relocation of fuel and cladding.

3.11 Subassembly-to-subassembly Heat Transfer

SASSYS-1 contains a model for transferring heat from the duct wall of one subassembly, through the interstitial sodium, to the duct wall of an adjacent subassembly. During normal, full power operation the subassembly-to-subassembly heat flow is usually small compared to the power generation rate, but at decay heat power levels the heat flow between a subassembly and its neighbors can be comparable to the power generation rate within the subassembly. This heat flow between adjacent subassemblies will affect subassembly-to-subassembly flow re-distribution at low flow rates; and at low powers and flow rates it will tend to cause all subassemblies to have similar temperature rises.

The subassembly duct wall is normally represented by the structure in a SAS channel; so this mode is implemented by transferring heat from the outer structure nodes of a SAS channel to the outer structure nodes of other SAS channels or to a constant temperature heat sink. Also, it is possible to transfer heat from the outer structure node of one channel to the coolant of another channel. This option was included in the code in order to treat the thimble flow region shown in Fig. 3.10-1. The equation for the structure to structure heat flux, $Q_{I,M}(j)$, from channel I to channel M at axial node j is

$$Q_{I,M}(j) = \frac{(HA)_{I,M}}{N_{PI} N_{SI} S_{st1}} \left[T_{sto}(I,J) - T_{sto}(M,j) \right] \tag{3.11-1}$$

where

$(HA)_{I,M}$ = heat transfer coefficient times area per unit height, between channels I and M

T_{sto} = structure outer node temperature

N_{PI} = number of pins per subassembly in channel I

N_{SI} = number of subassemblies represented in channel I

S_{stI} = structure perimeter per pin in channel I

The SAS channel treatment only accounts for one structure per channel; so the channel-to-channel heat flux seen by the structure in a channel will be a sum of the heat fluxes to all adjacent channels. This heat flux is

$$Q_I(j) = \sum_M Q_{I,M}(j) \tag{3.11-2}$$

Each SAS channel can transfer heat to up to eight other channels. A subassembly has six nearest neighbors, but a channel can represent more than one subassembly. Therefore, a channel can be in contact with more than six other channels.

If the constant temperature heat sink option is used, then the user supplies values of T_{snk} and H_{snk} for each axial zone in the channel, and these values are held constant during the calculations.

In contrast to many of the other temperature calculations in the codes, explicit forward time differencing is used for the channel to channel heat transfer. The channel to channel heat fluxes are calculated at the beginning of each main time step using the temperatures at that time. These heat fluxes are then held constant during a time step. This explicit forward differencing imposes stability limits on the time step size. The stability limit is typically in the range of .2-.5 seconds.

At this point, the subassembly-to-subassembly heat transfer model has only been implemented in the transient single phase heat transfer calculations. It is necessary to run a null transient to obtain the current steady-state temperatures when subassembly-to-subassembly heat transfer is used.

3.12 Interaction with Other Models

As mentioned in Section 3.1, the heat-transfer routines interact with a number of other models. These interactions are indicated in Fig. 3.1-1.

If PRIMAR-4 is being used, then the subassembly coolant outlet temperatures calculated in the heat-transfer routines are used by PRIMAR-4 to calculate the outlet plenum temperature. Also, if flow reversal occurs in a channel, then the temperature calculated in the heat-transfer routines for the coolant leaving the bottom of the subassembly is used by PRIMAR-4 in the calculation of the inlet plenum temperature. Section 3.3.6 describes how the inlet and outlet plenum temperatures are used in the calculations of the subassembly coolant inlet and reentry temperatures.

Before the onset of voiding, TSHTRN calculates the coolant temperatures used in the coolant channel hydraulics calculations, and the hydraulics routines calculate the coolant flow rates used by TSHTRN.

After the onset of voiding, coolant temperatures are calculate din TSBOIL. This module supplies the heat flux at the cladding outer surface, as defined in Eq. 3.5-2 and used in Eq. 3.5-9 to TSHTRV. TSBOIL uses the calculated cladding temperatures form TSHTRV to obtain extrapolated cladding temperatures, as in Eq. 3.5-3, for use in its coolant temperature calculations.

The point kinetics model supplies the power level used in the heat-transfer routines. In return, the heat-transfer routines supply the temperatures used to calculate reactivity feedback.

3.12.1 Reactivity Feedback

The temperatures calculated in the core thermal hydraulics routines are used to calculate various components of reactivity feedback. These reactivity components include Doppler feedback, axial expansion of the fuel and cladding, density changes in the sodium, core radial expansion and control rod drive expansion. These reactivity feedbacks are described in Chapter 4.

3.12.2 Coupling Between Core Channels and PRIMAR-4

As described in Chapter 5, the PRIMAR-4 calculations for a PRIMAR time step are carried out before the core channel coolant calculations. PRIMAR-4 must make estimates of the core flows for a new time step, and it also makes corrections for the differences between its estimates for the previous step and values computed by the core channel coolant routines. The coolant routines supply information to PRIMAR-4 for use in these estimates and corrections. Also, PRIMAR-4 supplies inlet and outlet coolant plenum pressures and temperatures for the use in the core channel calculations.

The information supplied by PRIMAR-4 is

$p_{in}(t_{p1})$ = inlet plenum pressure at the beginning of the PRIMAR time step

$p_x(t_{p1})$ = outlet plenum pressure at the beginning of the PRIMAR time step

$\frac{dp_{in}}{dt}$ =time derivative of the inlet plenum pressure

$\frac{dp_x}{dt}$ =time derivative of the outlet plenum pressure

ρ_{cin} =coolant density in the inlet plenum

ρ_{cout} =coolant density in the outlet plenum

T_{cin} =coolant temperature in the inlet plenum

and

T_{cout} = coolant temperature in the outlet plenum

The pressure p_{in} is at an elevation $z_{p\ell\ell}$ and p_x is at z_{plu}. At any time, *t*, during the PRIMAR time step, the inlet plenum pressure is

$$p_{in}(t) = p_{in}(t_{p1}) + (t - t_{p1})\frac{dp_{in}}{dt} \tag{3.12-1}$$

and the exit plenum pressure is

$$p_x(t) = p_x(t_{p1}) + (t - t_{p1})\frac{dp_x}{dt} \tag{3.12-2}$$

The information supplied to PRIMAR-4 by the core coolant routines for channel *ic* at the subassembly inlet *(L=1)* or outlet *(L=2)* is the following:

$$\Delta m_c(L) - \sum_{ic} N_{ps}(ic) \int_{p1}^{t_{p2}} w(L,ic)\,dt, \tag{3.12-3}$$

$$\Delta m_c T_c(L) - \sum_{ic} N_{ps}(ic) \int_{p1}^{t_{p2}} w(L,ic) T_{ex}(L,ic)\,dt, \tag{3.12-4}$$

$w(L,ic,t = t_{p2})$ = computed flow rate at t_{p2}

$T_{ex}(L,ic)$ = coolant temperature at the subassembly inlet or outlet

$\Delta E_v(L,ic)$ = heat added to the inlet or outlet plenum by condensing sodium vapor. (This term is zero before the onset of boiling.)

and the coefficients $C_o(L,ic)$, $C_i(L,ic)$, $C_2(L,ic)$, and $C_3(L,ic)$ used by PRIMAR-4 to estimate

the core channel flow. PRIMAR-4 estimates the flow into or out or each subassembly using

$$\frac{dw_e(L,ic)}{dt} = C_0(L,ic) + C_1(L,ic)\,p_{in} + C_2(L,ic)\,p_x + C_3(L,ic)\,w_e(L,ic)\,\left|w_e(L,ic)\right| \tag{3.12-5}$$

The core channel calculations use w as the flow rate per pin, whereas PRIMAR-4 estimates the total flow represented by a channel, so $N_{ps}(ic)$, the number of pins per subassembly times the number of subassemblies represented by the channel, comes into Eqs. 3.12-3, 3.12-4 and the calculations of the coefficients C_0, C_1, C_2, and C_3. In the pre-voiding module the coefficients are calculated as

$$C_0 = -\frac{gN_{ps}\left[I_5 + \rho_{cin}\left(z_c(1) - z_{p\ell\ell}\right) + \rho_{cout}\left(z_{p\ell u} - z(MZC)\right)\right]}{I_1} \tag{3.12-6}$$

$$C_1 = \frac{N_{ps}}{I_1} \tag{3.12-7}$$

$$C_2 = -C_1 \tag{3.12-8}$$

and

$$C_3 = -\frac{\left(I_2 w_2 + A_{fr} I_3 \left|w_2\right|^{1+b_{fr}} + I_4 \left|w_2\right|\right)}{\left|w_2\right| I_1 N_{ps}} \tag{3.12-9}$$

In this case, the coefficients for L=2 are equal to those for L=1.

3.13 Subroutine Descriptions and Flowcharts

The subroutines used in the core-channel thermal hydraulics calculations are described below, grouped by the phase of the calculation where they are used.

Steady-state Thermal Hydraulics:

SSTHRM-- Driver for the steady-state calculations:

SSCOOL-- Calculations steady-state coolant, structure, reflector, and gas plenum temperature for each axial node. Also calculates coolant pressure and saturation temperature at each axial node.

SSCLM1-- Calculates steady-state coolant pressures and saturation temperatures for the multiple pin option.

SSHTR-- Calculates steady-state fuel and cladding temperatures in the core and

blankets.

SSNULL-- Driver for the steady-state null transient.

Pre-Voiding Transient Temperature Calculations:

TSCL0-- Driver of the pre-voiding thermal hydraulics.

TSHTRN-- Driver for the pre-voiding transient temperature calculations. Calls TSHTN1, TSHTN2, TSHTN3, TSHTN4, TSHTM2, and TSHTM3 as appropriate.

TSHTN1-- Calculates reflector, coolant, and structure temperatures in a reflector zone.

TSHTN2-- Calculates cladding, coolant, structure, and plenum gas temperatures in the gas plenum region.

TSHTN3-- Calculates fuel, cladding, coolant, and structure temperatures in the core and axial blankets.

TSHTN4-- Calculates the axial node size and the coolant density and specific heat for each axial code.

TSHTN5-- Called from TSHTN3 to adjust fuel and cladding temperatures to account for the heat of fusion if melting is occurring.

TSHTM2-- Multiple pin version of TSHTN2.

TSHTM3-- Multiple pin version of TSHTN3.

Fuel and Cladding Temperatures During Boiling:

TSBOIL-- Driver for the boiling module.

TSHTRV-- Calculates fuel and cladding temperatures in the core and axial blankets.

Pre-voiding Coolant Flow Rates and Pressures:

TSCHV1-- Extrapolates coolant temperatures, computes coolant flow rate and pressures. Also tests for start of boiling. Sets variables for coupling with PRIMAR-4. Called by TSCLO every coolant step.

TSCNV2-- Called by TSCNV1 to compute flow-rate coefficients x_{I1}(JC), x_{I2}(JC), x_{I3}(JC), and x_{I5}(JC).

TSCNV3-- Called by TSCLO, only at the end of a heat-transfer step, to get heat-transfer coefficients H_{erc}(JC) and H_{sic}(JC). Calls TSCNV8 to get liquid heat-transfer coefficients h_c(JC).

TSCNV7-- Computes ρ_c, μ_c for liquid sodium.

TSCNV8-- Computes liquid heat-transfer coefficient h_c (JC).

TSCLM1-- Multiple pin version of TSCNV1.

Auxiliary Routines:

CFUEL-- Calculates the specific heat of the fuel as a function of temperature. For coding efficiency, one call to CFUEL gives the specific heats for all radial nodes at an axial node, rather than using as separate call to CFUEL for each radial node of each axial node.

CCLAD-- Calculates the specific heat of the cladding as a function of temperature. One call to CCLAD returns the values for all axial nodes int eh core and axial blankets.

KFUEL-- Calculates the thermal conductivity of the fuel as a function of temperature. One call to KFUEL provides the values for all radial nodes at an axial node.

KCLAD-- Calculates cladding thermal conductivity as a function of temperature. One call to KCLAD returns the values for all axial nodes in the core and axial blankets.

INTRP-- General interpolation routine that uses linear interpolation from a table to obtain y as a function of x. A single call to INTRP with an array of x's will return an array of resulting y's.

SHAPE-- Multiplies the array of axial power shapes by the current time-dependent power to obtain the current power, in watts, at each axial node in a channel.

HBSMPL-- Calculates the bond gap conductance at each axial node if the simple bond gap conductance model is used. Otherwise, DEFORM-II calculates the bond gap conductance; and HBSMPL is not called.

INVRT3-- Solves a tri-diagonal matrix equation of arbitrary size.

Figure 3.1-2 is a flowchart for subroutine TSCLO, Fig. 3.13-1 is a flowchart for subroutine TSHTRN, and Fig. 3.13-2 is a flowchart for subroutine TSHTN3. The logic in the other pre-voiding single pin transient heat-transfer routines is very simple and straightforward. Subroutine TSHTRV is similar to TSHTN3, except that TSHTRV does not calculate coolant and structure temperatures. Also, in TSHTRV the axial nodes are completely de-coupled, so the order in which they are treated is immaterial. For simplicity, the axial node loop in TSHTRV always starts at the bottom and works up.

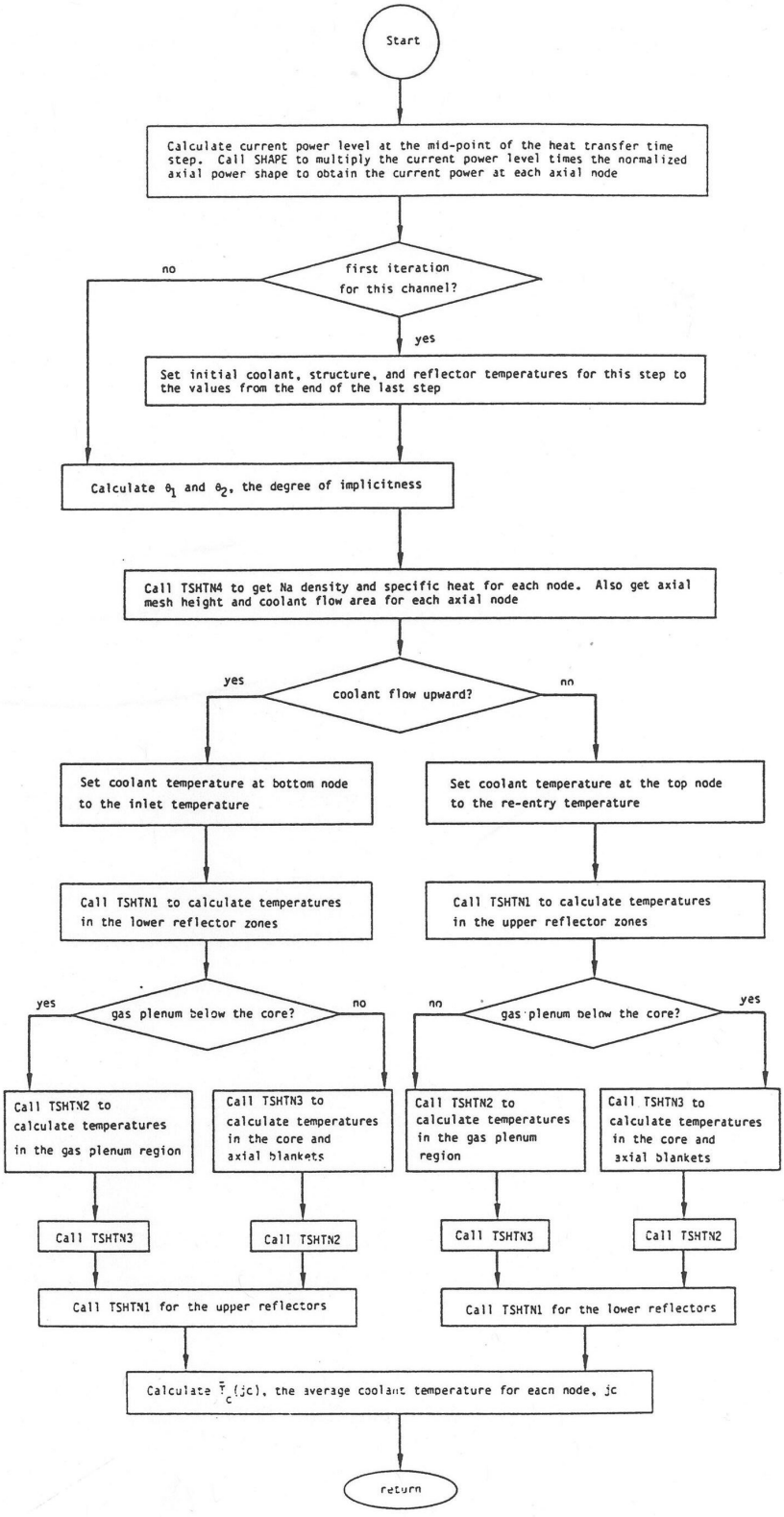

Figure 3.13-1: Flowchart for Subroutine TSHTRN

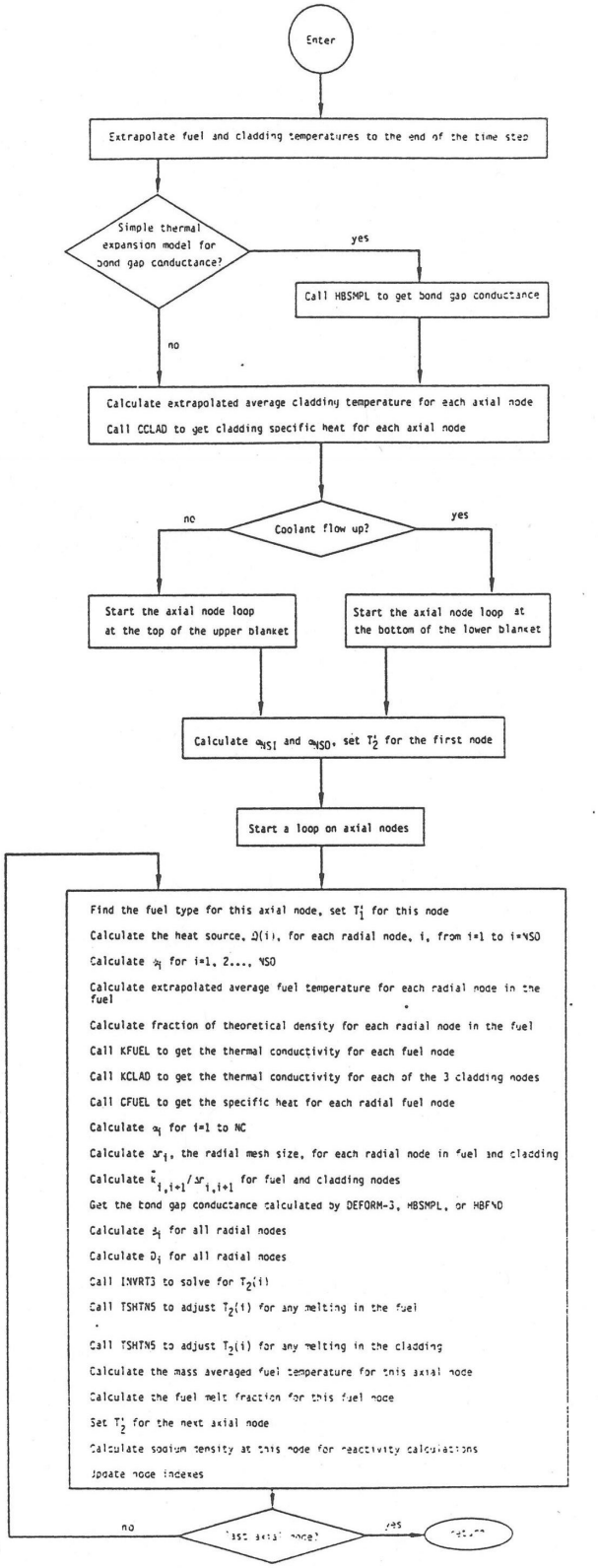

Figure 3.13-2: Flowchart for Subroutine TSHTN3

3.14 Input and Output

3.14.1 Input Description

The input variables used in the pre-voiding subassembly thermal hydraulics calculations are listed in Table 3.14-1. Some additional comments on some of these input variables are listed below.

3.14.1.1 Per Pin Basis

All of the core channel thermal hydraulic input to SASSYS-1 is on a per pin basis rather than a per subassembly basis. Thus, the initial flow rate, WO, is kg/s per pin; and the perimeters SRFSTZ and SER are perimeters per pin. Also, ACCZ is a coolant flow area per pin, and the variables DZIAB and DZIAT are ratios of inertial lengths to flow areas per pin.

3.14.1.2 Structure/Duct Wall and Wrapper Wires

Typically a SAS channel represents an average pin in a subassembly. In this case, the structure normally represents one pin's share of the duct wall, and it may also include the wrapper wire. If there are N pins in the subassembly, then the thickness used for the structure is the actual duct wall thickness, and the perimeter used for the structure is the duct wall perimeter divided by N. The wrapper wire can be either lumped with the cladding or included in the structure. Since wrapper wires are in much better contact with the cladding than with the duct wall, the most accurate treatment of the wrapper wire is probably to lump it with the cladding by increasing the specific heat of the cladding by enough to account for the total heat capacity of the cladding plus the wrapper wire. The cladding dimensions would not be changed.

The problem with lumping the wrapper wires with the duct wall to produce a single "structure" is that typically the duct wall has a much larger ratio of volume to wetted surface area than a wrapper wire, so the wrapper wire temperature will respond much more rapidly than the duct wall temperature to a change in coolant temperature. The heat capacity of the duct wall is considerably greater than the heat capacity of all of the wrapper wires in a subassembly, but the total perimeter of the wrapper wires is greater than the perimeter of the duct wall. If the duct wall and wrapper wires are lumped together, then the thickness of the structure should be determined by the thickness of the duct wall, since the duct wall contains most of the heat capacity. Then the perimeter of the structure should be chosen to conserve the total volume or total heat capacity of the duct wall plus wrapper wires.

A SAS channel can be used to represent a central pin rather than an average pin in a subassembly. In this case, the duct wall would probably be ignored, and the "structure: would represent only the wrapper wire. The perimeter of the structure would equal the perimeter of a wrapper wire, and the thickness of the structure would equal one half of the wrapper wire radius in order to conserve volume.

Table 3.14-1: Subassembly Thermal Hydraulics Input Variables

Variable	Reference Eq. No.	Input Variable	Input Block	Location Number	Suggested Value	External Reference
		NCHAN	1	1	1-34	
		IFUEL1	1	3	1-8	
		ICLAD1	1	4	1-3	
		ITKEL	1	7	0 or 1	
		IPOWOP	1	9	1	
		MAXSTP	1	11	--	
		IPO	1	12	20-50	
		IPOBOI	1	13	20-50	
		IBLPRT	1	14	0	
		INAS3D	1	29	0	
		ISSNUL	1	87	--	
		IPRSNL	1	88		
		EPSTEM	11	1	.1 or less	
		DTMXB	11	6	.01	
		DTFUEL	11	10	50.	
		DTCLAD	11	11	30.	
		POW	12	1		
ρ	3.3.1	COEFDS(1)	13	1	11080.	
		COEFDS(2)	13	2	2.04×10^{-5}	
		COEFDS(3)	13	3	8.70×10^{-9}	
k	3.3.1	COEFK	13	4		
k	3.3.1	EXKTB	13	11		
		EXKTM	13	71		
ρ	3.3.1	RHOTAB	13	91		
		RHOTEM	13	251		
k	3.3.1	XKTAB	13	420		
		XKTEM	13	580		
$\overline{c}_f$	3.3-16	CPFTAB	13	606		
		CPFTEM	13	766		
T_{sol}	3.3-92	TFSOL	13	786		
T_{liq}	3.3-93	TFLIQ	13	794		
U_{melt}	3.3-3	UFMELT	13	802		
U_{melt}	3.3-3	UEMELT	13	816		
c_e	3.3-32	CPCTAB	13	819		

Variable	Reference Eq. No.	Input Variable	Input Block	Location Number	Suggested Value	External Reference
$\rho_e c_e$		COCTEM	13	879		
		CROETB	13	990		
		CROETM	13	1050		
p_x	3.12-1	PX	14	1		
T_{in}	3.3-101	TOTAB	14	45		
		TOTME	14	65		
$z_{p\ell\ell}$	3.9-30	ZPLENL	14	87		
$z_{p\ell u}$	3.9-27	ZPLENU	14	88		
M_{mix}	3.3-99	XMXMSI	14	93		
M_{mix}	3.3-99	XMXMS0	14	94		
τ_{mix}	3.3-101	TIMMIX	14	95		
		IRHOK	51	3		
		NPLN	51	4	2-6	
		NREFB	51	5	1-5	
		NREFT	51	6	1-5	
		NZNODE	51	7		
NT		NT	51	14	4-11	
		IFUELV	51	15	1-IFUEL1	
		IFUELB	51	16	1-IFUEL1	
		ICLADV	51	17	1-ICLAD1	
		NGRDSP	51	18	0-10	
		IHGAP	51	24	0 or 1	
		NPIN	51	25	1 or more	
		NSUBAS	51	26	1 or more	
		MZUB	51	27	0-24	
		MZLB	51	28	0-24	
		ILAG	51	34	0	
		IEQMAS	51	118	0	
		IFRFAC	51	186		
		NCHCH	51	205		
		ICHCH	51	206		
		JJMLTP	51	214		
		IAXCON	51	284		
A_c	3.3-5	ACCZ	61	1	>0.	
Δ_z	3.3-6	AXHI	61	8	>0.	

Variable	Reference Eq. No.	Input Variable	Input Block	Location Number	Suggested Value	External Reference
D_h	3.3-9	DHZ	61	32	>0.	
d_{sti}	3.3-45	DSTIZ	61	39	>0.	
d_{sto}	3.3-47	DSTOZ	61	46	>0.	
		PLENL	61	53	>0.	
		RBR	61	54	>_ROUTFP	
		RER	61	78	>RBR	
r_{brp}	3.3-68	RBRPL	61	102	>0.	
r_{crp}	3.3-73	RERPL	61	103	>RBRPL	
		RINFP	61	104		
		ROUTFP	61	128	>RINFP	
		ZONEL	61	152	>0.	
S_{pt}	3.3-40	SRFSTZ	61	159		
		AREAPC	61	166	>0.	
d_{ro}	3.3-59	DRFO	61	169	>0.	
		RBRO	61	180	>0.	
		RERO	61	181	>0.	
S_{cr}	3.3-62	SER	61	182	>0.	
d_{ri}	3.3-56	DRFI	61	189	>0.	
N_{PI}	3.11-1	XXNPIN	61	274	>0.	
γ_s	3.3-22	GAMSS	62	2		
γ_c	3.3-6	GAMTNC	62	4		
γ_e	3.3-23	GAMTNE	62	5		
		PSHAPE	62	6		
P_r	3.3-22	PSHAPR	62	30		
		AHBPAR	63	2		
		BHBPAR	63	3		
		CHIBPAR	63	4		
		HBMAX	63	5		
		HBMIN	63	6		
		HBPAR	63	7		
k_{si}	3.3-43	XKSTIZ	63	11		
k_{so}	3.3-46	XKSTOZ	63	18		
$\varepsilon\sigma$	3.3-4	DEL	63	25		
k_r	3.3-57	XKRF	63	28		
$(\rho c)_{sti}$	3.3-45	RHOCSI	63	37	>0.	

Variable	Reference Eq. No.	Input Variable	Input Block	Location Number	Suggested Value	External Reference
$(\rho c)_{sto}$	3.3-47	RHOCSO	63	44	>0.	
$(\rho c)_r$	3.3-56	RHOCR	63	51	>0.	
$(\rho c)_g$	3.3-68	RHOCG	63	58	>0.	
R_g	3.3-71	RG	63	59	>0.	
α_f	3.10-4	FUELEX	63	73		
α_e	3.10-5	CLADEX	63	74		
Y_f	3.10-8	YFUEL	63	75		
Y_e	3.10-9	YCLAD	63	76		
		FULREX	63	77		
		CLDREX	63	78		
$(HA)_{I,M}$	3.11-1	HACHCH	63	82		
$1/\gamma_{ht}$	3.3-116	TAVINV	63	104	.5-5	
A_{fr}	3.8-3	AFR	64	1	.1875	
b_{fr}	3.8-3	BFR	64	2	-.2	
c_1	3.3-9	C1	64	3	.025	2-5
c_2	3.3-9	C2	64	4	.8	2-5
c_3	3.3-9	C3	64	5	4.8	2-5
		DWMAX	64	6	.2	
R_{eL}	3.9-3	RELAM	64	7	2100.	
A_{fL}	3.9-3	AFLAM	64	8	64.	
		WO	64	47		
K_{or}	3.9-12	XKORV	64	48		
		XKORGD	64	64		
$\left(\frac{\Delta z_i}{A}\right)_b$	3.9-6	DZIAB	64	65	>0.	
$\left(\frac{\Delta z_i}{A}\right)_f$	3.9-6	DZIAT	64	66		
T_{out}	3.3.-100	DTLMAX	64	69	15.	
U_1	3.10-1	TUPL	64	74		
U_2	3.10-2	UACH1	64	189		
		UACH2	64	190		

3.14.1.3 Empty Reflector Region

Sometimes a reflector zone is used to represent an empty section of a subassembly. The duct wall is usually represented by the structure; and since there is nothing but

sodium inside the duct wall, there is nothing for the reflector to represent. The code requires a "reflector" in every axial zone except the pin section, so some input for the reflector must be included. The reflector perimeter, SER, cannot be zero; but it can be set to a very small value, such as 10^{-9}, so that it would have no impact on coolant temperatures. Also, the total reflector thickness, DRFI plus DRFO, must be a reasonable value, 0.003 m or more, to prevent numerical instabilities in the reflector temperature calculations in the boiling module. The pre-voiding reflector temperature calculations are numerically stable for any reflector greater than zero.

3.14.1.4 Structure and Reflector Node Thickness

Two radial nodes are used in the reflectors and in the structure. The only restrictions on node thicknesses are that the total reflector thickness and the total structure thickness must be reasonable; 0.003 m or more, to prevent numerical instabilities in the temperature calculations in the boiling module. Usually, the node in contact with the coolant, the inner structure node or the outer reflector node, represents approximately 10% of the total thickness; and the other node represents the rest. Then the small node in contact the coolant will react rapidly to rapid changes in the coolant temperatures, whereas the larger node will dominate the longer-term response to the slow changes.

3.14.1.5 Coolant Re-entry Temperature

If PRIMAR-1 is being used, then the re-entry temperature calculation describe in Section 3.3.6 uses the input variable TUPL for the bulk temperature of the coolant in the outlet plenum. If PRIMAR-4 is being used, then the outlet plenum temperature is computed by PRIMAR-4; and TUPL is not used.

3.14.2 Output Description

Figure 3.14-1 shows a typical thermal hydraulic output for one step of the transient. The output is largely self-explanatory. Note that on the first page of this output the axial location, coolant temperature, saturation temperature, and pressure are the values at node boundaries; whereas the cladding, structure, plenum, and reflector temperatures are the values at node mid-points. Also, on the second page the radial fuel temperatures are the values at node mid-points except for the inner and outer fuel temperature, as indicated in Fig. 3.2-4; whereas the radii are the values of radial node boundaries.

CHANNEL 1 SAS4A 0.0 PRETEST ANALYSIS OF THE THORS NATURAL CIRCULATION TESTS 11/28/83 19.03.36 PAGE 69
PRIHAR4 OPTION, ONE CHANNEL

*** TRANSIENT STATE RESULTS ON TIME STEP 50 AT TIME = 25.000 (SEC) IN CHANNEL 1 ***

FLOWRATE (KG/S) 0.0081239

COOLANT PROFILE

AXIAL LOCATION (M)	COOLANT TEMPERATURE (K)	SATURATION TEMPERATURE (K)	PRESSURE (MPA)	CLADDING TEMPERATURE (K)	STRUCTURE TEMPERATURE (K) INNER	STRUCTURE TEMPERATURE (K) OUTER	PLENUM TEMPERATURE (K)	REFLECTOR TEMPERATURE (K) INNER	REFLECTOR TEMPERATURE (K) OUTER
VESSEL OUTLET			0.1443						
3.36974	1200.624	1199.702	0.1443		1200.624	1200.624		1200.624	1200.624
3.18559	1200.624	1200.795	0.1456		1200.624	1200.624		1200.624	1200.624
3.00144	1200.624	1201.830	0.1470		1200.624	1200.624		1200.624	1200.624
2.81729	1200.624	1202.958	0.1483		1200.624	1200.624		1200.624	1200.624
2.63314	1200.624	1204.028	0.1496		1200.624	1200.624		1200.624	1200.624
2.49344	1200.623	1204.829	0.1506		1200.624	1200.624		1200.624	1200.624
2.35374	1200.621	1205.627	0.1516		1200.623	1200.623		1200.623	1200.623
2.35174	1200.621	1205.634	0.1517		1200.622	1200.624		1200.621	1200.621
2.25064	1200.620	1206.350	0.1525		1200.621	1200.623		1200.620	1200.620
2.14954	1200.642	1207.013	0.1534		1200.625	1200.623		1200.628	1200.629
2.04844	1200.735	1207.673	0.1542		1200.658	1200.630		1200.676	1200.682
1.94734	1200.983	1208.330	0.1550		1200.770	1200.667		1200.830	1200.846
1.86267	1201.412	1208.877	0.1557	1201.175	1201.004	1200.761			
1.77801	1202.120	1209.423	0.1564	1201.726	1201.419	1200.955			
1.69334	1203.196	1209.966	0.1571	1202.601	1202.104	1201.319			
1.60867	1204.706	1210.507	0.1578	1203.874	1203.138	1201.932			
1.52401	1206.684	1211.046	0.1585	1205.598	1204.586	1202.878			
1.43934	1209.121	1211.583	0.1592	1207.783	1206.486	1204.230			
1.35467	1211.963	1212.118	0.1599	1210.413	1208.834	1206.033			
1.27000	1215.109	1212.650	0.1606	1213.399	1211.586	1208.315			
1.18534	1218.427	1213.180	0.1613	1216.629	1214.653	1211.027			
1.10067	1191.641	1213.711	0.1620	1208.505	1202.851	1199.039			
1.01600	1154.046	1214.245	0.1628	1177.533	1170.685	1166.855			
0.93134	1107.039	1214.784	0.1635	1136.220	1128.487	1124.780			
0.84667	1052.422	1215.327	0.1642	1086.130	1077.852	1074.402			
0.76200	992.352	1215.876	0.1649	1029.223	1020.745	1017.673			
0.67734	929.241	1216.432	0.1657	967.782	959.434	956.831			
0.59267	865.710	1216.994	0.1664	904.330	896.415	894.343			
0.50800	804.314	1217.563	0.1672	841.487	834.251	832.728			
0.42334	747.588	1218.137	0.1680	781.813	775.460	774.449			
0.33867	697.872	1218.716	0.1688	727.789	722.458	721.830			
0.25400	657.181	1219.299	0.1696	681.615	677.410	677.152			
0.16933	627.150	1219.885	0.1704	645.155	642.137	642.072			
0.08467	627.150	1220.469	0.1712	627.150	627.150	627.150			
0.0	627.150	1221.052	0.1720	627.150	627.150	627.150			
-0.08467	627.150	1221.632	0.1728	627.150	627.150	627.150	627.150		
-0.18627	627.150	1222.624	0.1742		627.150	627.150		627.150	627.150
VESSEL INLET			0.1742						

Figure 3.14-1: Sample Subassembly Thermal Hydraulics Output

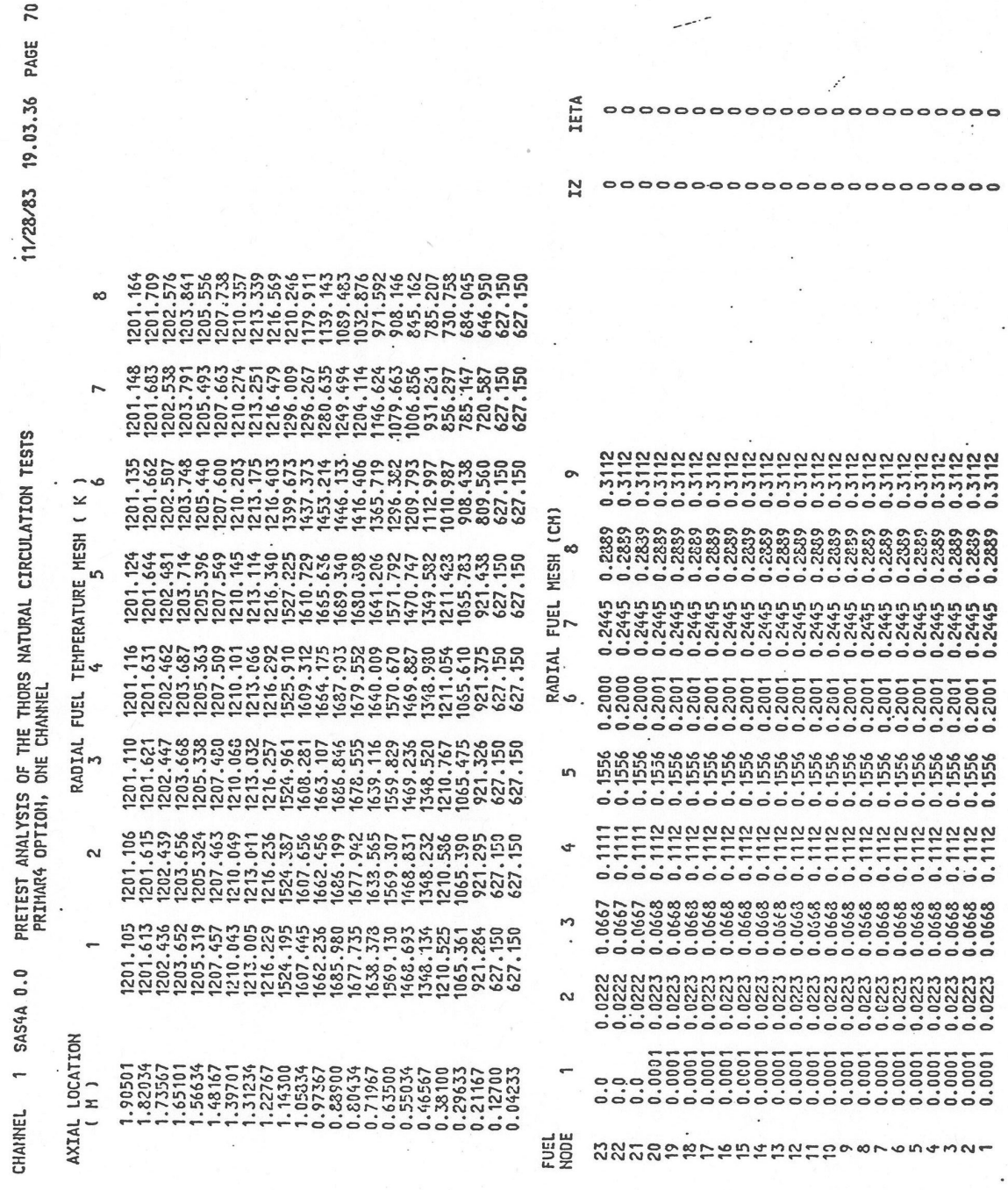

CHANNEL 1 SAS4A 0.0 PRETEST ANALYSIS OF THE THORS NATURAL CIRCULATION TESTS 11/28/83 19.03.36 PAGE 70
PRIHAR4 OPTION, ONE CHANNEL

AXIAL LOCATION (M) — RADIAL FUEL TEMPERATURE MESH (K)

1	2	3	4	5	6	7	8
1.90501	1201.105	1201.106	1201.110	1201.116	1201.124	1201.135	1201.148	1201.164
1.82034	1201.613	1201.615	1201.621	1201.631	1201.644	1201.662	1201.683	1201.709
1.73567	1202.436	1202.439	1202.447	1202.462	1202.481	1202.507	1202.538	1202.576
1.65101	1203.652	1203.656	1203.668	1203.687	1203.714	1203.748	1203.791	1203.841
1.56634	1205.319	1205.324	1205.338	1205.363	1205.396	1205.440	1205.493	1205.556
1.48167	1207.457	1207.463	1207.480	1207.509	1207.549	1207.600	1207.663	1207.738
1.39701	1210.043	1210.049	1210.063	1210.101	1210.145	1210.203	1210.274	1210.357
1.31234	1213.005	1213.011	1213.032	1213.066	1213.114	1213.175	1213.251	1213.339
1.22767	1216.229	1216.236	1216.257	1216.292	1216.340	1216.403	1216.479	1216.569
1.14300	1524.195	1524.387	1524.961	1525.910	1527.225	1399.673	1296.009	1210.246
1.05834	1607.445	1607.656	1608.281	1609.312	1610.729	1437.373	1296.267	1179.911
0.97367	1662.236	1662.456	1663.107	1664.175	1665.636	1453.214	1280.635	1139.143
0.88900	1685.980	1686.199	1686.846	1687.903	1689.340	1446.133	1249.494	1089.483
0.80434	1677.735	1677.942	1678.555	1679.552	1680.898	1416.406	1204.114	1032.876
0.71967	1638.373	1638.565	1639.116	1640.009	1641.206	1365.719	1146.624	971.592
0.63500	1569.130	1569.307	1559.829	1570.670	1571.792	1296.382	1079.663	908.146
0.55034	1468.693	1468.831	1469.236	1469.887	1470.747	1209.793	1006.856	845.162
0.46567	1348.134	1348.232	1348.520	1348.980	1349.582	1112.997	931.261	785.207
0.38100	1210.525	1210.586	1210.767	1211.054	1211.423	1010.987	856.297	730.758
0.29633	1065.361	1065.390	1065.475	1065.610	1055.783	908.438	785.147	684.045
0.21167	921.284	921.295	921.326	921.375	921.438	809.560	720.587	646.950
0.12700	627.150	627.150	627.150	627.150	627.150	627.150	627.150	627.150
0.04233	627.150	627.150	627.150	627.150	627.150	627.150	627.150	627.150

FUEL NODE	1	2	3	4	5	6	7	8	9	IZ	IETA
23	0.0	0.0222	0.0667	0.1111	0.1556	0.2000	0.2445	0.2889	0.3112	0	0
22	0.0	0.0222	0.0667	0.1111	0.1556	0.2000	0.2445	0.2889	0.3112	0	0
21	0.0	0.0222	0.0667	0.1111	0.1556	0.2000	0.2445	0.2839	0.3112	0	0
20	0.0001	0.0223	0.0668	0.1112	0.1556	0.2001	0.2445	0.2889	0.3112	0	0
19	0.0001	0.0223	0.0668	0.1112	0.1556	0.2001	0.2445	0.2889	0.3112	0	0
18	0.0001	0.0223	0.0668	0.1112	0.1556	0.2001	0.2445	0.2889	0.3112	0	0
17	0.0001	0.0223	0.0668	0.1112	0.1556	0.2001	0.2445	0.2889	0.3112	0	0
16	0.0001	0.0223	0.0668	0.1112	0.1556	0.2001	0.2445	0.2889	0.3112	0	0
15	0.0001	0.0223	0.0668	0.1112	0.1556	0.2001	0.2445	0.2889	0.3112	0	0
14	0.0001	0.0223	0.0668	0.1112	0.1556	0.2001	0.2445	0.2889	0.3112	0	0
13	0.0001	0.0223	0.0668	0.1112	0.1556	0.2001	0.2445	0.2889	0.3112	0	0
12	0.0001	0.0223	0.0668	0.1112	0.1556	0.2001	0.2445	0.2889	0.3112	0	0
11	0.0001	0.0223	0.0668	0.1112	0.1556	0.2001	0.2445	0.2889	0.3112	0	0
10	0.0001	0.0223	0.0668	0.1112	0.1556	0.2001	0.2445	0.2889	0.3112	0	0
9	0.0001	0.0223	0.0668	0.1112	0.1556	0.2001	0.2445	0.2889	0.3112	0	0
8	0.0001	0.0223	0.0668	0.1112	0.1556	0.2001	0.2445	0.2889	0.3112	0	0
7	0.0001	0.0223	0.0668	0.1112	0.1556	0.2001	0.2445	0.2889	0.3112	0	0
6	0.0001	0.0223	0.0668	0.1112	0.1556	0.2001	0.2445	0.2889	0.3112	0	0
5	0.0001	0.0223	0.0668	0.1112	0.1556	0.2001	0.2445	0.2889	0.3112	0	0
4	0.0001	0.0223	0.0668	0.1112	0.1556	0.2001	0.2445	0.2889	0.3112	0	0
3	0.0001	0.0223	0.0668	0.1112	0.1556	0.2001	0.2445	0.2889	0.3112	0	0
2	0.0001	0.0223	0.0668	0.1112	0.1556	0.2001	0.2445	0.2839	0.3112	0	0
1	0.0001	0.0223	0.0668	0.1112	0.1556	0.2001	0.2445	0.2889	0.3112	0	0

Figure 3.14-1: Sample Subassembly Thermal Hydraulics Output (Cont'd.)

CHANNEL 1 SAS4A 0.0 PRETEST ANALYSIS OF THE THORS NATURAL CIRCULATION TESTS 11/28/83 19.03.36 PAGE 71
PRIMAR4 OPTION, ONE CHANNEL

AXIAL LOCATION (M)	CLADDING TEMPERATURE (K)			AVERAGE COOLANT TEMPERATURE (K)	STRUCTURE TEMPERATURE (K)		AVERAGE FUEL TEMPERATURE (K)	RADIAL LOCATION (CM)			
								FUEL		CLAD	
	INNER	MIDPOINT	OUTER		INNER	OUTER		INNER	OUTER	INNER	OUTER
1.90501	1201.165	1201.175	1201.186	1201.200	1201.004	1200.761	1201.135	0.0	0.3112	0.3112	0.3492
1.82034	1201.709	1201.726	1201.744	1201.766	1201.419	1200.955	1201.682	0.0	0.3112	0.3112	0.3492
1.73567	1202.576	1202.601	1202.627	1202.658	1202.104	1201.319	1202.506	0.0	0.3112	0.3112	0.3492
1.65101	1203.841	1203.874	1203.909	1203.951	1203.138	1201.932	1203.747	0.0001	0.3112	0.3112	0.3492
1.56634	1205.557	1205.598	1205.642	1205.695	1204.586	1202.878	1205.439	0.0001	0.3112	0.3112	0.3492
1.48167	1207.738	1207.788	1207.840	1207.902	1206.486	1204.230	1207.599	0.0001	0.3112	0.3112	0.3492
1.39701	1210.358	1210.413	1210.471	1210.542	1208.834	1206.038	1210.202	0.0001	0.3112	0.3112	0.3492
1.31234	1213.340	1213.399	1213.461	1213.536	1211.536	1208.315	1213.174	0.0001	0.3112	0.3112	0.3492
1.22767	1216.569	1216.629	1216.692	1216.768	1214.653	1211.027	1216.401	0.0001	0.3112	0.3112	0.3492
1.14300	1210.227	1208.505	1206.835	1205.034	1202.851	1199.039	1400.460	0.0001	0.3112	0.3112	0.3492
1.05833	1179.826	1177.533	1175.318	1172.843	1170.685	1166.855	1438.522	0.0001	0.3112	0.3112	0.3492
0.97367	1139.112	1136.220	1133.496	1130.542	1128.487	1124.780	1454.994	0.0001	0.3112	0.3112	0.3492
0.88900	1089.468	1086.130	1083.003	1079.731	1077.852	1074.402	1448.894	0.0001	0.3112	0.3112	0.3492
0.80434	1032.837	1029.223	1025.815	1022.387	1020.745	1017.673	1420.434	0.0001	0.3112	0.3112	0.3492
0.71967	971.552	967.782	964.226	960.796	959.434	956.831	1371.251	0.0001	0.3112	0.3112	0.3492
0.63500	908.106	904.330	900.768	897.475	896.415	894.343	1303.302	0.0001	0.3112	0.3112	0.3492
0.55034	845.123	841.487	838.056	835.012	834.251	832.728	1217.457	0.0001	0.3112	0.3112	0.3492
0.46567	785.171	781.818	778.653	775.951	775.450	774.449	1120.946	0.0001	0.3112	0.3112	0.3492
0.38100	730.726	727.789	725.017	722.730	722.458	721.280	1017.249	0.0001	0.3112	0.3112	0.3492
0.29633	684.020	681.615	679.345	677.526	677.410	677.152	912.334	0.0001	0.3112	0.3112	0.3492
0.21167	646.931	645.155	643.479	642.165	642.137	642.072	811.611	0.0001	0.3112	0.3112	0.3492
0.12700	627.150	627.150	627.150	627.150	627.150	627.150	627.150	0.0001	0.3112	0.3112	0.3492
0.04233	627.150	627.150	627.150	627.150	627.150	627.150	627.150	0.0001	0.3112	0.3112	0.3492

FUEL NODE	AXIAL LOCATION (M)	FRACTION MOLTEN	ABOVE SOLDUS	ABOVE LIQDUS	GAP CONDUCTANCE W/M2-K	
23	1.90501	0.0	0.0	0.0	1.0000D+07	0.0
22	1.82034	0.0	0.0	0.0	1.0000D+07	0.0
21	1.73567	0.0	0.0	0.0	1.0000D+07	0.0
20	1.65101	0.0	0.0	0.0	1.0000D+07	0.0
19	1.56634	0.0	0.0	0.0	1.0000D+07	0.0
18	1.48167	0.0	0.0	0.0	1.0000D+07	0.0
17	1.39701	0.0	0.0	0.0	1.0000D+07	0.0
16	1.31234	0.0	0.0	0.0	1.0000D+07	0.0
15	1.22767	0.0	0.0	0.0	1.0000D+07	0.0
14	1.14300	0.0	0.0	0.0	1.0000D+07	0.0
13	1.05834	0.0	0.0	0.0	1.0000D+07	0.0
12	0.97367	0.0	0.0	0.0	1.0000D+07	0.0
11	0.88900	0.0	0.0	0.0	1.0000D+07	0.0
10	0.80434	0.0	0.0	0.0	1.0000D+07	0.0
9	0.71967	0.0	0.0	0.0	1.0000D+07	0.0
8	0.63500	0.0	0.0	0.0	1.0000D+07	0.0
7	0.55034	0.0	0.0	0.0	1.0000D+07	0.0
6	0.46567	0.0	0.0	0.0	1.0000D+07	0.0
5	0.38100	0.0	0.0	0.0	1.0000D+07	0.0
4	0.29633	0.0	0.0	0.0	1.0000D+07	0.0
3	0.21167	0.0	0.0	0.0	1.0000D+07	0.0
2	0.12700	0.0	0.0	0.0	1.0000D+07	0.0
1	0.04233	0.0	0.0	0.0	1.0000D+07	0.0

Figure 3.14-1: Sample Subassembly Thermal Hydraulics Output (Cont'd.)

3.15 Thermal Properties of Fuel and Cladding

All material property data for fuel and cladding are cast as functions or subroutines to allow for modularization and the ease of making changes. This also allows for the incorporation of different materials data in a straightforward manner. In a number of the correlations used, the units are inconsistent with the SI unit system adopted by SASSYS-1 and SAS4A. The routines that use these correlations carry out the appropriate units conversions internally.

The thermal properties for fuel and cladding are described in this section. Sodium properties are described in Chapter 12.

3.15.1 Fuel Density

The fuel density can be obtained either form a user-supplied table of density vs temperature or from a correlation with

$$\rho_f = \frac{\rho_o}{1 + C_1(T - 273) + C_2(T - 273)^2} \tag{3.15-1}$$

where

ρ_o = The theoretical density at 273 K, kg/m^3

C_1, C_2 = Input coefficients

T = Temperature, K

This applies between 273 K and the solidus temperature.

The liquid fuel density is given by

$$\rho_\ell = \frac{\rho_o}{1 + C_3(T - 273)} \tag{3.15-2}$$

where

C_3 = Input coefficient

This applies to temperatures above the liquidus. For the range between the solidus and liquidus temperatures, a linear interpolation is performed.

These equations are found in the function RHOF. Suggested values of coefficients are from the Nuclear Systems Materials Handbook [3-8].

ρ_c = COEFDS(1) = 11.05x10^3 kg/m^3 (mixed oxide)

C_1 = COEFDS(2) = 2.04x10^{-5} K^{-1}

C_2 = COEFDS(3) = 8.70x10^{-9} K^{-2}

C_3 = COEFDS(2) = 9.30x10^{-5} K^{-1}

3.15.2 Fuel Thermal Conductivity

Four different options exist for the fuel thermal conductivity. These are controlled through the input parameter IRHOK.

IRHOK = 0

The thermal conductivity as function of temperature is input in table form through the variable arrays XKTAB and XKTEM.

IRHOK =1

For this option, the conductivity equations are given by:

$$k_1(T) = 1.1 + \frac{1x10^2}{T(.4888 - .4465 f_D)} \quad \text{for } 800°C \le T \le 2000°C \tag{3.15-3}$$

$$k_2(T) = k_1(800)\frac{168.844}{12.044 + (0.196)T} \quad \text{for } T \le 800°C \tag{3.15-4}$$

$$k_3(T) = k_1(2000) \quad \text{for } T > 2000°C \tag{3.15-5}$$

where

k_1, k_2, k_3 = Fuel thermal conductivity, W/m-k

T = Temperature, ºC

f_D = Fuel fraction of theroretical density

IRHOK = 2

This form of the conductivity is given by

$$k_1(T) = \left[(C_1 - f_D)\, f_D - 1\right]\left[\frac{1}{(C_2 + C_3 T)} + C_4 T^3\right] \quad \text{for } 0.75 \le f_D \le 0.95 \tag{3.15-6}$$

$$k_2(T) = (3f_D - 1)\left[\frac{1}{C_5 + C_6 T} + C_7 T^3\right] \qquad (3.15\text{-}7)$$

for $f_D > 0.95$

where

$C_1, C_2, C_3, C_4, C_5, C_6, C_7$ = Input variables

k_1, k_2 = Fuel conductivity W/m-k

T = Temperature, K

If *T* is greater than the melting temperature, it is set to the melting temperature.

Suggested values:

C_1= COEFK(1) = 2.1

C_2= COEFK(2) = 2.88×10^{-3}

C_3= COEFK(3) = 2.52×10^{-5}

C_4= COEFK(4) = 2.83×10^{-10}

C_5= COEFK(5) = 5.75×10^{-2}

C_6= COEFK(6) = 5.03×10^{-4}

C_7= COEFK(7) = 2.91×10^{-11}

IRHOK = 3

This conductivity form is [3-9]

$$k_1(T) = \frac{4.005x10^3}{(T - 273) + 402.4} + 0.6416x10^{-10}T^3 \qquad (3.15\text{-}8)$$

where

T = Temperature, K

k = Conductivity in W/m-k

This is the correlation for UO_2 and is converted to mixed oxide by subtracting 0.2.

$$k_2(T) = k_1(T) - 0.2 \qquad (3.15\text{-}9)$$

The porosity correction term was derived for use in the COMETHE-IIIJ [2-10] code and is given by

$$f_p = 1 - 1.029\,\varepsilon - 3.2\,\varepsilon^2 - 40.1\,\varepsilon^3 + 158\,\varepsilon^4 \qquad (3.15\text{-}10)$$

where

f_p = Porosity multiplier

ε = 1 - ρ_f = Fractional porosity

ρ_f = fractional fuel density = actual density/theoretical density

The conductivity is therefore given by

$$k(T) = f_p\, k_2(T). \qquad (3.15\text{-}11)$$

Two different routines contain the above correlations, FK and KFUEL. The function FK returns a single value of the conductivity for a single invocation and is used in the steady-state calculation. The subroutine KFUEL returns the conductivity values for each radial node in the current axial segment. It is used in the transient calculational procedure.

REFERENCES

NOTICE

Several references in this document refer to unpublished information. For a list of available open-literature citations, please contact the authors.

APPENDIX 3.1:
DEGREE OF IMPLICITNESS FOR FLOW AND TEMPERATURE CALCULATIONS

A typical calculation in SASSYS-1 involves finding the value of a temperature or a flow rate at the end of a time step given the values of relevant parameters at the beginning of the step, as well as the values of driving functions at the beginning and end of the step. Linearized finite difference approximations to the relevant differential equations are usually used, and the accuracy of the finite differencing in time will depend both on the size of the time step and on the degree of implicitness in the solution. By picking appropriate values for the degree of implicitness, it is possible to improve the accuracy of the solution.

The differential equations used for temperatures and flow rates are of the form

$$\frac{dy}{dt} = f(y,t) \tag{A3. 1-12}$$

Where y is the flow rate or temperature being calculated, and f is a function of y and time. The finite difference approximation used for Eq. A3.1-1 is

$$\frac{y_2 - y_1}{\Delta t} = \theta_1 f(y_1, t_1) + \theta_2 f(y_2, t_2) \tag{A3. 1-13}$$

where

t_1 = time at the beginning of the time step

t_2 = time at the end of the time step

y_1 = y at t_1

y_2 = y at t_2

$$\Delta t = t_2 - t_1 \tag{A3. 1-14}$$

$$\theta_1 + \theta_2 = 1.0 \tag{A3. 1-15}$$

The parameters θ_1 and θ_2 determines the degree of implicitness of the solution: for a fully explicit solution θ_1 = 1.0 and θ_2 = 0.0, whereas for a fully implicit solution θ_1 = 0.0 and θ_2 = 1.0.

After linearizing, equation A3.1-1 can be put in the form

$$\frac{dy}{dt} = f(y_1, t_1) + (t - t_1)\frac{df}{dt} + (y - y_1)\frac{df}{dy} \quad \text{(A3. 1-16)}$$

or

$$\frac{dy}{dt} = A + B\ (t - t_1) + C(y - y_1) \quad \text{(A3. 1-17)}$$

where

$$A = f\left(y_1, t_1\right) \quad \text{(A3. 1-18)}$$

$$B = df\ /\ dt \quad \text{(A3. 1-19)}$$

$$C = df\ /\ dy \quad \text{(A3. 1-20)}$$

For instance, Eq. 3.80t for the coolant flow rate in a channel is

$$I_1 \frac{dw}{dt} = p_b - p_t - w^2 I_2 - A_{fr} w\ |w|^{I+b_{fr}} I_3 - w|w| I_4 - g I_5 \quad \text{(A3. 1-21)}$$

Linearizing the w^2, $w|w|^{1+b_{fr}}$, and $w|w|$ terms gives

$$w^2 \simeq w_1^2 + 2w_i\left(w - w_1\right) \quad \text{(A3. 1-22)}$$

$$w|w|^{1+b_{fr}} \simeq w_1|w_1|^{1+b_{fr}} + \left(2 + b_{fr}\right)|w_1|^{1+b_{fr}}\left(w - w_1\right) \quad \text{(A3. 1-23)}$$

and

$$w|w| \simeq w_1|w_1| + |w_1|\left(w - w_1\right) \quad \text{(A3.1-24)}$$

Also, p_b and p_t are approximated as

$$p_b(t) = p_b(t_1) + (t - t_1)\frac{dp_b}{dt} \quad \text{(A3. 1-25)}$$

$$p_t(t) = p_t(t_1) + (t - t_1)\frac{dp_t}{dt} \quad \text{(A3. 1-26)}$$

where

$$\frac{dp_b}{dt} = \frac{p_b(t_2) - p_b(t_1)}{t_2 - t_1} \tag{A3. 1-27}$$

and

$$\frac{dp_t}{dt} = \frac{p_t(t_2) - p_t(t_1)}{t_2 - t_1} \tag{A3. 1-28}$$

Then Eq. A3.1-10 has the form of Eq. A3.1-6 if

$$A = \left\{ p_b(t_1) - p_t(t_1) - w_1^2 I_2 - A_{fr}\ w_1 |w_1|^{1+b_{fr}} I_3 - w_1 |w_1| I_4 - g I_5 \right\} / I_1 \tag{A3. 1-29}$$

$$B = \frac{\frac{dp_b}{dt} - \frac{dp_t}{dt}}{I_1} \tag{A3. 1-30}$$

and

$$C = -\frac{\left[2 w_1\ I_2 - (2 + b_{fr}) A_{fr} |w_1|^{1+b_{fr}} - |w_1| I_4 \right]}{I_1} \tag{A3. 1-31}$$

The exact solution for Eq. A3.1-6 is

$$y - y_1 = \left(A\tau - B\tau^2 \right) \left(1 - e^{-(t - t_1)/\tau} \right) + B\tau (t - t_1) \tag{A3. 1-32}$$

where

$$\tau = -\frac{1}{C} \tag{A3. 1-33}$$

The finite difference approximation used for Eq. A3.1-6 is

$$\frac{y_2 - y_1}{\Delta t} = A + \theta_2 B \Delta t + \theta_2 C (y_2 - y_1) \tag{A3. 1-34}$$

where

$$\Delta t = t_2 - t_1 \tag{A3. 1-35}$$

The solution of Eq. A3.1-23 for y_2 is

$$y_2 - y_1 = \frac{A\Delta t + \theta_2 B \Delta t^2}{1 + \theta_2 \Delta t / \tau} \tag{A3. 1-36}$$

Figure A3.1-1 shows y_2 - y_1, as given by Eq. A3.1-25, as a function of θ_2 for the case where A = 1, B = .5, Δt = 2, and τ = 1. Also shown is the exact solution from Eq. A3.1-21. Note that a value θ_2 can be found such that the finite difference solution of Eq. A3.1-25 exactly matches the differential equation solution, given by Eq. A3.1-21, for this case. Also note that neither a fully explicit solution, θ_2 = 0, nor a fully implicit solution, θ_2 = 1.0, is very accurate for particular case. An explicit solution would be numerically unstable for Δt greater than τ; and values considerably smaller than the time constant τ.

For any values of the parameters in Eq. A3.1-21 and Eq. A3.1-25, a value of θ_2 can be chosen such that the finite difference solution matches the solution of the differential equation by setting $t = t_2$ in Eq. A3.1-21 and combining this equation with Eq. A3.1-25 to give

$$\left(A\tau - B\tau^2\right)\left(1 - e^{-\Delta t/\tau}\right) + B\tau\,\Delta t = \frac{A\Delta t + \theta_2 B \Delta t^2}{1 + \theta_2 \Delta t / \tau} \tag{A3. 1-37}$$

solving for θ_2 gives

$$\theta_2 = \frac{\dfrac{\Delta t}{\tau} - \left(1 - e^{-\Delta t/\tau}\right)}{\dfrac{\Delta t}{\tau}\left(1 - e^{-\Delta t/\tau}\right)} \tag{A3. 1-38}$$

Note that A and B cancelled out of Eq. A3.1-27, and θ_2 is a function only of $\Delta t/t$.

Figure A3.1-2 shows θ_2, given by Eq. A3.1-27, as a function of $\Delta t/\tau$. This figure also shows some approximations to this function, as discussed below. For small values of $\Delta t/\tau$, θ_2 approaches 0.5, where as for large values of $\Delta t/\tau$, θ_2 approaches 1.0.

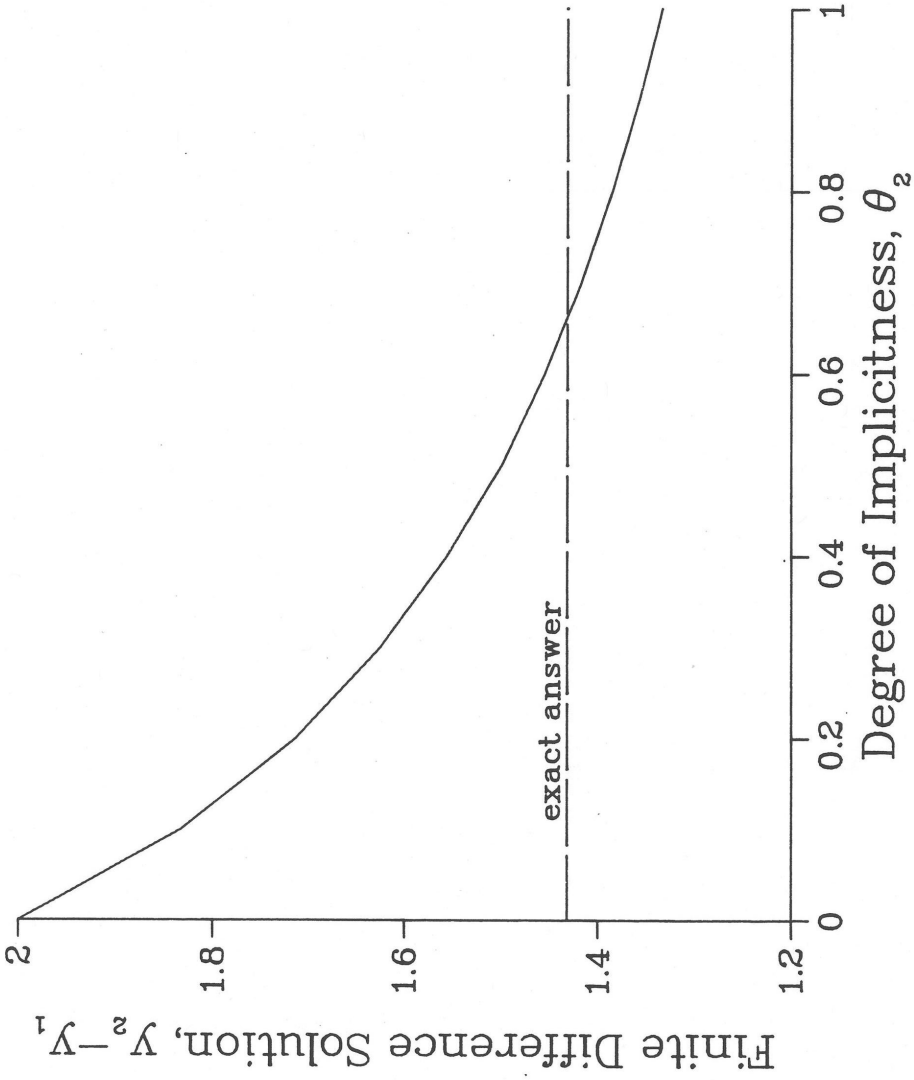

Fig. A3.1-1. Finite Difference Solution as a Function of the Degree of Implicitness

Figure A3.1-1: Finite Difference Solution as a Function of the Degree of Implicitness

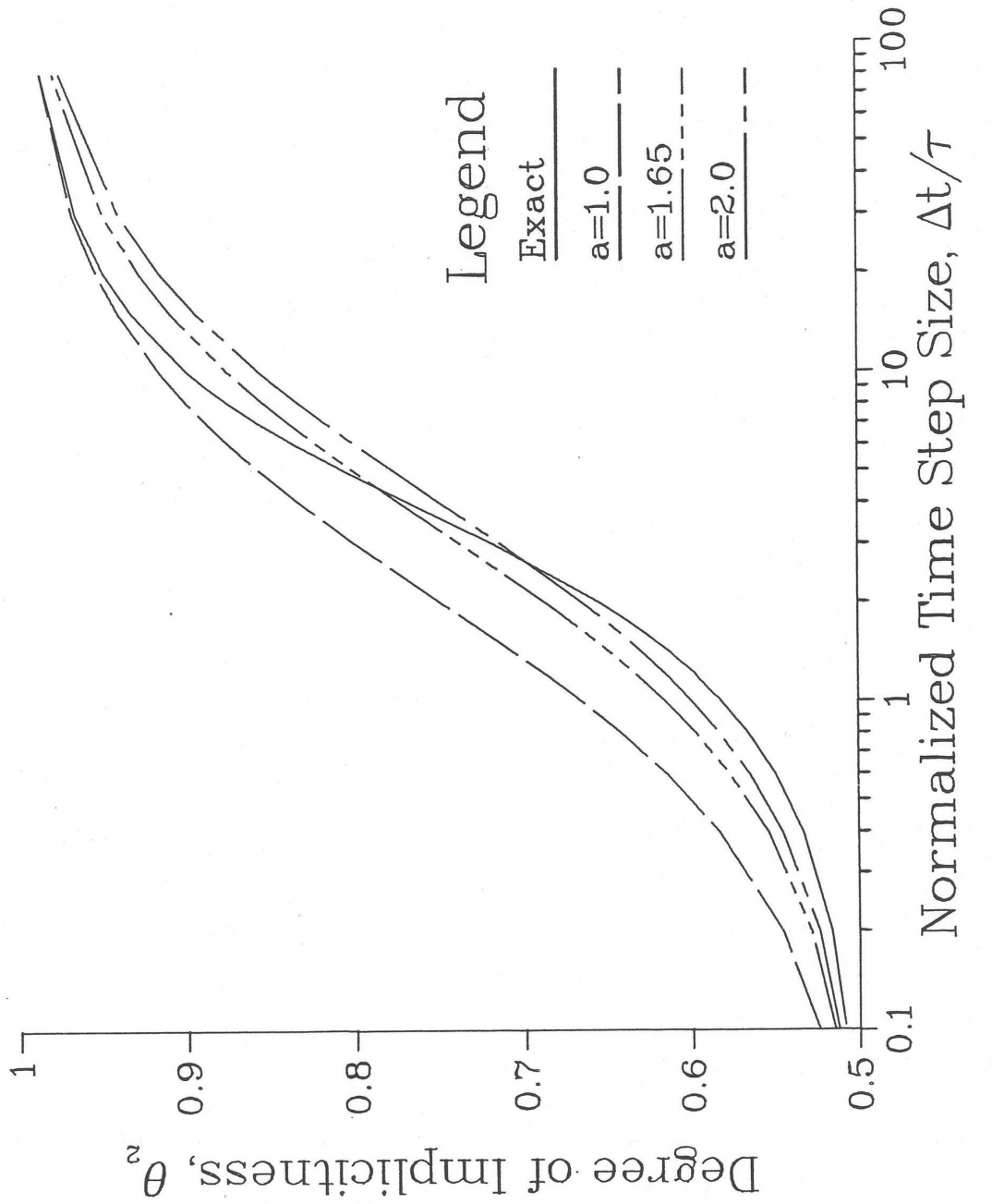

Figure A3.1-2: Degree of Implicitness as a Function of Normalized Time Step Size

For any equation that can be put in the form of Eq. A3.1-5 or A3.1-6, Eq. A3.1-22 can be used to fine τ, and then Eq. A3.1-27 can be used to find the appropriate value of θ_2 for any value of Δt. Note that if driving pressures and coolant flows are being solved for simultaneously, as is done in PRIMAR-4, then the value of B in Eq. A3.1-6 is not known until the pressures have been solved for. In such cases, a direct analytic solution of the differential equation, as in Eq. A3.1-22, could not be made except by iterating between Eq. A3.1-22 and the pressure solution. On the other hand, the calculation of θ_2, as in Eq. A3.1-27, requires only Δt and τ; and the calculation of τ requires only information that is available at the beginning of a time step; so an appropriate value for θ_2 can be found for use in finite difference approximations without iteration, even if driving pressures and flow rates are being solved for simultaneously.

Even if finite differencing in time does not introduce any error into a solution, there are usually other sources of error, such as the linearization approximations of Eq. A3.1-11 through Eq. A3.1-17. Also, the term represented by $B(t\text{-}t_1)$ in Eq. A3.1-6 may in fact not be linear in time. Therefore, simpler and easier to compute approximations to the expression on the right-hand side of Eq. A3.1-27 might sometimes be used without losing much overall accuracy. A simple approximation, θ_2' that approaches the correct limits for very small and very large values of $\Delta t/\tau$ is

$$\theta_2' = \frac{a + \dfrac{\Delta t}{\tau}}{2a + \dfrac{\Delta t}{\tau}} \qquad \text{(A3. 1-39)}$$

where the parameter a can be chosen to give some best overall fit. Figure A3.1-2 shows this function for various values of the parameter a. The curve for a = 1.65 gives a fairly good fit, although no value of a will give a good fit over the whole range.

A better fit to θ_2 can be obtained by an expression of the form

$$\theta_2' = \frac{a + bx + x^2}{2a + cx + x^2} \qquad \text{(A3. 1-40)}$$

where

$$x = \frac{\Delta t}{\tau} \qquad \text{(A3. 1-41)}$$

with a = 6.12992, b = 2.66054, and c = 3.56284, this expression fits the exact value of Eq. A3.1-27 to within 1% over the whole range of $\Delta t/\tau$, as shown in Fig. A3.1-3.

In general, when linear approximations are valid, and when a single known time constant dominates the behavior, Eq. A3.1-27 or Eq. A3.1-29 will give a value of θ_2 that will provide accurate finite difference solutions. For cases where a number of different time constants are important, none of these expressions for θ_2 will give a precise finite

difference solution for all time-step sizes. Even in this case, though, θ_2 should approach 0.5 for small time steps, and it should approach 1.0 for large time steps. Therefore, an expression of the form given by Eq. A3.1-28 may be appropriate in such cases.

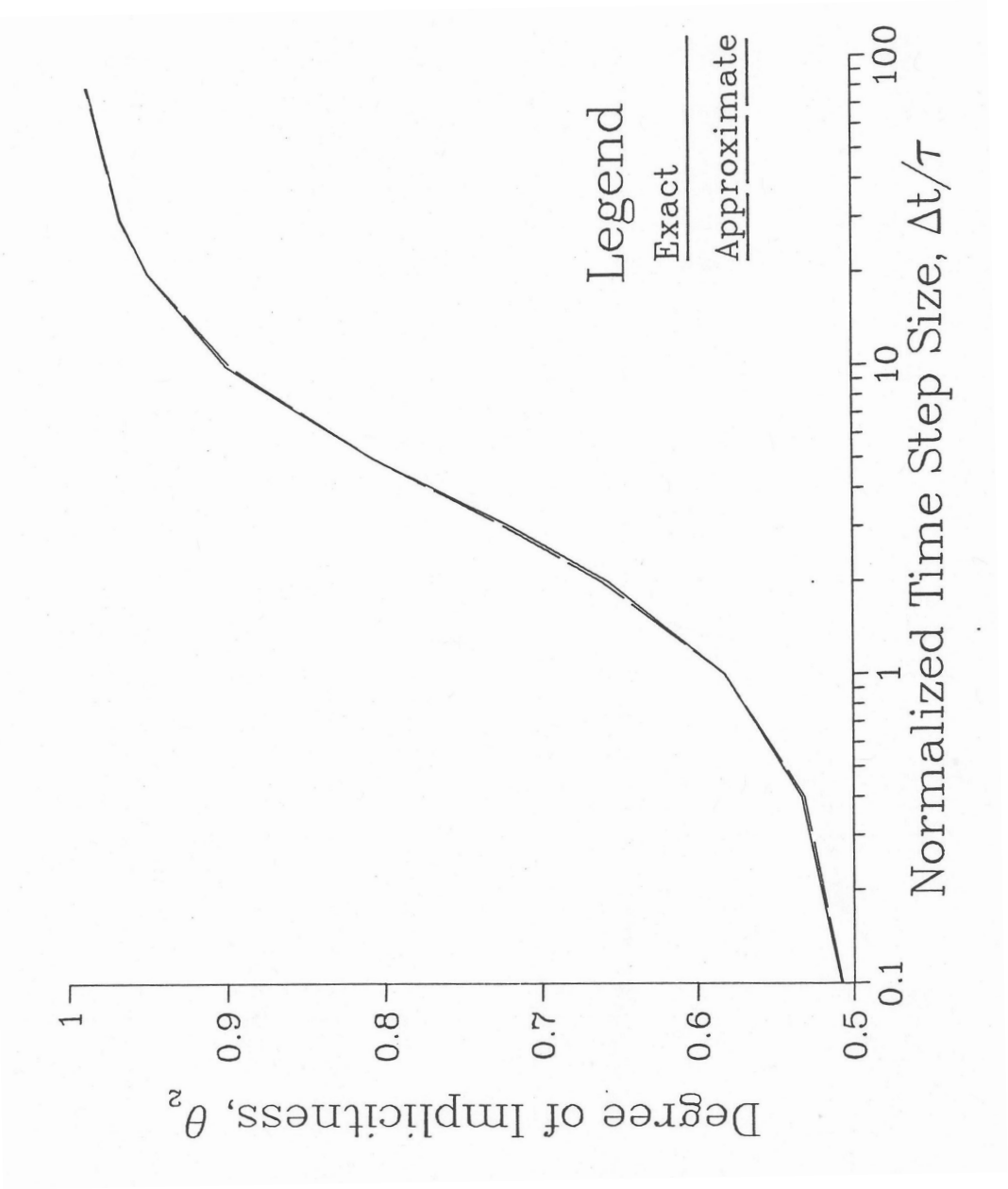

Figure A3.1-3: Approximate Correlation for the Degree of Implicitness